

**ANALYSIS OF ARCHITECTURAL GEOMETRIES AFFECTING STRESS DISTRIBUTIONS OF
GOTHIC FLYING BUTTRESSES**

by

RICHARD D. Y. KIM

A THESIS

submitted in partial fulfillment of the requirements for the degree

MASTER OF SCIENCE

Department of Architectural Engineering and Construction Science

College of Engineering

KANSAS STATE UNIVERSITY

Manhattan, Kansas

2016

Approved by:

**Major Professor
Kimberly Kramer**

Copyright

RICHARD KIM

2016

Abstract

The flying buttress is one of the most prominent characteristics of Gothic architecture. Understanding stress distribution from the upper vaulted nave (high vault) to the flying buttress system would contribute greatly to preservation efforts of such iconic structures. Many investigations have emphasized structural analysis of Gothic flying buttresses, but only limited research how architectural design affects load distribution throughout the Gothic members exist. The objective of this investigation was to inspire engineers and architectural preservationists to develop further research in Gothic structural analysis and restoration by increasing understanding how architectural design of flying buttresses affects the load path being transmitted from the main superstructure to the lateral force resisting system. Several flying buttress designs under similar analytical parameters were compared in order to understand how member geometries affect stress distribution. Because Gothic design is architecturally complex, finite element analysis method was used to obtain member stress distribution (regions of compressive and tensile stresses). Architectural elevation schematics of the flying buttresses of prominent Gothic cathedrals were referenced when modeling the structural members to a computer software program (RAM Elements).

Table of Contents

List of Figures	vii
List of Tables	ix
List of Equations	x
Acknowledgements	xi
Dedication	xii
1 Introduction	1
2 Objective and Methodology	3
3 Anatomy of the Flying Buttress	5
4 Historic Structural Masonry	6
4.1 masonry properties and assumptions	6
4.2 mechanics of the masonry arch	7
4.2.1 lines of thrust	8
4.2.1.1 active line of thrust	9
4.2.1.2 passive line of thrust.....	9
4.3 gothic architectural elements	9
4.3.1 the gothic arch	9
4.3.2 the pinnacle	10
4.3.3 the flying buttress	11
4.4 historical structural masonry in Europe	11
4.4.1 stone type	12
4.4.2 mortar type	12
4.4.3 integration between stone and mortar of ancient masonry structures	13
5 Method of Analysis	14
5.1 classical method	14
5.2 linear elastic analysis	15
5.3 linear elastic finite element analysis	16
6 Analysis Plan and Procedure	18
6.1 first trial.....	18
6.2 second trial.....	19
6.2.1 Cathedral d'Amiens.....	20
7 Analysis of Three Gothic Structures	22
7.1 Cathédrale Notre-Dame de Paris.....	23
7.1.1 structural history and description.....	24
7.1.2 load path.....	25

7.1.3 finite element analysis.....	25
7.1.3.1 input.....	26
7.1.3.2 output.....	27
7.1.3.2.1 areas vulnerable in tension	29
7.1.3.2.2 areas remaining in compression	30
7.2 Cathédrale Saint-Étienne, Bourges.....	31
7.2.1 structural history and description	31
7.2.2 load path.....	32
7.2.3 finite element analysis.....	33
7.2.3.1 input.....	33
7.2.3.2 output.....	34
7.2.3.2.1 areas vulnerable in tension	37
7.2.3.2.2 areas remaining in compression	37
7.3 Cathédrale d'Amiens.....	39
7.3.1 structural history and description.....	39
7.3.2 load path.....	40
7.3.3 finite element analysis.....	41
7.3.3.1 input.....	42
7.3.3.2 output.....	43
7.3.3.2.1 areas vulnerable in tension	46
7.3.3.2.2 areas remaining in compression	47
8 Parametric studies	48
8.1 modulus of elasticity of limestone	48
8.2 unit weight of limestone.....	48
8.3 inclination, span distance and thickness of flying buttress	48
8.4 omitting quatrefoil regions of flying buttress of Cathédrale d'Amiens	49
8.5 changing magnitude of lateral load	50
9 Results and Conclusion	52
9.1 most effective design	52
9.2 least effective design	53
9.3 discussion of results.....	53
9.4 limitations	55
9.5 recommendations for further research.....	56
References.....	59
Appendix A – Computations and Assumptions	62

Appendix B – Architectural Drawings	68
Appendix C – Model Renderings	75
Appendix D – Source Permission.....	120

List of Figures

Figure 1.1 – Romanesque Architecture.....	1
Figure 1.2 – Gothic Architecture.....	1
Figure 2.1 – Flying Buttress of Clermont-Ferrand.....	3
Figure 2.2 – Flying Buttress of Amiens.....	3
Figure 2.3 – Flying Buttress of Notre-Dame de Paris.....	3
Figure 3.1 – Gothic Cathedral Cross Section.....	5
Figure 4.1 – the Arch.....	6
Figure 4.2 – Masonry Arch and Wooden Framework.....	7
Figure 4.3 – Inverted Catenary Curve.....	7
Figure 4.4 – Active and Passive Lines of Thrust.....	8
Figure 4.5 – the Roman Arch.....	10
Figure 4.6 – the Gothic Arch.....	10
Figure 4.7 – the Pinnacle Affecting Line of Thrust.....	10
Figure 4.8 – Gothic Cross Section.....	11
Figure 5.1 – Illustrated Example of the Classical Method.....	14
Figure 5.2 – Deflection of Cross Section of Finite Element Model.....	16
Figure 6.1 – First Trial Model Construction.....	19
Figure 6.2 – Second Trial Model Construction.....	19
Figure 6.3 – Shell Segmentation of Cathédrale d'Amiens.....	20
Figure 7.1 – Map of France.....	22
Figure 7.2 – Regions of Boundary Conditions.....	22
Figure 7.3 – Plan View of Notre-Dame de Paris.....	24
Figure 7.4 – Cross section of Notre-Dame de Paris.....	25
Figure 7.5 – Schematic of Analysis of Notre-Dame de Paris.....	27
Figure 7.6 – Schematic Reference.....	28
Figure 7.7 – Flying Buttress 1 of Notre-Dame de Paris.....	28
Figure 7.8 – Schematic Reference.....	28
Figure 7.9 – Flying Buttress 2 of Notre-Dame de Paris.....	28
Figure 7.10 – Plan View of Cathédrale Saint-Étienne, Bourges.....	31
Figure 7.11 – Cross Section of Cathédrale Saint-Étienne, Bourges.....	32
Figure 7.12 – Schematic of Analysis of Cathédrale Saint-Étienne, Bourges.....	33
Figure 7.13 – Schematic Reference.....	35
Figure 7.14 – Flying Buttress 1 of Cathédrale Saint-Étienne, Bourges.....	35

Figure 7.15 – Schematic Reference.....	35
Figure 7.16 – Flying Buttress 2 of Cathédrale Saint-Étienne, Bourges.....	35
Figure 7.17 – Schematic Reference.....	35
Figure 7.18 – Flying Buttress 3 of Cathédrale Saint-Étienne, Bourges.....	35
Figure 7.19 – Schematic Reference.....	36
Figure 7.20 – Flying Buttress 4 of Cathédrale Saint-Étienne, Bourges.....	36
Figure 7.21 – Schematic Reference.....	36
Figure 7.22 – Flying Buttress 5 of Cathédrale Saint-Étienne, Bourges.....	36
Figure 7.23 – Schematic Reference.....	36
Figure 7.24 – Flying Buttress 6 of Cathédrale Saint-Étienne, Bourges.....	36
Figure 7.25 – Plan View of Cathédrale d'Amiens.....	39
Figure 7.26 – Cross Section of Cathédrale d'Amiens.....	40
Figure 7.27 – Original Schematic of Analysis of Cathédrale d'Amiens.....	42
Figure 7.28 – Current Schematic of Analysis of Cathédrale d'Amiens.....	42
Figure 7.29 – Schematic Reference.....	44
Figure 7.30 – Flying Buttress 1 of Cathédrale d'Amiens.....	44
Figure 7.31 – Schematic Reference.....	44
Figure 7.32 – Flying Buttress 2 of Cathédrale d'Amiens.....	44
Figure 7.33 – Schematic Reference.....	45
Figure 7.34 – Flying Buttress 1 & 3 of Cathédrale d'Amiens.....	45
Figure 7.35 – Schematic Reference.....	45
Figure 7.36 – Flying Buttress 2 of Cathédrale d'Amiens.....	45
Figure 8.1 – Cathédrale d'Amiens Without Quatrefoil Regions.....	50
Figure 8.2 - Cathédrale d'Amiens With Quatrefoil Regions.....	50
Figure 9.1 – Tensile Stress Distribution of Notre-Dame de Paris.....	52
Figure 9.2 – Tensile Stress Distribution of Cathédrale Saint-Étienne, Bourges.....	52
Figure 9.3 – Tensile Stress Distribution of Cathédrale d'Amiens	52
Figure 9.4 – Quatrefoil Design.....	53
Figure 9.5 – Cinqfoil Design.....	53
Figure 9.6 – Profile of Notre-Dame de Paris.....	53
Figure 9.7 – Profile of Cathédrale Saint-Étienne, Bourges.....	53
Figure 9.8 – Profile of Cathédrale d'Amiens	53
Figure 9.9 – Section View of Nave and Flying Buttress System.....	55
Figure 9.10 – Section View of Aisle and Nave.....	56

List of Tables

Table 7.1 - Mechanical Properties of Limestone.....	26
---	----

List of Equations

Equation 9.1 – Wind Pressure.....57

Acknowledgements

I would like to thank my major professor, Kimberly Kramer, for all the enthusiasm, guidance and encouragement throughout my undergraduate and graduate years at Kansas State University.

I would also like to thank LEYS Bérangère for taking the time to direct me to authentic resources that I would never have found on my own.

Je souhaite également remercier LEYS Bérangère pour avoir pris le temps de me montrer les ressources académiques authentiques que je n'aurais jamais découverts par moi-même .

Dedication

I wish to dedicate my endeavors to my parents, my academic advisors, engineering mentors and friends. I thank you for encouraging me to press on forward when I wanted to give in.

“For every house is built by someone, but the builder of all things is God.”

– Hebrews 3:4

“Toute maison est construite par quelqu'un, mais celui qui construit toute chose, c'est Dieu.”

– Hébreux 3:4

1 Introduction

Construction methods and philosophies from our ancient predecessors clash with our modern practices with regards to architecture and engineering. Many possible reasons why buildings constructed centuries ago tend to have significant value than most buildings constructed today exist. Most Gothic buildings required an entire or several human generations to plan, design and construct. Such time invested in these structures may be a reason why most historical structures are worth preserving today. Another explanation is that architects and masons lacked of deeper understanding of the mechanics of materials, which drove engineers and architects to be conservative in their design practices. To some degree, the lack of understanding of how materials behave may have been an advantage to explore numerous creative solutions to pursue unimaginable endeavors, such as Gothic design.

Gothic design can be argued as a design philosophy in which structural aesthetics and form coexist in perfect union. One cannot exist without the other. After centuries of engineering knowledge passed down from the ancient Roman Empire, the Gothic era was the period where such understanding truly flourished that enabled the Gothic movement come to life.

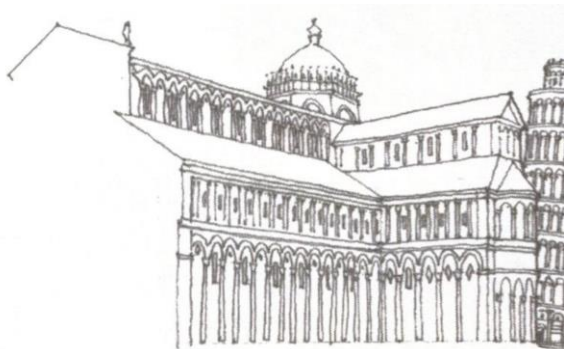


Figure 1.1 - Romanesque Architecture



Figure 1.2 - Gothic Architecture

Images courtesy of Francis D. K. Chang, *A Visual Dictionary of Architecture (2nd Ed.)*; John Wiley & Sons, Inc.

This principle Gothic structural element is derived from other Gothic elements such as the groined vault and the pointed arch. The Gothic movement emphasized two things: height and light. Achieving both of these elements resulted in the architectural design to be slender in appearance as depicted in **Figure 1.2**. Allowing light into the interior parts of the structure required walls that were substantially less thick than buildings of the Romanesque era (**Figure 1.1**), but this posed a grand problem for builders if height is something they wanted to achieve. This became a stability

issue as masons noticed the walls bowing outwards when the height of the structure increased. Without compromising the slender appearance of the structure, Gothic structural elements, such as the point arch, was manipulated in such a way that an arch *suspended* between regions vulnerable in tension in order to transmit thrust loads or wind loads from the nave to the foundation system. Hence, this *suspended* appearance was given the name *flying buttress*.

Once the builders found this remarkable solution, this structural element allowed builders to construct such tall structures, which allowed the entire structure to remain in compression. The beauty of this design process from Romanesque to Gothic was the *skeletonization* process of structural masonry (Ball, 2008), which helped visualize how loads were being transmitted throughout the structure. The understanding of manipulating load paths for masonry to remain in compression allowed Gothic builders to achieve both height and large openings throughout the structure.

Design assumptions, architectural schematics, and etc. will be referenced throughout this research since the nature of this study is heavily dependent on illustrations. **Appendix A** contains information regarding model computations and assumptions. **Appendix B** contains authentic architectural cross sections and plan drawings taken from a digital archive. **Appendix C** contains comprehensive stress model renderings for the selected gothic structures. Lastly, **Appendix D** references source permission from various publishers and proprietors of exclusive material (architectural cross sections, site photographs, etc.)

2 Objective and Methodology

Repair, restoration and understanding historic load bearing masonry structures can be a complex issue in terms of finding a solution that is structurally sound while respecting its architectural integrity. The assessment of such historical structures is difficult to determine such as loads, mechanical properties, decay of materials, geometry and etc. Investigating historical masonry structures is a question of stability rather than the strength of materials (Viola, Panzacci & Tornabene, 2004).

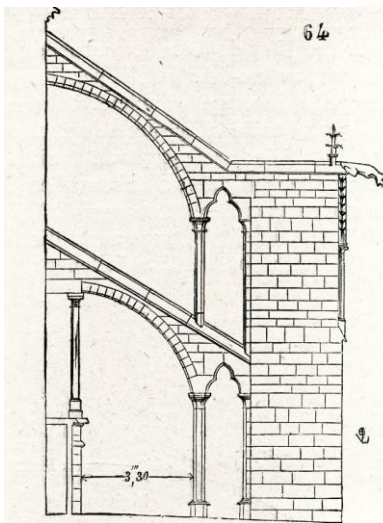


Figure 2.1 - Flying Buttress of Clermont-Ferrand

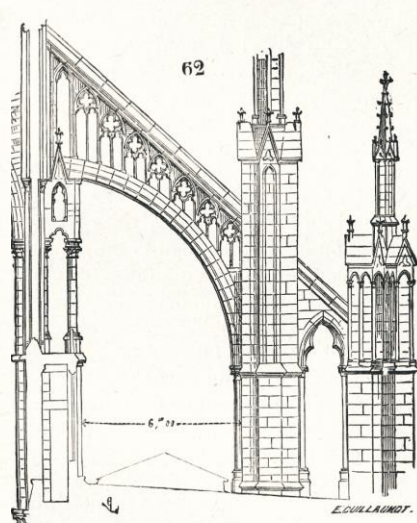


Figure 2.2 – Flying Buttress of Amiens

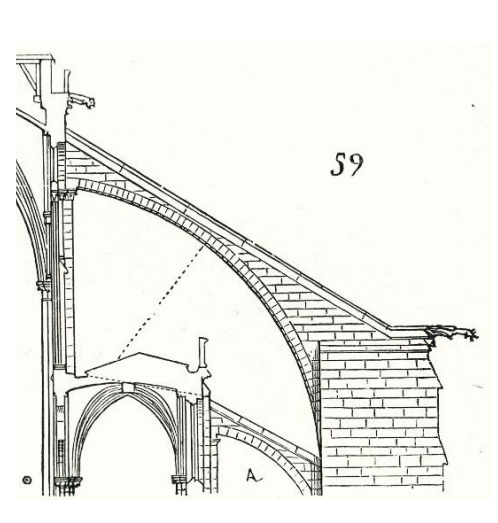


Figure 2.3 – Flying Buttress of Notre-Dame de Paris

Images courtesy of mappinggothic.org, Media Center for Art History, Department of Art History and Archaeology, Trustees of Columbia University

The primary objective of this study is to see how architectural geometries of flying buttresses affect the stress distribution of the member through a two-dimensional finite element analysis. **Figure 2.1**, **Figure 2.2** and **Figure 2.3** demonstrates the variety of architectural designs of flying buttresses to counteract the thrust loads from the high vault. Such geometric variety of flying buttresses will affect stresses to be distributed differently from one design to the other. Specific analysis with regards to wind, seismic, foundation settlement and vibrations (from bells) are not addressed in this research. Assumptions and reasonable simplifications are made to the model since geometry will be the primary factor in determining member stress distribution.

A similar study by Maria A. Nikolinakou and Andrew J. Tallon titled *New Research in Early Gothic Flying Buttresses* investigated how design parameters such as cross section thickness, length, flyer

width, and inclination affected the trajectory of the thrust lines of flying buttresses. Unlike Nikolinakou and Tallon's study, this research focuses more on tensile and compressive stress distributions with respect to architectural geometries rather than trajectories of thrust lines. However, thrust lines are mentioned throughout the investigation.

Three different structures were selected for the finite element models of flying buttress designs which yield results identifying regions that are susceptible to tension stresses and which regions remain in compression. RAM Elements has been used to analyze the stress distributions for all of the selected structures. Furthermore, the advantage of modeling three different designs should also yield how one geometry is more effective at keeping elements in compression over other geometries.

3 Anatomy of the Flying Buttress

The flying buttress is a structural element that resists lateral loads from the high vault to the external buttresses, as demonstrated in **Figure 3.1**. The flying buttress enabled walls to be more slender and delicate in appearance, thereby allowing more light into the structure while achieving height. This was one of the most effective solutions to transmit wind loads as Gothic structures became taller and taller. The location of flying buttresses were intuitively positioned since Gothic structures were essentially structural skeletons. Wherever a structural skeleton was susceptible of bowing outward due to tension, a flying buttress was implemented to effectively alleviate loads that caused tension within the masonry structure. The structural elements labeled in **Figure 3.1** (as well as **Figure 4.8**) will be consistently used throughout the research as the flying buttress has direct and indirect relationships to its neighboring structural elements.

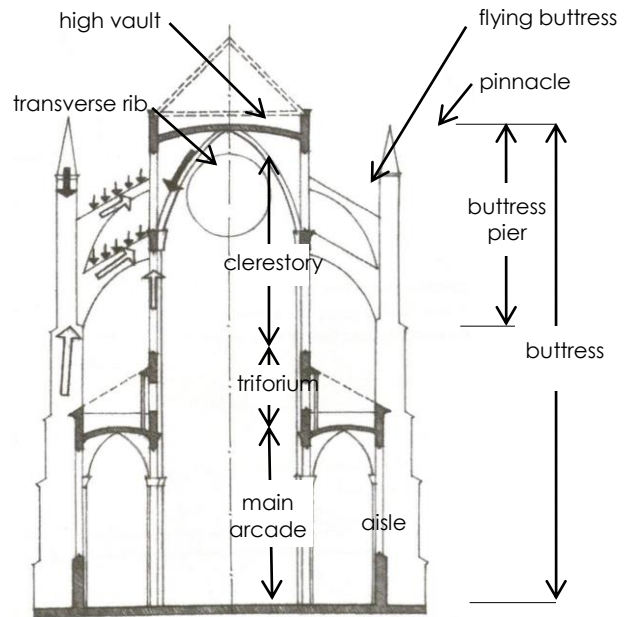


Figure 3.1 – Gothic Cathedral Cross Section

Image courtesy of Francis D. K. Chang,
A Visual Dictionary of Architecture (2nd Ed.);
John Wiley & Sons, Inc.

The earliest flying buttress (also mentioned as *flyers*) designs were simple in nature since this design was one of the first of its kind, such as the buttresses from the Notre-Dame de Paris (refer to **Figure 7.4**) Upon careful observation and experience of architects and builders, other cathedrals began to experiment with other forms of flying buttress designs. Some designs, such as the Cathédrale d'Amiens (refer to **Figure 7.26**) and Cathédrale Notre-Dame de Chartres, may have emphasized aesthetics while others may have emphasized function.

4 Historic Structural Masonry

Architectural masonry or stone is categorized as a brittle material. These materials have adequate strength in compression; however, they lack strength in tension. In addition, the brittle nature of the material lacks ductility, which serves as a useful quality for structural members. For this application, such as an arch or a flying buttress, these members are an assemblage of stones arranged in a particular configuration (**refer to Figure 4.1**), rather than a monolithic, homogenous member.

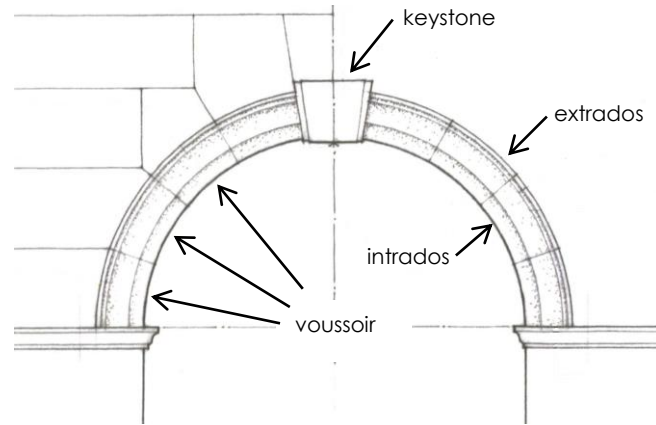


Figure 4.1 – the Arch

Image courtesy of Francis D. K. Chang, *A Visual Dictionary of Architecture* (2nd Ed.); John Wiley & Sons, Inc.

4.1 masonry properties and assumptions

The Stone Skeleton (1995) by Jacques Heyman discusses several assumptions upon analyzing masonry structures. Several structural assumptions are to be made with regards to structural masonry arches or flying buttresses. With regards to each masonry unit, is it assumed that friction is sufficient enough that the units are effectively interlocked to where one cannot slide on one another. However, it is possible that one can find sufficient evidence of slipping in certain parts of the masonry structure. For this investigation, the structure is assumed not to experience any evidence of slipping for two primary reasons. Thorough site investigation has not been made to assess the condition of the flying buttresses for the cathedrals selected in this research. In addition, substantial slipping of the masonry units that may jeopardize the stability of the structure is most likely to have been repaired by now after centuries of existence. The second assumption is masonry has limited tensile strength, but it is the mortar joints that are the most vulnerable to tensile stresses. Therefore, the second assumption implies that only compressive stresses can be transmitted between masonry units. The third assumption is masonry has *infinite* compressive strength capacity. This is a reasonable assumption with respect to average compressive stresses in masonry because the average stresses are low compared to the allowable compressive strength. In theory, the approximate maximum height of a masonry structure crushing from self-weight can reach as high as two kilometers or 1.24 miles (assuming stability is not an issue).

4.2 mechanics of the masonry arch

With these basic structural assumptions in consideration, commencing with a fundamental shape (the arch) that influenced other complex forms of structural masonry design will help better understand the behavior of the flying buttress. *The Stone Skeleton* (1995) by Jacques Heyman illustrates a comprehensive example of the voussoir arch (refer to **Figure 4.1**). The arch is composed of identical wedge-shaped masonry units arranged in a semi-circular arch. Normally, timber form-work is used to maintain the geometric form, as well as propping up the units in place until an arch is completed (refer to **Figure 4.2**). As the form work support is gradually removed, the abutments will slightly give way due to the thrust action caused by self-weight alone. Two possible fates of the masonry arch exist. The arch can collapse due to the movement of the abutments. Or, as the abutments give way, this will slightly change the geometry of the arch which causes forces to find new paths to travel through each masonry unit. As a new load path is established, the system is able to accommodate the change without compromising the stability of the structure.

From the previous structural assumptions, the voussoirs cannot slip and the units cannot deform themselves. Therefore, tensile cracks will inevitably occur as a result of the abutments shift. Depending on the nature of the cracks, these cracks can be idealized as hinges. A hinge is idealized when a crack is severe enough to where it limits the thrust lines to travel throughout the arch. In other words, a severe crack increases the chance of locating where the thrust lines travel throughout the masonry arch since the reduced bearing interface on both sides of the crack is the only area remaining in compression

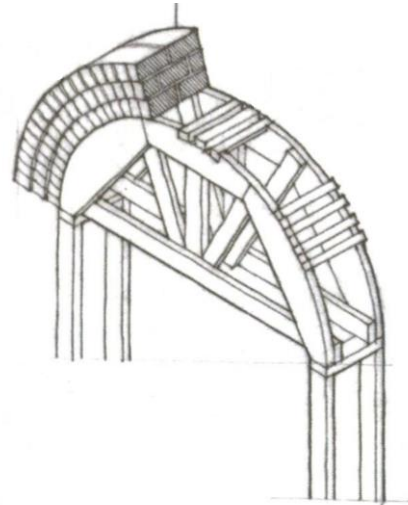


Figure 4.2 – Masonry Arch and Wooden Formwork

Image courtesy of Francis D. K. Chang, *A Visual Dictionary of Architecture* (2nd Ed.); John Wiley & Sons, Inc.

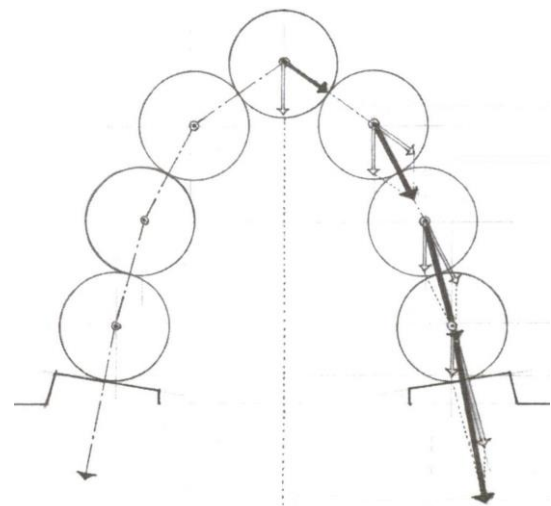


Figure 4.3 – Inverted Catenary Curve

Image courtesy of Francis D. K. Chang, *A Visual Dictionary of Architecture* (2nd Ed.); John Wiley & Sons, Inc.

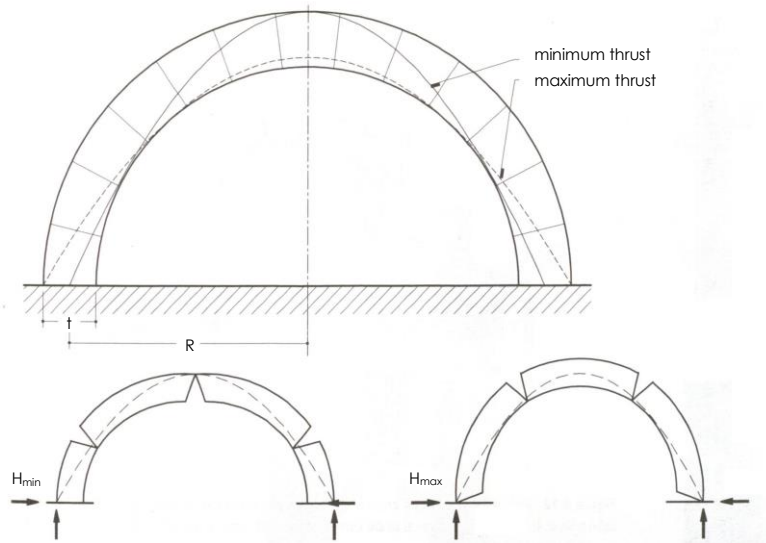


Figure 4.4 – Active and Passive Lines of Thrust

Image courtesy of E. Allen, W. Zalewski and Boston Structures Group, *Form and Forces – Designing Efficient, Expressive Structures*; John Wiley & Sons, Inc.

4.2.1 lines of thrust

It was not until the 17th century when a British scientist, Robert Hooke, discovered a mathematical expression for structural arches. His discovery is summarized with an elegant phrase: “as hangs the flexible line, so but inverted will stand the rigid arch.” His observation can be seen as a hanging chain, which forms a catenary curve experiencing completely in tension under its own weight as shown in **Figure 4.3**. When

inverted, this arch stands completely in tension when rigid (Allen & Zalewski, 2010). Since masonry is strong under compression, an inverted catenary curve can be approximated for a particular masonry arch to verify if the compression line (line of thrust) remains within the masonry arch. The line of thrust is a way to understand which regions of the member safely remain in compression or which regions are vulnerable in tension as shown in **Figure 4.4**. This figure illustrates the development of tensile stresses on the opposite side of the thrust line touching the arch profile. It may be intuitive how and why the thrust lines are drawn in a particular member, especially if the hinges are located along the arch.

The line of thrust within the same masonry arch can be determined several ways. The design of the arch determines the possible minimum and maximum horizontal force. In reality, movement occurs and the masonry arch accommodates to such movements by creating hinges. Upon the formation of such hinges, this statically determines where the line of thrust passes through since it limits where the compression forces can transmit from the structure to the foundation. There are two primary types of lines of thrust: *active* and *passive*.

4.2.1.1 active line of thrust

An active line of thrust signifies a small inward movement along the arch supports as shown on the bottom right of **Figure 4.4**. In other words, an active line of thrust depicts the largest allowable horizontal force that the arch can withstand (Allen & Zalewski, 2010). This line of thrust is present when an external force is applied to the masonry arch. The flying buttresses is not meant to operate in its passive state. It was designed to withstand constant outward thrust from the nave vault with an approximate value of 20 tonnes per bay for certain cathedrals (Heyman, 1995).

4.2.1.2 passive line of thrust

A passive line of thrust signifies a small outward movement along the arch supports, as a function with regards to the masonry units' weight and shape along the arch as depicted on the bottom left of **Figure 4.4** (Allen & Zalewski, 2010).

4.3 gothic architectural elements

Many ecclesiastical structures prior to the Gothic architectural influence were influenced the Romanesque style, which typically had an elevation height of no more than two to three stories. Another important feature of Romanesque buildings is the massive, thick walls. It was not until the second half of the twelfth century where masons from Ile-de-France (region in France) vigorously pursued development of wall design. This so-called early Gothic period saw an increasing emphasis on height (Mark, 1993). Several key architectural elements allow the Gothic movement feasible since the Gothic movement placed an emphasis of light and the pursuit of the heavens.

4.3.1 the gothic arch

The concept of the pointed arch was a refined and modified design since the pointed arch (**Figure 4.6**) allows the gravity loads to transfer downwards more effectively than a semi-circular arch. The configuration of the semi-circular arch (**Figure 4.5**) is relatively difficult for loads to travel in the vertical direction; hence this design favors loads to be transmitted more along the horizontal direction. Therefore, the horizontal thrust at the ends of the semi-circular arch tends to be problematic at some instances than the Gothic pointed arch.

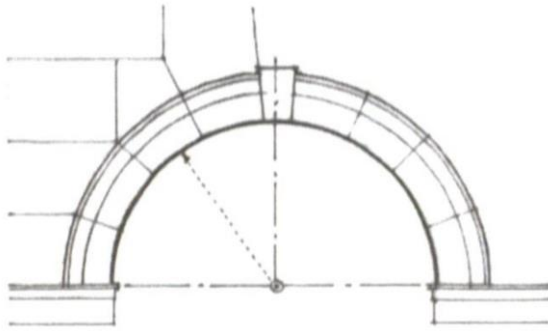


Figure 4.5 – the Roman Arch

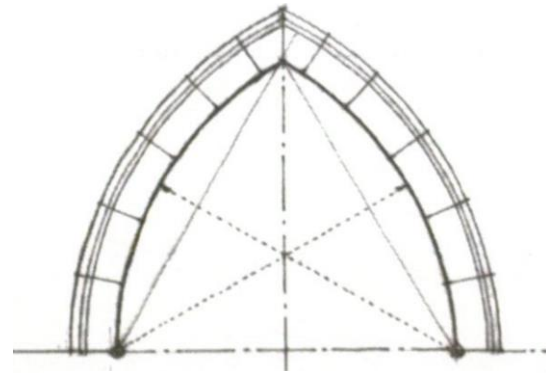


Figure 4.6 – the Gothic Arch

Images courtesy of Francis D. K. Chang, *A Visual Dictionary of Architecture* (2nd Ed.); John Wiley & Sons, Inc.

After decades of observing the nature of the Gothic pointed arch, the creation of the flying buttresses began to flourish. The flying buttress is essentially a bisected pointed arch that is butted against a vertical wall. Or, one may think of the global Gothic structural expression as one massive Gothic pointed arch. Manipulating the Gothic arch and modifying gradients to effectively transmit lateral and gravity loads of tall, delicate structures was the key to make the Gothic movement possible.

4.3.2 the pinnacle

The purpose of the pinnacle may seem unclear whether or if, not both, these structural elements are considered to be purely for aesthetics or considered to play a substantial role in the flying buttress system. Conservatively, the weight of the pinnacle can be estimated to be around one-hundredth of the total weight of the pier. For this reason, the pinnacle does not contribute to the overall stability of the flying buttress system, but it is localized at the head of the pier (Heyman, 1995).

In fact, the pinnacle does play a considerable role in stabilizing the horizontal thrust and the ends (culée) of the flying buttresses. The left portion of **Figure 4.7** shows how the flying buttress system is vulnerable to tension since the thrust line nearly touches the perimeter of the cross section

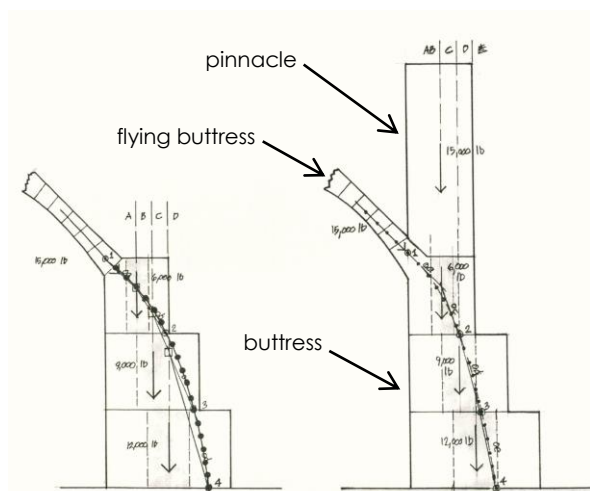


Figure 4.7 – the Pinnacle Affecting Line of Thrust

Image courtesy of E. Allen, W. Zalewski and Boston Structures Group, *Form and Forces – Designing Efficient, Expressive Structures*; John Wiley & Sons, Inc.

profile. However, the weight of the pinnacle helps direct the thrust line closer to the interior section of the external buttress, as indicated on the right portion of the **Figure 4.7**.

Without the weight of the pinnacles, the horizontal thrust may be substantial enough to cause sliding failure or overturning at the head of the (external) buttress. The weight of the pinnacles help increase the frictional capacity along the potential failure line or counteract the overturning moment caused by the thrust. The mode of failure depends on the interaction between the masonry units and the mortar joints.

4.3.3 the flying buttress

The flying buttress is one of the most essential structural and architectural characteristic of the Gothic style. This unique structural member is an evolutionary adaptation of the groined vault and the pointed (Gothic) arch. It simply acts as a linear brace to resist the thrust loads from the vault or wind loading from the roof as shown in **Figure 4.8**. The brace is composed of one or more rows of ashlar masonry all behaving in compression, which in turn are typically supported by segmented arches below (Mark, 1993). Prior to the design of the flying buttress, ordinary solid buttresses were implemented, but the outcome resulted in an uneconomical design with a heavy appearance. Modifying the solid buttress with a void that creates a shape of an arch enables the structure to reach new heights while allowing light in interior spaces (Nikolinakou & Tallon). The figure above shows two end regions of the flying buttress. The head is the upper end region and the culée is the lower end region of the flying buttress member.

4.4 historical structural masonry in Europe

Limestone was the most widely used material for load-bearing walls and piers for most historic European structures (Mark, 1993). In conjunction with the type of stone used for the construction of cathedrals, the type of mortar used centuries ago behaves considerably different than mortar used in modern construction.

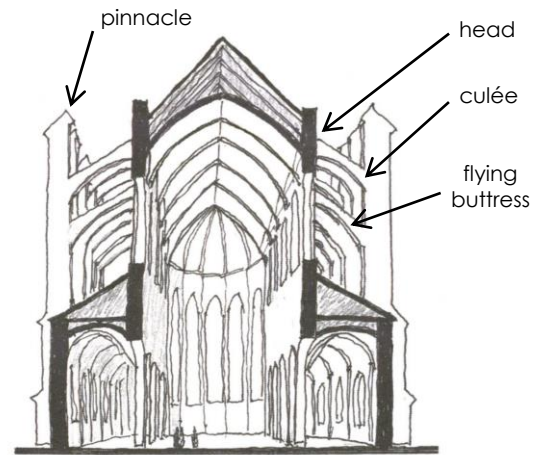


Figure 4.8 – Gothic Cross Section

Image courtesy of E. Allen, W. Zalewski and Boston Structures Group, *Form and Forces – Designing Efficient, Expressive Structures*; John Wiley & Sons, Inc.

4.4.1 stone type

The compressive strength of limestone varies with a range from a minimum value of 200 kg/cm² or 2.84 ksi to a maximum value of 2000 kg/cm² or 28.4 ksi (Mark, 1993). The tensile strength of unreinforced masonry structure usually ranges from 5 to 10 percent of the compressive strength of masonry. However, the tensile strength of grout between the masonry units is significantly lower than the tensile strength of the masonry unit. Therefore, it is imperative to understand the mechanical properties and the interaction between the masonry units and mortar.

4.4.2 mortar type

Architectural Technology – up to the Scientific Revolution (1993) by Robert Mark provides a thorough explanation with regards to mortar properties and its interaction with stone masonry units. Mortars used in historic masonry structures were generally composed of pure lime, or lime and sand mixtures. Pure lime mortars are not hydraulic which can take months or even centuries to dry. Mortar passes through two independent stages: setting and carbonation.

For the 'setting' stage, pure lime mortar is deemed to be 'set' when all excess water has evaporated either absorbed by the adjacent porous masonry units or evaporated into the atmosphere. The rate of evaporation depends on many factors such as the amount of excess water, humidity, porosity of the stone and the mass of the structure. Currently, lime mortars are described to be as 'slow-setting' in contrast with modern Portland cement, which with an accelerator sets approximately in ten hours. Lime mortar sets within days or weeks, but never to the extent of months or years at a time.

For the 'carbonation' stage, this is a much slower chemical process than the 'setting' stage. The set mortar paste, which is made from calcium hydroxide, reacts with carbon-dioxide in order form calcium-carbonate. The 'carbonation' stage is a fundamental process in developing mortar that is more durable, which depends on numerous factors such as relative humidity, temperature and atmospheric carbon-dioxide concentration. According to a scientific research titled *Forced and natural carbonation of lime-based mortars with and without additives: Mineralogical and textural changes* (2004) by Cultrone, Sebastián and Huertas, calcium-carbonate is a fundamental composition of limestone. Normally, this chemical reaction undergoes a slow process due to an insufficient amount of carbon dioxide available in the atmosphere. Unfortunately, the diffusion of carbon dioxide beyond a thin surface layer of carbonated mortar deep into the masonry joint occurs at a painfully slow rate. Although lime mortar that is only set is not very strong even in

compression, neither the strength of the mortar nor the strength of the masonry units is as important as their combined properties.

Understanding the chemical processes may provide insight to the mechanical properties of mortar, which may help architectural preservationists when applying modern materials with different mechanical properties.

4.4.3 integration between stone and mortar of ancient masonry structures

With regards to pure lime mortars taking over centuries to dry, one may ask if mortar was any useful during medieval and Gothic periods for ancient masonry structures. Mortar is essential for several reasons, even for ancient masonry structures.

An article written by Ray Tschoepe titled *The Short Course on Historic Mortar* (2016) thoroughly discusses the importance of mortar interaction between the masonry units. The slow setting mortar does have its advantages. The mortar helps lubricate the masonry units while helping the overall structural element consolidate and settle in place with the help of the slow, soft setting properties of mortar. This also helps with the leveling of masonry units as they are set in place. The curing of the mortar helps the load transfer throughout the masonry units by creating an even interface between the units. This helps mitigate any stress concentrations if a masonry unit happened to have an uneven surface. Another practical reason for the use of mortar between masonry units is to keep the interior part of the structure weatherproof. Lastly, the soft mortar should act as a cushion in order to allow expansion and contraction of the porous masonry units. The fact that some mortar takes centuries to cure luckily coincides for Gothic structures, since many of these cathedrals took centuries to complete.

The strength and deformation characteristics of masonry structure are difficult to predict in terms of quantifying the resilience of masonry units interacting with mortar. Unfortunately, even test results of discrete sample of materials do not correspond well with the same materials that are used in large quantities in buildings. Studies of masonry walls that are perpendicularly loaded with respect to the mortar bed have demonstrated that mortar can survive under conditions in which its crushing strength can be exceeded by as much as 300 percent based on a reference titled *Structural Masonry* (1971) by Sven Sahlin.

5 Method of Analysis

Structural failure of historic masonry structures is based on instability rather than the strength of the material with respect to structural form. In other words, the structure needs to remain entirely in compression with certain regions experiencing tensile stresses that do not exceed the allowable tensile stress of the mortar or masonry unit. In addition, the material stresses found in structural masonry are generally very low. Traditional design methods of masonry structures are based on rule of proportionality and geometry, which is logical for structures that experience stresses at low levels (Allen & Kalewski 2010). Scientists over the course of centuries have tried to develop explanations to understand stability of structures simply through observation of nature.

5.1 classical method

A paper conducted by Pere Roca, Miguel Cervera, Guiseppe Gariup and Luca Pela titled *Structural Analysis of Masonry Historical Constructions. Classical and Advanced Approaches* (2010) provides a brief and thorough history of classical methods applied to masonry arches up until the 19th century. The history begins with Robert Hooke, a British scientist who discovered a mathematical expression for structural arches. Meanwhile, another British scientist, David Gregory, independently derived the equation of the catenary curve. In fact, he extended Hooke's

discovery that arches are stable when the catenary curve remains within the arch with variable thickness as demonstrated in **Figure 5.1**.

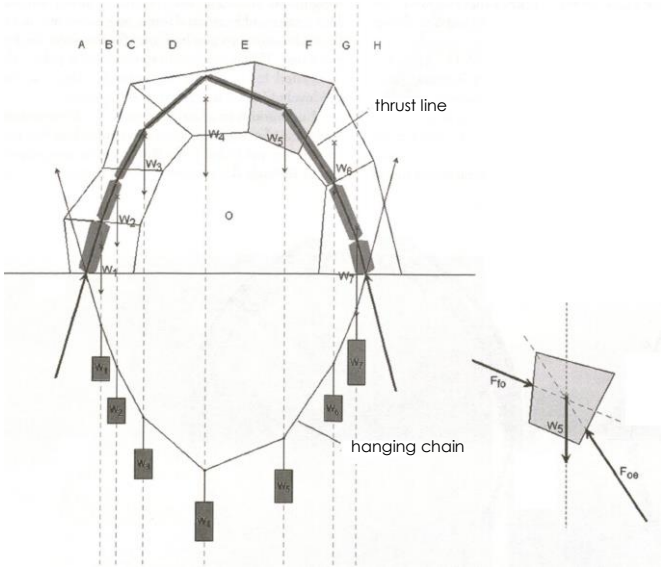


Figure 5.1 - Illustrated Example of the Classical Method

Image courtesy of E. Allen, W. Zalewski and Boston Structures Group, *Form and Forces – Designing Efficient, Expressive Structures*; John Wiley & Sons, Inc.

During the 18th century, French researchers La Hire, Couplet and Coulomb investigated the stability of arches from a different point of view. Couplet observed that collapse of arches is due to the development of hinges. Coulomb published a theory with regards to the stability of arches. He presents his theory that correlates possible modes of failure through mathematical expressions. Coulomb mentions that failure due to sliding is a rare phenomenon and advised to consider failure from overturning. In

addition, he mentions a theory of *maxima and minima* (optimization method) in order to determine where unfavorable hinges occur within the masonry arch.

All of these past discoveries were further developed in the 19th century in graphic form: the thrust line theory as demonstrated in **Figure 4.4** and **Figure 5.1**.

Figure 5.1 is a demonstration of a custom catenary curve for the illustrated masonry arch. The weight of each masonry unit is positioned according to its respective center of mass. A fictitious vertical line is created that passes through each center of mass and the catenary curve below. This will create points of intersection along the catenary curve below the arch. Then, the weight of each masonry unit is suspended along the points of intersection, which will result in a *weighted* catenary curve. This *weighted* catenary curve is inverted in order to verify if it remains within the profile of the masonry arch.

5.2 linear elastic analysis

Using linear elastic analysis to determine the ultimate response of masonry structure is not ideal. Such analysis to assess the strength capacity and structural safety of masonry structures, especially arches and vaults, may result in a very conservative or unrealistic approach. However, linear elastic analysis has been always used prior to more sophisticated approaches with regards to preliminary assessments of structural models (Roca, Cervera, Gariup & Pela, 2010). Defining meshes, loads and reactions are some of many preliminary information needed before continuing with more detailed models with more sophisticated parameters.

Since this investigation was conducted with basic parameters with simplified assumptions, linear elastic analysis was applied when determining preliminary stress distributions of flying buttresses with regards to geometry.

5.3 linear elastic finite element analysis

Formulating a mechanical and mathematical expression of some Gothic flying buttresses is a cumbersome approach, and frankly impossible, for analysis due to its complex architectural design. In fact, the Finite Elements Method (FEM) is currently the best approach that yields satisfactory results for historic structures (Barrallo & Sanchez-Beitia). **Figure 5.2** is one of many results generated by a Finite Element Analysis software (RAM Elements). This image depicts a meshed cross section of the Notre-Dame de Paris that shows both the original profile and its exaggerated deformed shape. Model renderings of principal major and minor stress of all the cathedrals analyzed in this research can be found in **Appendix C**.

Graphical line of thrust methods are much more intuitive to understand and implement. Unfortunately, this approach is limited if the geometry of Gothic flying buttresses become elaborate.

Finite element analysis (RAM Elements) was used due to the design nature of Gothic flying buttresses and to implement a uniform procedure to produce a solution that was cohesive and consistent for all selected designs. Only lines and nodes that make up the structural profile were displayed when the traced cross sectional profile was imported from AutoCad to RAM Elements. RAM Elements conveniently tabulated all nodes in their respective x, y and z coordinates. Shells were created by carefully segmenting the cross section profile into four-sided polygons. Interior lines (also recognized as *members*) and nodes were created in order to effectively create the four-sided polygons within the profile section. This software only recognized at least four nodes of reference when creating a shell. Therefore, members that were automatically generated from the imported cross section profile and newly generated members used to construct shells are deleted. Once all the shells were created, RAM Elements allowed the user to determine the mechanical

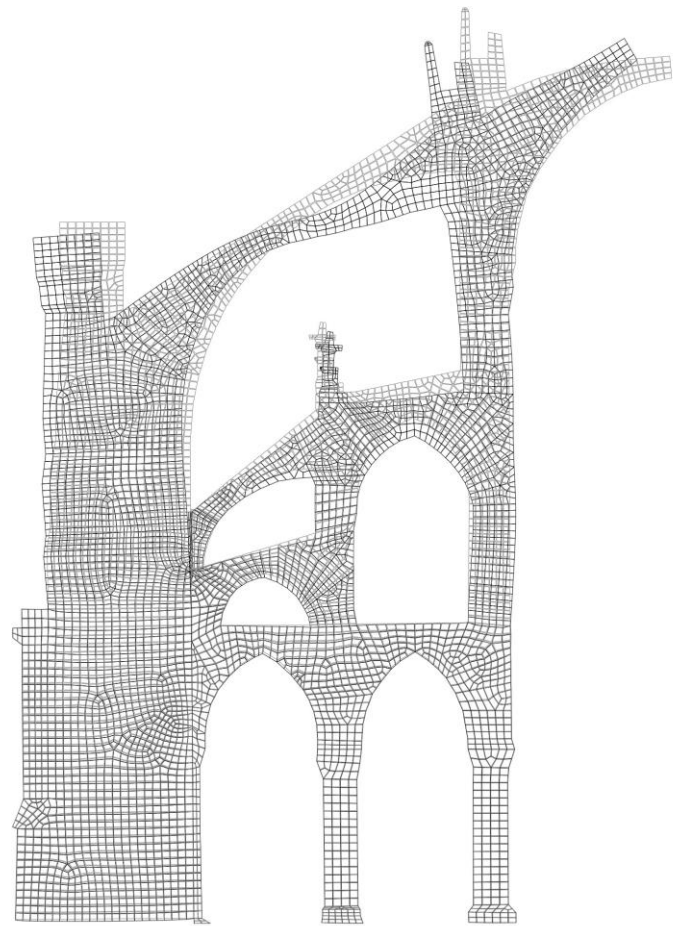


Figure 5.2 – Deflection of Cross Section of Finite Element Model

properties, thickness and loading conditions of the shells and determining the degrees of freedom of all the nodes existing in the model. As for the loading condition for the shells, RAM Elements only allowed a distributed load (ton/m or klf) to act on the sides of shells, not a concentrated load.

6 Analysis Plan and Procedure

RAM Elements was the only FEM software used to analyze the stress distributions of the selected cross sections. For all of the flying buttresses, the cross sections of the three cathedrals were scanned and uploaded to AutoCAD. The cross section images were realistically proportioned based on the scale provided on each image (the cross sections were scaled and modeled in metric units). Once scaled accurately, the cross section profile was traced over the image. Then, the traced cross sections were imported to RAM Elements and modified to ameliorate the computing process without substantially deterring too much from the original detailed geometries of the flying buttresses.

The profile is traced solely based on what the details of the drawings provide. The cross section drawings do not provide sufficient detail with respect to the foundation system. There is sufficient mass extending to the bottom of the soil for the external buttresses, but there are no foundation details provided below the base of the columns. Hence, the bottom portion of the traced profiles only show a partial *foundation system* for the external buttresses while the column bases are shown resting on grade with no particular foundation system (refer to **Figure 7.3**, **Figure 7.10** and **Figure 7.25**)

6.1 first trial

The first version of all of the models were traced over in great detail. The reason for such attention to detail was to satisfy the objective of the thesis: observing how the architectural geometries affect the stress distribution of the flying buttresses. However, this posed some problems when creating shells with numerous points in the model. The entire cross section (left and right sides of the main arcade) was modeled for all cathedrals.

6.2 second trial

In order to mitigate the computer models from crashing, some changes have been made in order to simplify the analysis as depicted in **Figure 6.1** and **Figure 6.2**. Fortunately, the cross sections of the Notre-Dame de Paris, the Cathédrale Saint-Étienne and Cathédrale d'Amiens were all symmetrical. Therefore, half of the cross section from the line of symmetry was omitted.

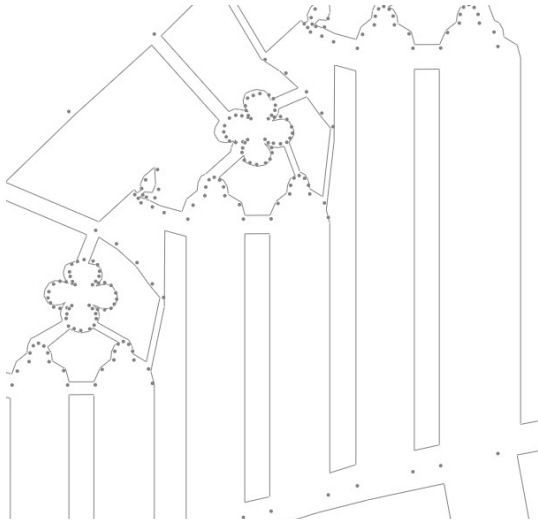


Figure 6.1 – First Trial Model Construction

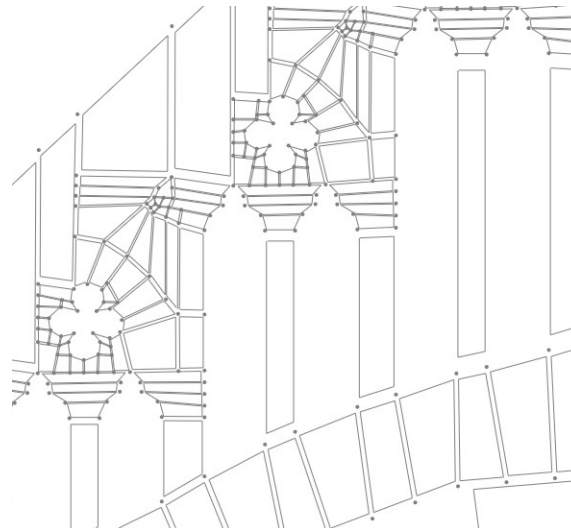


Figure 6.2 – Second Trial Model Construction

All the points were modeled along the perimeter of the structure to create a detailed profile of the cross section. The points were originally marked between each brick and mortar joint to obtain a very accurate profile of each cathedral based on cross section images in **Figure 7.3**, **Figure 7.10** and **Figure 7.25**. From a global perspective, the distance between nodes were so incremental that it would not have made a great difference if every other node(s) was deleted, yet retaining an accurate profile of the structure (**shown in Figure 6.1**). This judgment was made in order to economize time, effort and the computing process by omitting nodes in the model without jeopardizing the authenticity of the original profile as demonstrated in **Figure 6.2**. Some cluster of points that make up the architectural embellishments were structurally insignificant. These points were modified to simple geometries. The trapezoidal-like shape between the quatrefoil design (see **Figure 8.4**) appeared as a void from the cross section drawings. However, based on the images from mappinggothic.org, these trapezoidal regions are actually solid masonry; hence, the creation of additional shells in those regions in **Figure 6.2**.

6.2.1 Cathedral d'Amiens

This trial is specifically applied to the Cathedral of Amiens due to its geometric complexity of the flying buttresses. Additional simplifications had to be made since the shells were segmented in a manner that closely represented the cross section drawings. However, some parts that were intricate in design had to be omitted in order to create shells that were adequate enough for the computer software to effectively analyze the entire structure.

In addition, the labels below both sides of the cross section of Cathédrale d'Amiens read *état actuel* (current state) on the bottom right side and *état antérieur à 1497* (previous state from 1497) on the bottom left side. Since the cross sections are symmetrical and the only design modification was the addition of the lower flyer, two models of the same cross section (*état actuel* and *état antérieur à 1497*) were investigated using the same horizontal loads. The two separate models were used to understand how this design change accommodated to effectively transmit lateral loads down to the columns and external buttress than the previous design.

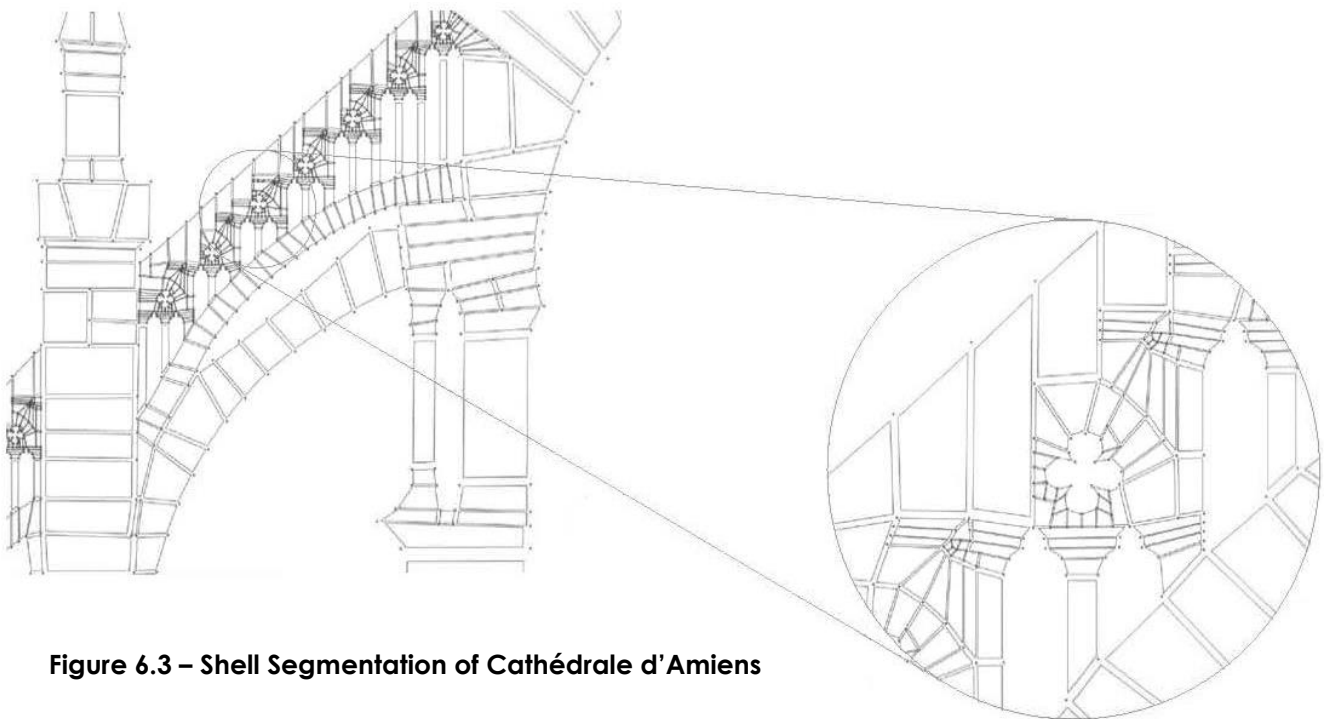


Figure 6.3 – Shell Segmentation of Cathédrale d'Amiens

The augmented, circular image in **Figure 6.3** shows some of the smaller shells created in order to respect the geometric profile of the architectural design. The large image in **Figure 6.3** shows its relationship to the smaller image as a reference. The smaller shells have a rough dimension size of 3.08 cm x 4.52 cm.

7 Analysis of Three Gothic Structures

All three Gothic structures chosen for analysis are in France. One of the structures is situated in the heart of Paris. For the other two structures in relation to the French capital, one is approximately 250 km south of Paris (Bourges) and the other is situated approximately 160 km north of Paris (Amiens). The cathedrals were chosen relatively in close proximity to one another in order to keep some design parameters fixed such as construction techniques, stone type, etc. Such subtle details may be of use for further detailed analysis.

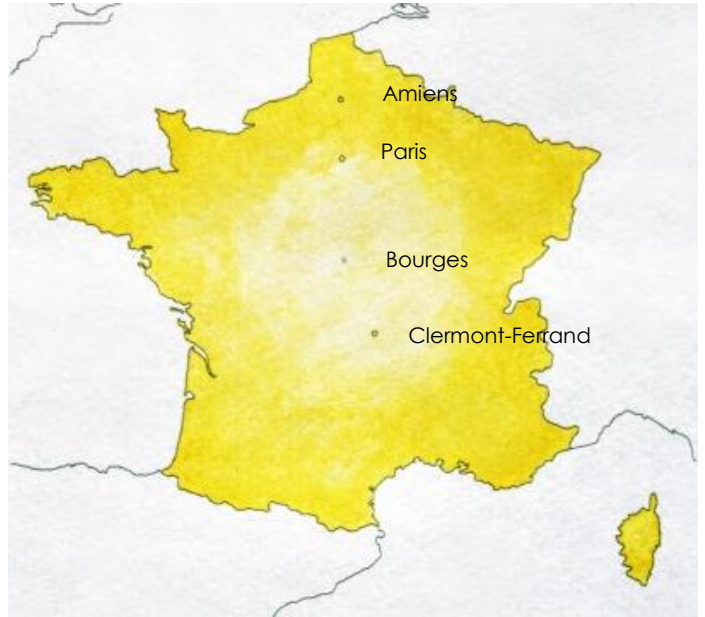


Figure 7.1 – Map of France

As mentioned before, only half of the cross section was taken into consideration due to symmetry for the two-dimensional analysis.

Before proceeding forward with the implementation of the horizontal thrust onto the flying buttress system, a horizontal reaction had to be solved at the keystone of the upper vaulted nave. The solution for the horizontal reaction at the keystone was done by idealizing it as a vertical roller (refer to images in **Appendix A**).

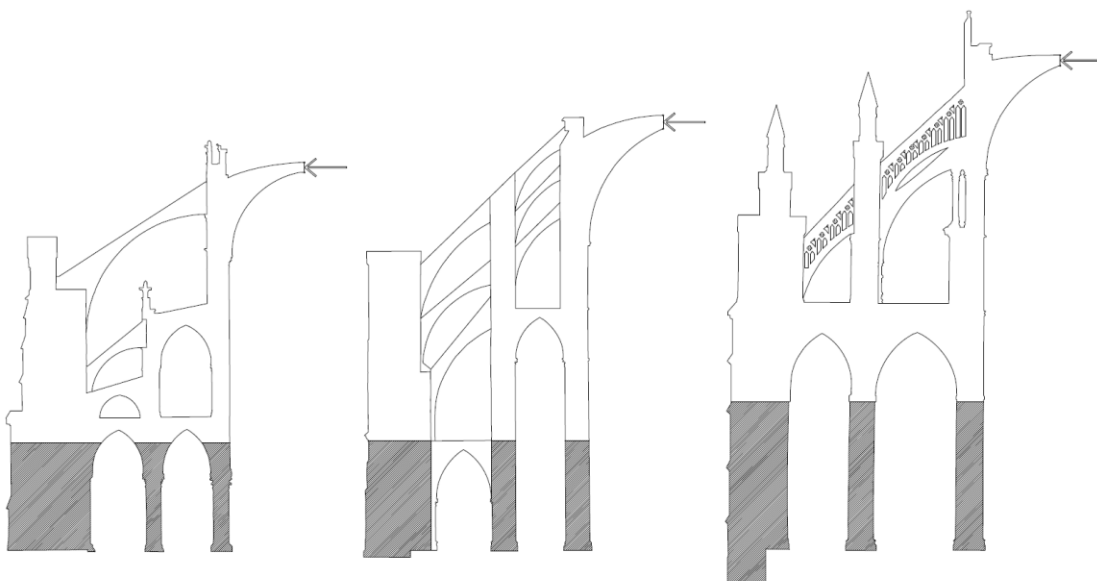


Figure 7.2 – Regions of Boundary Conditions

Once the horizontal reaction was determined, the magnitude of the horizontal thrust was considered in addition to the horizontal reaction all acting on the keystone. Due to the lack of detailed information of the roof construction for all three cathedrals, all of the lateral loads distributed throughout the flying buttress system were assumed to originate from the loads induced at the keystone of the high vault.

In terms of boundary conditions, the nodes that fall within the shaded region of the arcades (*first storey*) are assumed to be fixed, as shown in **Figure 7.2**. This is under the assumption that this region does not experience any sort of differential settlement, lateral displacement and rotation. All nodes above the first storey arcade, or regions that are unshaded, are free to translate along the horizontal and vertical direction and free to rotate along the y-axis (out-of-plane axis). However, only nodes that form the keystone is only allowed to translate vertically and horizontally without any rotation. The restriction of rotation at that region is to allow an even interface of load transfer between the shells at the nave in order to effectively disperse stresses throughout the flying buttress system.

The arrow in **Figure 7.2** indicates a 20 tonne (44 kip) load applied at each cathedral for visual purposes. However, RAM Elements only recognize superimposed shell loads as distributed loads. Therefore, the side dimension of the shell was taken where the load was applied in order to determine the loads in tonnes per linear meter (or kips per linear foot).

7.1 Cathédrale Notre-Dame de Paris

The Notre-Dame de Paris was constructed in the fourth arrondissement (district) of the French capital. This structure is considered to be one of the finest and one of the original examples of French Gothic Architecture (mappinggothic.org). This cathedral houses some of the most important relics in all of Christendom such as the fragment of the Cross of Christ and the Crown of Thorns (notredamedeparis.fr). According to **Figure 7.3**, the length and width of the Notre-Dame de Paris was constructed approximately 130 meters (426 ft) by 50 meters (164 ft) with an approximate ceiling height of 33 meters (108 ft) measuring from the floor to the upper nave.

7.1.1 structural history and description

The Notre-Dame de Paris was one of the early structures to implement the flying buttress. The cathedral began construction around 1155 A.D. with ambitions of being the tallest structure in all of France. The keystone has a height of 33 meters (108 ft) and a steeper timber roof structure than most buildings at the time, which became problematic with wind pressures at such high altitude (Mark, 1993). The height of the structure coupled with the design needed an effective solution to transmit lateral loads down to the foundation system.

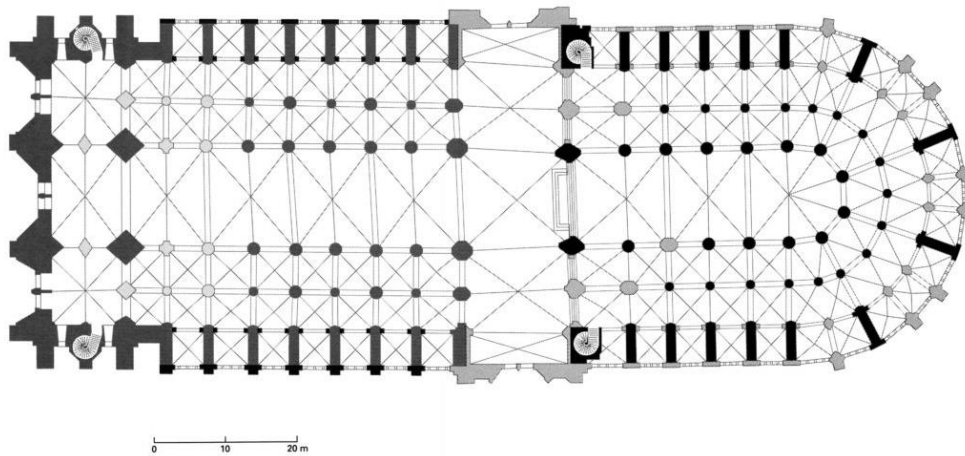


Figure 7.3 – Plan View of Notre-Dame de Paris

Image courtesy of mappinggothic.org, Media Center for Art History, Department of Art History and Archaeology, Trustees of Columbia University

Based on archeological findings from drawings and early photographs, the lateral thrust from the weight of the nave vaults were primarily resisted by the masonry arches that also supported the roof above the gallery (Clark & Mark, 1984). Earlier structures were sufficiently braced against wind loads by the adjacent substructure adjacent to the vault. Unfortunately, masons could not mimic this practice for such a tall clerestory in order to brace for such wind loading. Archeologist hypothesize that the cracking during construction or bowing of the clerestory and walls lead to the implementation of the flying buttress system to increase the structural resistance to wind loads.

Appendix B, p.68 shows an identical plan view of Notre-Dame de Paris with shaded regions that correspond to the location of the flying buttresses shown on **Figure 7.4**.

7.1.2 load path

The flying buttress continuously experiences thrust loads from wind and the pure self-weight of the masonry ribbed vault. The thrust transferred by wind depends on how the roof structure is attached to the masonry structure. According to **Figure 7.4**, the thrust transmitted by the self-weight of the ribbed vaults of the upper nave appears to coincide with the positioning of the flying buttress. Visually, the timber roof frame appears to be somewhat in line with the angle of the outermost flying buttress in hopes to effectively transfer the lateral loads to the exterior pier (refer to **Appendix B**, p.69). The ends of the flying buttresses are designed with a fairly high thickness measured normal to the intrados of the flying buttress. The head of flying buttress is approximately measured to be 2.77 meters (8.85 ft). The considerable thickness towards the ends of the flying buttresses allows more possibilities for the lines of thrust to adequately travel through the Gothic member. The same figure can be found in **Appendix B**, p.69 with span length, head thickness and culée thickness for both flying buttresses in detail. The construction of the upper triforium and minor buttressing seems to be in place in order to further effectively transmit lateral loads and mitigate any tensile stresses experienced by the main interior column for stability reasons.

7.1.3 finite element analysis

The profile of the cross section of the Notre-Dame de Paris was relatively not an elaborate design compared to the cathedrals in Bourges and Amiens. The design of the flying buttresses did not



Figure 7.4 – Cross Section of Notre-Dame de Paris

Image courtesy of mappinggothic.org, Media Center for Art History, Department of Art History and Archaeology, Trustees of Columbia University

have any interior openings or profiles that deviated from a clean arc shape. In summary, RAM element was able to quickly compute the stresses throughout the cross section based on the following parameters and boundary conditions of the model.

7.1.3.1 input

In addition to the design parameters made mentioned in the beginning of **section 7**, the material type selected was limestone. The information provided in **Table 7.1** only refers to the mechanical properties of the masonry units alone (references found in **Appendix A**).

properties	imperial units	metric units
poisson's ratio, ν	0.25	0.25
unit weight, γ	0.0868 lb/in ³	0.002403 kg/cm ³
coefficient of thermal expansion, α	4.45x10 ⁻⁶ 1/F	8.01x10 ⁻⁶ 1/C
modulus of elasticity, E	3.92x10 ⁶ psi	2.75x10 ⁵ kg/cm ²

Table 7.1 – Mechanical Properties of Limestone

Furthermore, the maximum distance allowed between nodes was set to 30 cm (11.8 in.) and the merge node tolerance was set at 0.254 cm (0.1 in.) when solving the finite element analysis model in a two-dimensional shell (XY) setting.

20 tonne (44 k) horizontal thrust load was applied at the keystone of the upper vaulted nave. **Appendix A** explains in detail determining the value of the horizontal thrust load for the cathedrals.

The thickness of the shells unique to the Notre-Dame de Paris varies for the external piers, flying buttresses, interior columns and the nave. The thickness of the mentioned structural elements were determined from **Figure 7.3** by using the scale provided below the plan drawing. The external pier has a thickness of 160 cm (63 in.), the flying buttresses with a thickness of 90 cm (35 in.), the center column with a thickness of 175 cm (69 in.), the most interior column with a thickness of 160 cm (63 in.), and the nave with a thickness of 90 cm (35 in.). Refer to **Appendix C**, p. 82 that shows the varying thickness of the profile.

7.1.3.2 output

The output explains which regions experience stresses in tension and compression for each flying buttress. The flying buttress members are labeled and indicated on **Figure 7.5**. An explanation is provided as to why these areas are developing certain tensile stress regions based on design model parameters and loading conditions. Load transfer and effects of adjacent structural members are mentioned since they directly affect the behavior of the flying buttresses. For the following section, the finite element renderings will correspond to a similar schematic like **Figure 7.5**. The only difference is the finite element rendering of a particular flying buttress will correspond to the member highlighted in yellow in the adjacent figure (**Figure 7.6** and **Figure 7.8**).

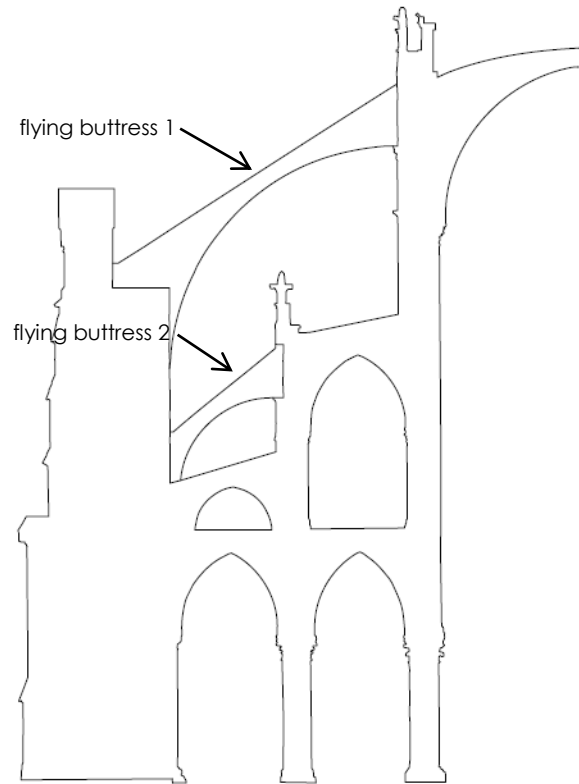


Figure 7.5 – Schematic of Analysis of Notre-Dame de Paris

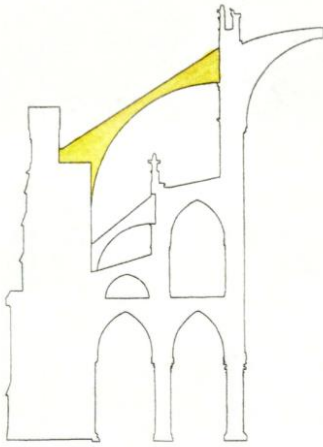


Figure 7.6 – Schematic Reference

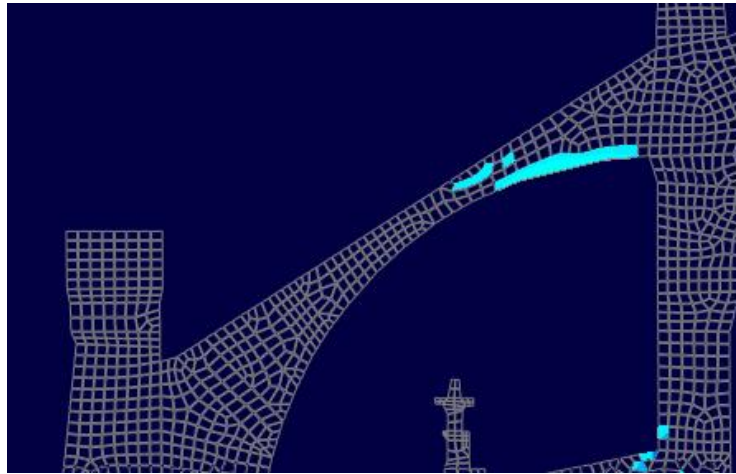


Figure 7.7 – Flying Buttress 1 of Notre-Dame de Paris

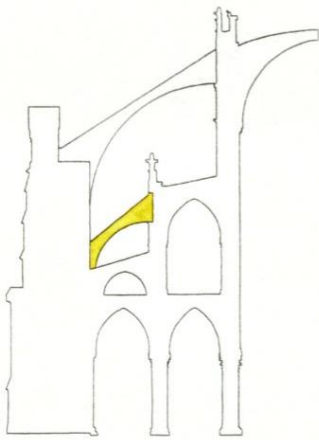


Figure 7.8 – Schematic Reference

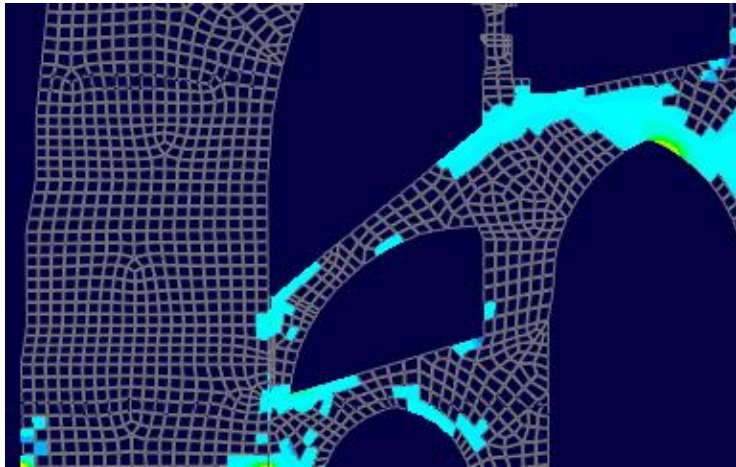


Figure 7.9 – Flying Buttress 2 of Notre-Dame de Paris

7.1.3.2.1 areas vulnerable in tension

Tensile stress are indicated in light blue in **Figure 7.7** and **Figure 7.9** with the maximum principal stress range from 4.031×10^{-4} ton/cm² (5.733×10^{-3} ksi) to 4.281×10^{-3} ton/cm² (6.089×10^{-2} ksi). These figures are zoomed closely to their respected flying buttress elements indicated by the schematics on their left shaded in yellow (**Figure 7.6** and **Figure 7.8**). **Figure 7.7** and **Figure 7.9** only show tensile stresses in order to easily identify the vulnerable regions of the masonry structure instead of displaying the entire stress ranges. **Appendix C**, p.75 – 80 shows comprehensive stress renderings from RAM Elements that contain complete stress ranges of the entire cross section profile with respect to minimum and maximum principal stresses. **Appendix C**, p.81 also provides an exaggerated deflected shape of the cross section profile, which may provide insight how certain regions experience tensile or compressive stresses.

According to **Figure 7.7**, the first flying buttress experiences tension stress past the midpoint (toward the nave) along the extrados. Another stress concentration is located close to the head of the flying buttress on the intrados of the flying buttress.

The second flying buttress, from **Figure 7.9**, experiences considerable tensile stress regions on the head and culée regions (refer to **Figure 4.8**) along the extrados of the flying buttress. Other noticeable stress regions remain on the culée and slightly past the mid-span (toward the nave) along the intrados of the Gothic member.

The two flying buttresses experience tensile stress regions near the head of the flying buttresses due to the low slope. The low slopes of the flying buttresses create a difficult path for the lines of thrust to travel effectively from the high vault to the piers and columns below. In other words, the low slope does not effectively capture or direct the thrust loads to the flying buttress. Instead, the thrust line travels to the columns. Ideally, flying buttresses with steeper slopes accommodate closely to the inverted catenary curve, which idealizes the load path (lines of thrust) for the flying buttress system.

7.1.3.2.2 areas remaining in compression

The remaining regions that are not shaded in color in **Figure 7.7** and **Figure 7.9** are regions that experience compression with values ranging from -2.182×10^{-3} ton/cm² (-2.103×10^{-2} ksi) to -2.433×10^{-4} ton/cm² (-3.461×10^{-3} ksi). As mentioned before, **Appendix C** contains complete stress renderings of the entire profile section. The colors corresponding to their respective stress ranges are indicated on the top right corner of each rendering.

Since Notre-Dame de Paris was one of the first structures to incorporate the use of flying buttresses, masons and architects were designing for a phenomenon that was unfamiliar at the time. In order to fully capture the effects of lateral thrust from the roof and the high vault, the head and the culée regions of the flying buttress have considerable thickness for effective load transfer.

By observation, the first flying buttress is the primary member for resisting majority of the lateral loads originating from the vaulted nave and the roof. In addition to being the primary structural member of lateral resistance, the span distance of the first flying buttress explains such thickness of the exterior pier in order to ensure the lateral loads are effectively transmitted down to the foundation system.

Furthermore, the schematic of the cross section illustrates that the second flying buttress (and the arch directly below) may not appear to be part of the original design since the inverted catenary curve profile does not clearly trace back to the high vault; hence, the considerable tension stress concentration appearing at the upper head region of the second flying buttress. This appears to be a sudden design modification in order to counteract the lateral thrust from the triforium and the high vault.

7.2 Cathédrale Saint-Étienne, Bourges

The date of construction of Cathédrale Saint-Étienne is unknown, but records of construction changes were dated from the early 12th century (mappinggothic.org). Two continuous flying buttresses connect the nave to the interior and exterior piers. According to **Figure 7.10**, the length and width of the Cathédrale Saint-Étienne was constructed approximately 118 meters (387 ft) by 45 meters (148 ft) based on the scale provided. The approximate ceiling height of 35.5 meters (116 ft) measuring from the floor to the upper nave (mappinggothic.org).

7.2.1 structural history and description

Masons were able to learn from their experiences from Notre-Dame de Paris and refine their design and building techniques for the Cathédrale Saint-Étienne in Bourges, France. The masons were able to build the cathedral at Bourges taller than the one in Paris near the end of the twelfth century. The flying buttresses in Bourges are lighter and steeper than the original design in Paris (Mark, 1993).

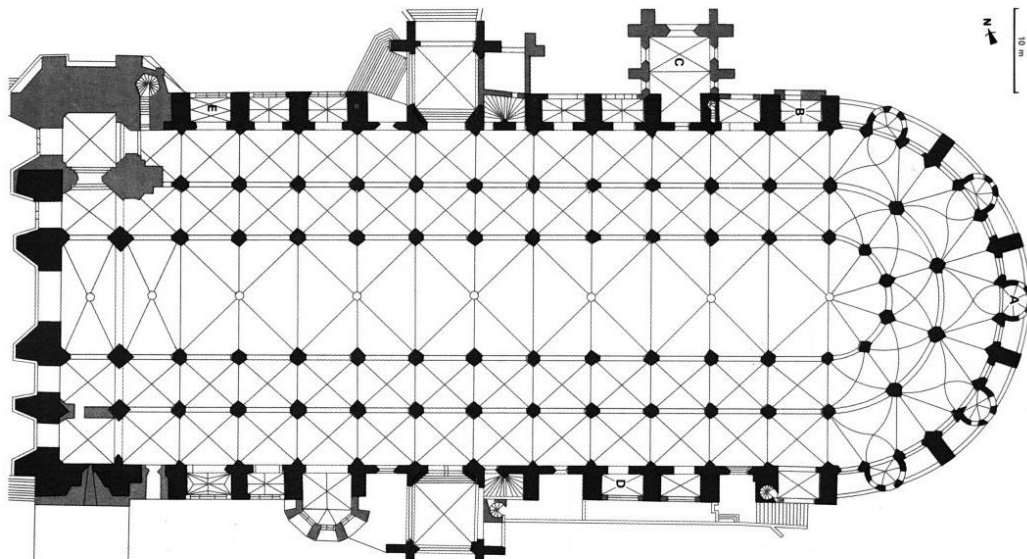


Figure 7.10 – Plan View of Cathédrale Saint-Étienne, Bourges

Image courtesy of mappinggothic.org, Media Center for Art History, Department of Art History and Archaeology, Trustees of Columbia University

Generally, the structure resembles similarly than the one in Paris except for the omission of the transepts and the floor gallery. This design change allowed more light into interior spaces. According to some investigations, the cathedral of Bourges showed less stress levels than other great Gothic cathedrals. At the same time, their efforts in improving their design and construction techniques allowed them to cut cost and quantity of masonry for this structure (Mark, 1982).

Appendix B, p.70 shows an identical plan view of Cathédrale Saint-Étienne, Bourges with shaded regions that correspond to the location of the flying buttresses shown on **Figure 7.11**.

The cross section of Cathédrale Saint-Étienne, Bourges in **Figure 7.11** does not correspond to what is shown in reality. The cross section drawing that represents the structure's current state of condition can be found in **Appendix B**, p.72. Nevertheless, the cross section shown in **Figure 7.11** was chosen since the design was relatively more complex than the *modified* or *current* design (refer to **Appendix B**) with regards to the quantity and position of the flying buttresses. The cross section in **Figure 7.11** may have been the *original* design of the flying buttress system before any changes have been made. The flying buttresses are positioned differently in the *modified* design. Moreover, the *modified* design shows two less flying buttresses than the *original* design.

7.2.2 load path

Determining the transfer of wind loads from the roof to the flying buttress system is difficult since the timber roof frame is not provided on the cross section. A similar assumption can be made with regards to wind load transfer like the Notre-Dame de Paris since the outermost flying buttress appears to align with the timber roof frame. Based on **Figure 7.11**, a total of six flying buttresses on one side of the cross section is shown. Three flying buttresses are above the upper triforium and

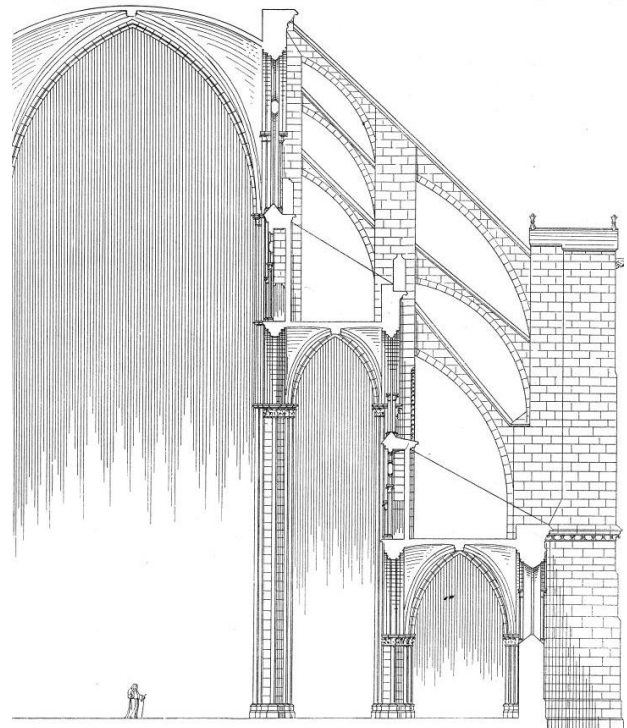


Figure 7.11 – Cross Section of Cathédrale Saint-Étienne, Bourges

Image courtesy of mappinggothic.org, Media Center for Art History, Department of Art History and Archaeology, Trustees of Columbia University

another three at the lower triforium. Only four out of the six flying buttresses make a continuous path from the upper nave to the exterior pier. The remaining two flying buttresses are placed more in the line of action of the upper nave vault and the roof structure at the upper triforium. The head thickness of the flying buttresses for the Cathédrale Saint-Étienne varies. The smallest head thickness is approximated to be 1.29 meters (3.28 ft) and the largest head thickness is approximated to be 2.7 meters (6.56 ft). The same figure can be found in **Appendix B**, p.71 with span length, head thickness and culée thickness for some flying buttress in detail. A scale can be found in this figure on the bottom right part of the schematic (each increment is equivalent to one meter).

7.2.3 finite element analysis

The profile of the cross section of the Cathédrale Saint-Étienne was also not an elaborate design in a sense that there were no interior openings within the flying buttress member or profiles that deviated from a clean arc shape. Due to the simple and elegant design of the Cathédrale Saint-Étienne, RAM Elements was able to quickly compute the stresses throughout the cross section based on the following design parameters and boundary conditions of the model.

7.2.3.1 input

Aside from using different cross sections for each of the Gothic structures, all of the boundary conditions, mechanics of materials properties, node fixities, loads, axis of orientation and assumptions remain the same for Cathédrale Saint-Étienne, Bourges as mentioned in **section 7** and **section 7.1.3.1**.

The thickness of the shells unique to the Cathédrale Saint-Étienne, Bourges varies for the external piers, flying buttresses, interior columns and the nave. According to the plan and provided scale in **Figure 7.10**, the external pier has a thickness of 180 cm (71 in.), the flying buttresses with a thickness of 90 cm (35in.), the interior columns with a thickness of 180 cm

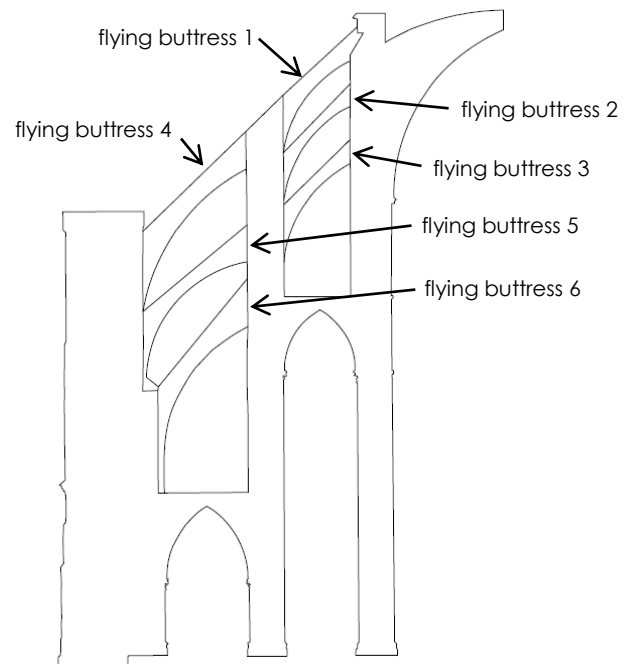


Figure 7.12 – Schematic of Analysis of Cathédrale Saint-Étienne, Bourges

(71 in.), and the nave with a thickness of 180 cm (71in.). All of the thicknesses were approximated in reference to the plan drawing.

7.2.3.2 output

The output explains which regions of the flying buttress experience stresses in tension and compression for each flying buttress. The flying buttresses are labeled and indicated in **Figure 7.12**. An explanation is provided as to why these areas are developing certain tensile and compressive stress regions based on design model parameters and loading conditions. Load transfer and effects of adjacent structural members are mentioned since they directly affect the behavior of the flying buttress. For the following section, the finite element renderings will correspond to a similar schematic like **Figure 7.12**. The only difference is the finite element rendering of a particular flying buttress will corresponded to the member highlighted in yellow in the adjacent figure. Refer to **Appendix C**, p. 90 that shows the varying thickness of the profile.

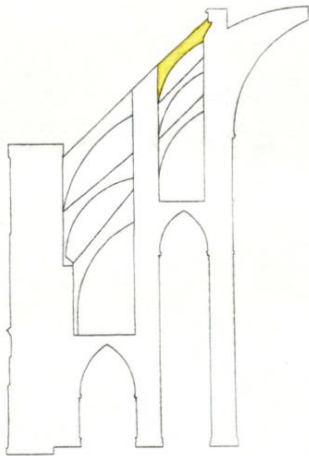


Figure 7.13 – Schematic Reference

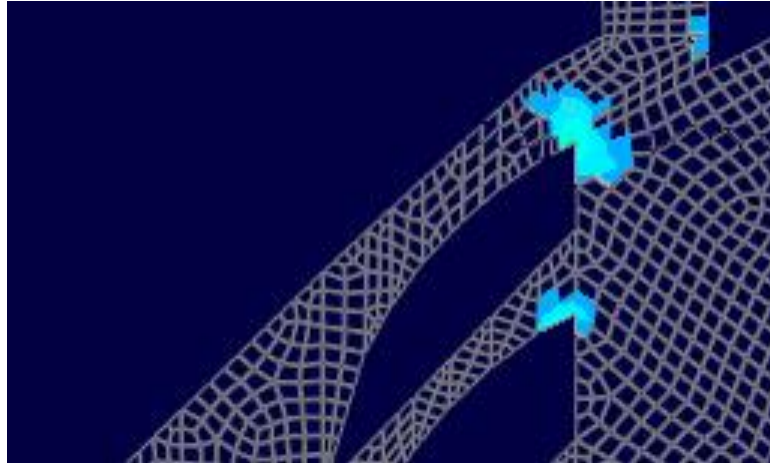


Figure 7.14 – Flying Buttress 1 of Cathédrale Saint-Étienne, Bourges



Figure 7.15 – Schematic Reference

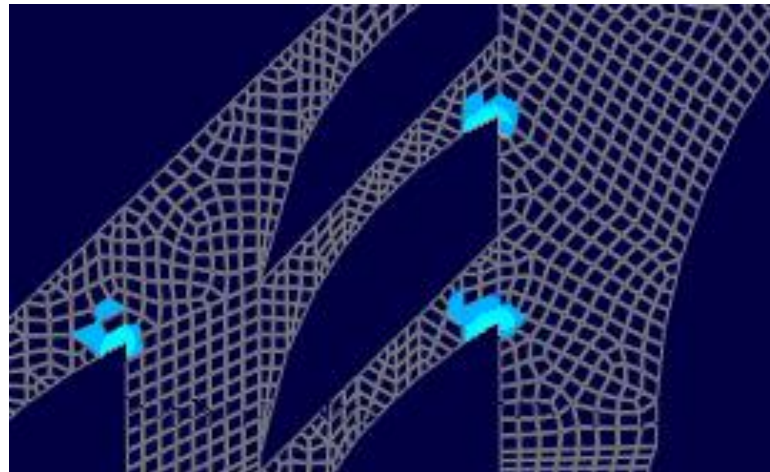


Figure 7.16 – Flying Buttress 2 of Cathédrale Saint-Étienne, Bourges

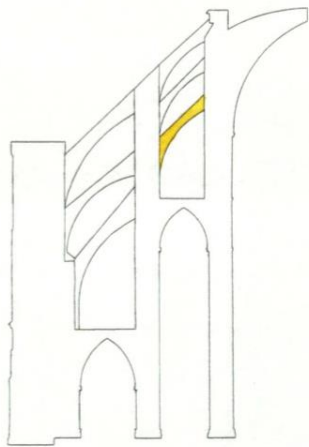


Figure 7.17 – Schematic Reference

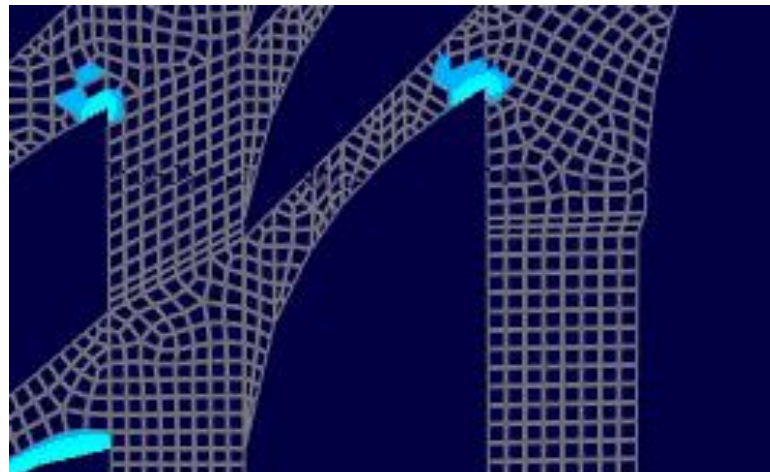


Figure 7.18 – Flying Buttress 3 of Cathédrale Saint-Étienne, Bourges

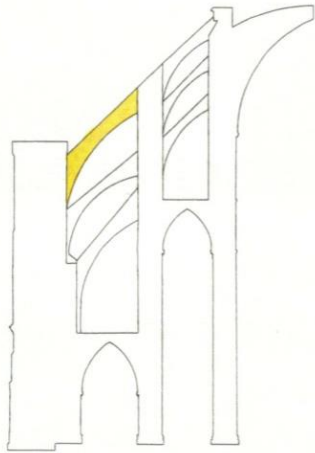


Figure 7.19 – Schematic Reference

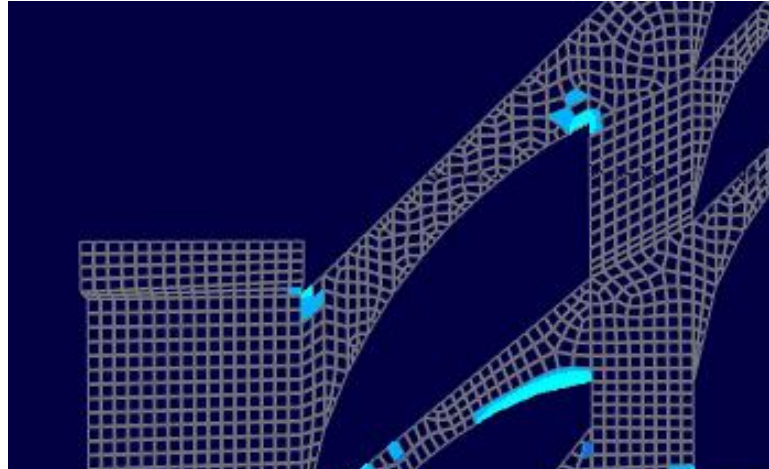


Figure 7.20 – Flying Buttress 4 of Cathédrale Saint-Étienne, Bourges

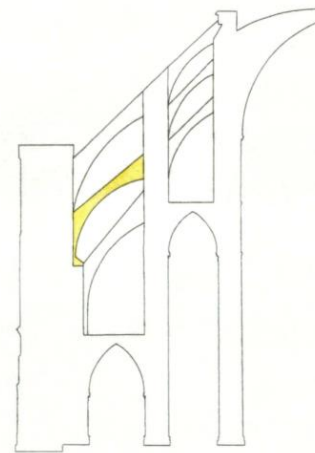


Figure 7.21 – Schematic Reference

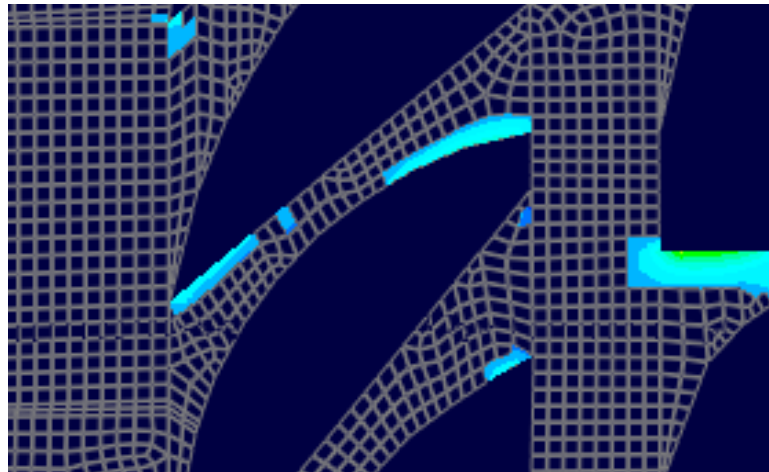


Figure 7.22 – Flying Buttress 5 of Cathédrale Saint-Étienne, Bourges

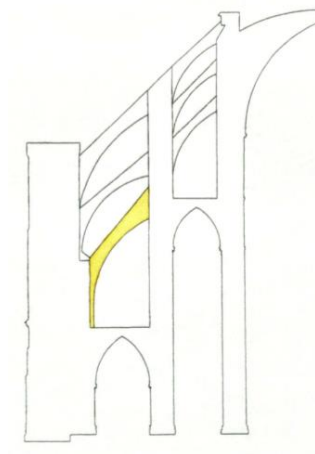


Figure 7.23 – Schematic Reference

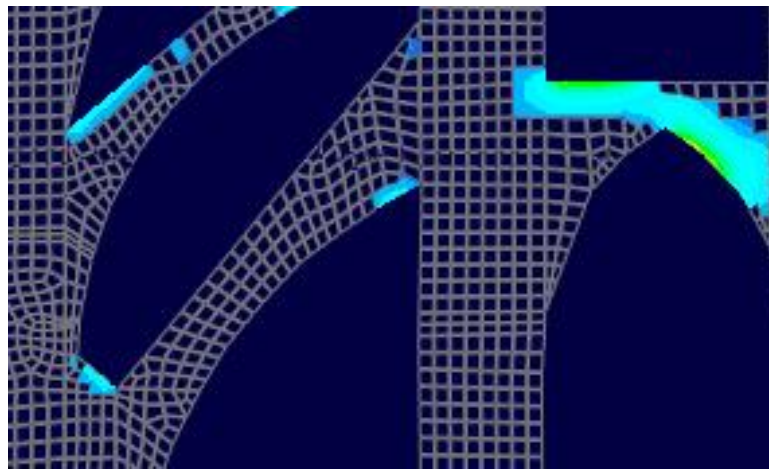


Figure 7.24 – Flying Buttress 6 of Cathédrale Saint-Étienne, Bourges

7.2.3.2.1 areas vulnerable in tension

Tensile stress are indicated in light blue in **Figure 7.14**, **Figure 7.16**, **Figure 7.18**, **Figure 7.20**, **Figure 7.22** and **Figure 7.24** with the maximum principal stress range from 1.413×10^{-3} ton/cm² (2.009×10^{-2} ksi) to 0.01 ton/cm² (0.142 ksi). These figures are zoomed closely to their respected flying buttress elements indicated by the schematics on their left shaded in yellow (**Figure 7.13**, **Figure 7.15**, **Figure 7.17**, **Figure 7.19**, **Figure 7.21** and **Figure 7.23**). As mentioned before, the figures on the right side only show tensile stresses in order to easily identify the vulnerable regions of the masonry structure instead of displaying the entire stress ranges. **Appendix C**, p.83 - 88 shows comprehensive stress renderings from RAM Elements that contain complete stress ranges of the entire cross section profile with respect to minimum and maximum principal stresses, as well as the deflected shape of the profile section.

The flying buttresses above the inner aisle appear to experience tensile stress regions on the lower head region. Only the third flying buttress shows a small pocket of tensile stress concentration on the upper culée region. In reference to **Figure 7.11**, the thickness of the culée is noticeably larger than the thickness of the head.

The flying buttresses above the outer aisle appear to experience similar tensile stress regions along the intrados of the head region. The third flying buttress experiences tensile stresses on the upper corner of the culée region whereas the fourth flying buttress experiences tensile stresses along the lower portion of the extrados. However, the sixth flying buttress does not experience any tensile stress regions along the lower region. In addition, the head depth of the outer aisle flying buttresses are substantially thicker than the inner aisle flying buttresses. Flying buttresses 4 and 5 have approximately similar slope. The sixth flying buttresses has the steepest pitch based on the given cross section.

7.2.3.2.2 areas remaining in compression

The remaining regions that are not shaded in color (**Figure 7.14**, **Figure 7.16**, **Figure 7.18**, **Figure 7.20**, **Figure 7.22** and **Figure 7.24**) are regions that experience compression with values ranging from -2.335×10^{-3} ton/cm² (-3.321×10^{-2} ksi) to -1.567×10^{-4} ton/cm² (-2.229×10^{-3} ksi). As mentioned before, **Appendix C** contains complete stress renderings of the entire profile section with colors corresponding to their respective stress ranges. Each stress range is indicated on the top right corner of each rendering.

The flying buttress system for the Cathédrale Saint-Étienne, Bourges is unique since there are three flying buttresses each occurring above the inner and outer aisles as shown in **Figure 7.11**. In addition, the placement of the flying buttresses seems to indicate that the designers began to further understand how the thrust loads from the nave and roof distribute accordingly across the flying buttress system. Masons and architects initially thought that lateral loads traveled in a linear manner, which explains why flying buttresses 1 & 4 and 3 & 5 were designed along the same *line of action*. Flying buttresses 2 and 6 remain to be incongruent with the rest of the flying buttresses.

The second flying buttress was installed as an attempt to capture the thrust loads from the upper vaulted nave by constructing several meters below the first buttress since the thrust loads would have already traveled further below at that elevation if an inverted catenary curve was projected along the structural profile of the nave.

The sixth flying buttress appears to perform the best in terms of keeping majority of the masonry units in compression. The placement and the slope appear to be appropriate to capture the thrust loads transferred from the flying buttresses above the inner aisle. The sixth flying buttress can arguably be the only Gothic structural member that respects the (weighted) inverted catenary profile, which may reflect the designers' understanding of the thrust lines originating from the triforium and the flying buttresses above the interior aisle (flying buttresses 1, 2 and 3).

7.3 Cathédrale d'Amiens

The Cathédrale d'Amiens dates back from the 13th century and it remained to be the largest in France at the time (mappinggothic.org). According to the plan and scale provided in **Figure 7.25**, the length and width of the Cathédrale d'Amiens was constructed approximately 145 meters (476 ft) by 70 meters (230 ft). The ceiling height has an approximate ceiling height of 42 meters (138 ft) measuring from the floor to the high vault (mappinggothic.org).

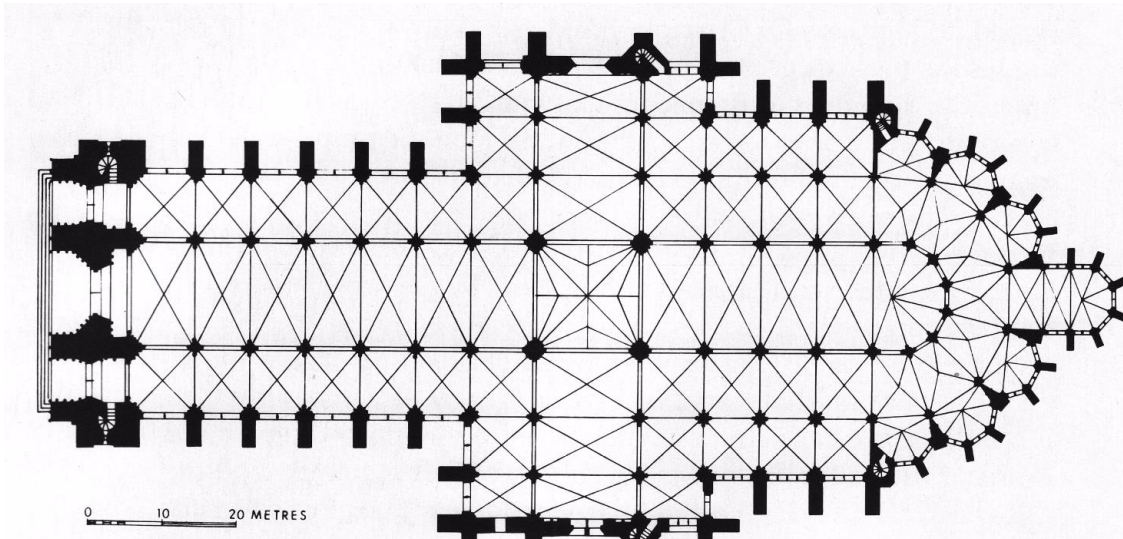


Figure 7.25 – Plan View of Cathédrale d'Amiens

Image courtesy of mappinggothic.org, Media Center for Art History, Department of Art History and Archaeology, Trustees of Columbia University

7.3.1 structural history and description

The Cathédrale d'Amiens is also considered to be one of the finest examples of High Gothic architecture. The nave stands 42 meters (138ft) high which will induce considerable amount of wind loads being transferred from the roof to the flying buttresses. The result of the delicate Gothic ribs coupled with high wind loads and the tie restrains between the walls caused wall along the nave to bend into an S shape (Mark, 1982). This observation was noted when nodal testing showed that the upper region of the leeward pier buttresses experienced tension perhaps due to strong storms. In addition, the pinnacles placed on the exterior corner of the pier buttresses helped compensate such outward thrust. The weight of the pinnacles helps the thrust line remain in compression just enough to overpower the regions susceptible to tension. The use of these pinnacles to counteract tensile stresses within the flying buttresses do not contribute much to the

overall stability of the buttresses. The mass of the pinnacles themselves cannot substantially compare with the overall weight of the buttresses. Such use of pinnacles can only conclude that the masons intuitively responded to the structural behavior of masonry during the construction process (Mark, 1993). **Appendix B**, p.73 shows an identical plan view of Cathédrale d'Amiens with shaded regions that correspond to the location of the flying buttresses shown on **Figure 7.26**.

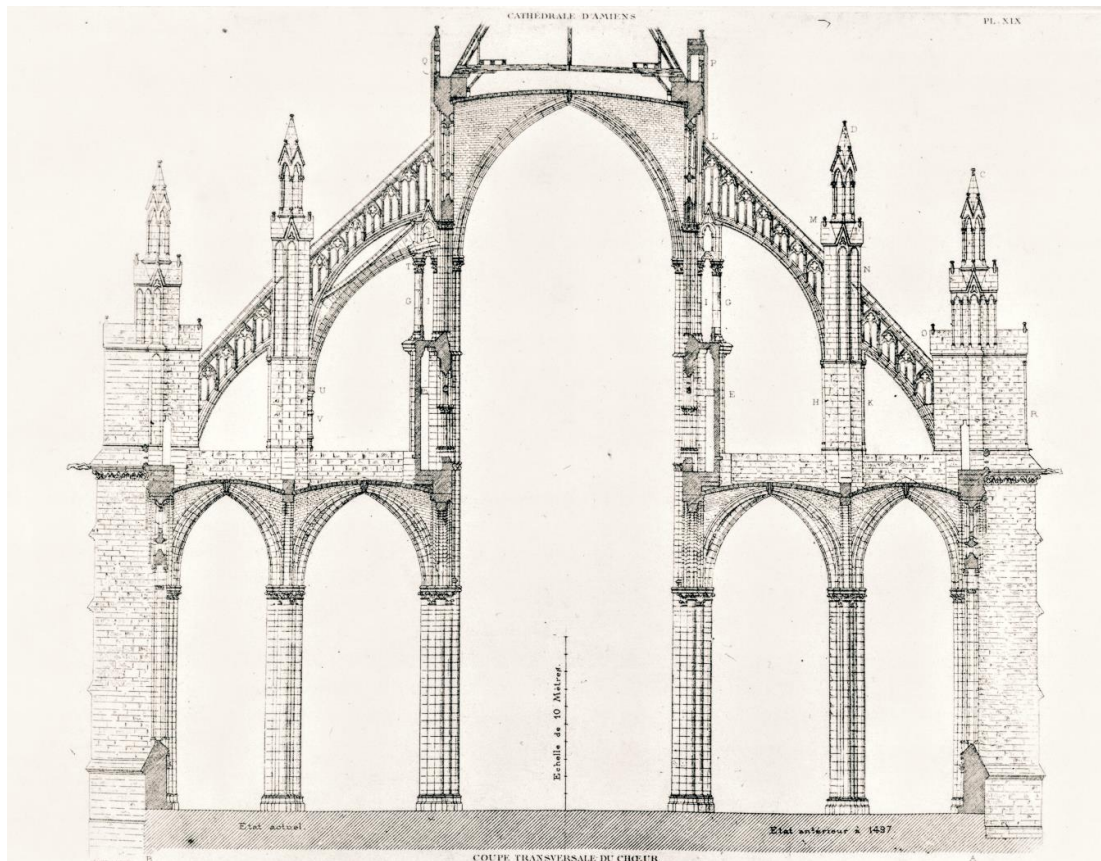


Figure 7.26 – Cross Section of Cathédrale d'Amiens

Image courtesy of mappinggothic.org, Media Center for Art History, Department of Art History and Archaeology, Trustees of Columbia University

7.3.2 load path

According to **Figure 7.26**, the elevation where the timber roof frame rests upon the masonry ledge is considerably high in relation to the location of the head of the flying buttress. There is an approximate elevation difference of 3.6 meters (11.8 ft) from the top head of the flying buttress to the elevation where the timber roof frame rests on the stone ledge. The difference in elevation between the two points of interest may be difficult for the lateral loads from the roof structure travel effectively down to the flying buttress system. The same figure can be found in **Appendix B**,

p.74 with span length, head thickness and culée thickness for all of the flying buttresses in detail. A scale can be found in this figure on the bottom center part of the schematic (each increment is equivalent to one meter).

In addition, there is a great amount of uncertainty whether the timber roof frame is accurately shown on the cross section drawings since the schematics do not concisely convey how the timber roof frame connects to the masonry ledge. In addition, interior photos of the roofs are provided in the archives of mappinggothic.org, but they do not provide enough detail to determine or idealize the connection at the masonry ledges. Understanding the attachment of the roof structure to the stone superstructure will considerably affect how the loads are actually applied to the flying buttress system.

Furthermore, the striking difference with regards to the design at Amiens is the intricate voids within the flying buttress. The design remains to be consistent for the flying buttresses above the inner and outer aisles. Just by visual inspection of **Figure 7.26**, the strength capacity of the flying buttresses to withstand the wind loads seems inadequate since the masonry units that compose the extrados and the intrados ribs will be the primary regions that will transfer lateral loads from the upper vaulted nave down to the interior and exterior piers. The intricate interior quatrefoil design (refer to **Figure 8.4**) serves to stabilize the extrados and intrados ribs. Centuries later, masons noticed the inadequacies of the original design of the flying buttresses. A second solid flying buttress was installed just below the original flying buttress above the inner aisle region in order to mitigate tensile stresses from developing even further to the point of structural instability.

7.3.3 finite element analysis

Creating the profile of the cross section of the Cathédrale d'Amiens was a tedious process due to the elaborate design of the flying buttresses. There were many instances where the shells had to be segmented into smaller shapes in order to retain the overall detailed geometric design. Cutting the cross section in half from the axis of symmetry greatly reduced time and effort with regards to creating and solving the model. However, the model was solved approximately 8 minutes due to the number of tiny shells between the intrados and extrados of the flying buttresses. The results were based on the following design parameters and boundary conditions of the model.

7.3.3.1 input

Aside from using different cross sections for each of the Gothic structures, all of the boundary conditions, mechanics of materials properties, node fixities, loads, axis of orientation and assumptions remain the same for Cathédrale d'Amiens as mentioned in **section 7.1.3.1**.

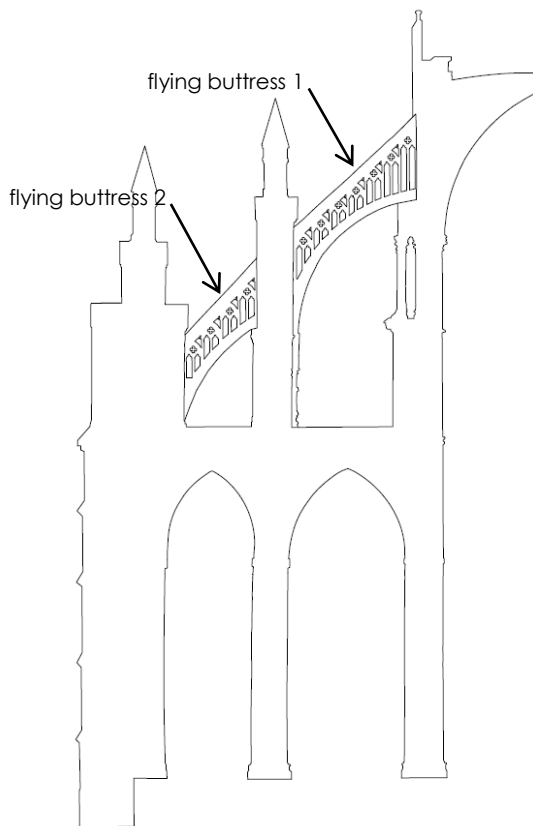


Figure 7.27 – Original Schematic of Analysis of Cathédrale d'Amiens

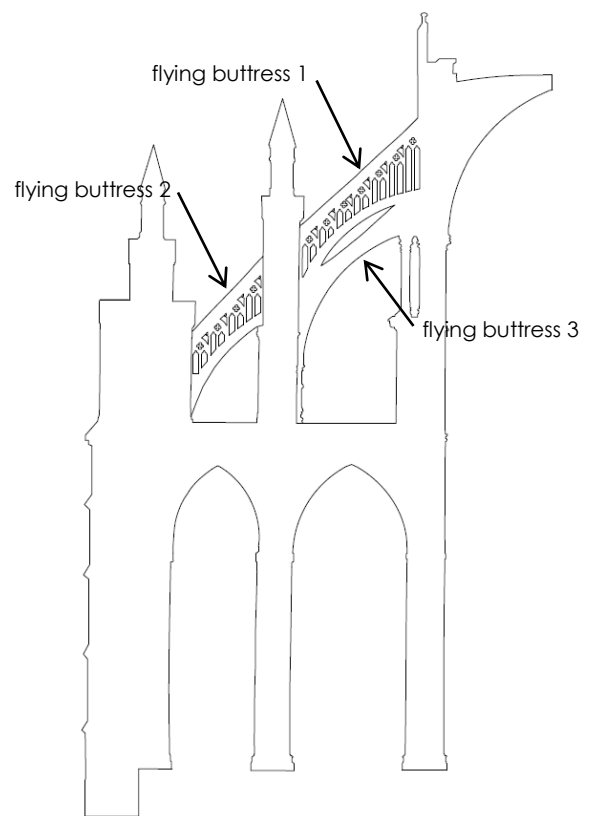


Figure 7.28 – Current Schematic of Analysis of Cathédrale d'Amiens

The thickness of the shells corresponding to the plan view of Cathédrale d'Amiens vary for the external piers, flying buttresses, interior columns and the nave. Based on the scale provided in **Figure 7.25**, the external pier has a thickness of 175 cm (69 in.), the flying buttresses with a thickness of 90 cm (35 in.), the center column with a thickness of 100 cm

(39 in.), the most interior column with a thickness of 100 cm (39 in.), and the nave with a thickness of 100 cm (39 in.). Refer to **Appendix C**, p. 98 that shows the varying thickness of the profile.

7.3.3.2 output

The output explains which regions of the flying buttress experience stresses in tension and compression for each flying buttress. The flying buttresses are labeled and indicated on **Figure 7.27** and **Figure 7.28**. An explanation is provided as to why these areas are developing certain compressive and tensile stress regions based on design model parameters and loading conditions. Load transfer and effects of adjacent structure members are mentioned since they directly affect the behavior of the flying buttresses.

For the following section, the finite element renderings will correspond to similar schematics like **Figure 7.27** and **Figure 7.28**. The only difference is the finite element rendering of a particular flying buttress corresponding to the member highlighted in yellow in the adjacent figure.

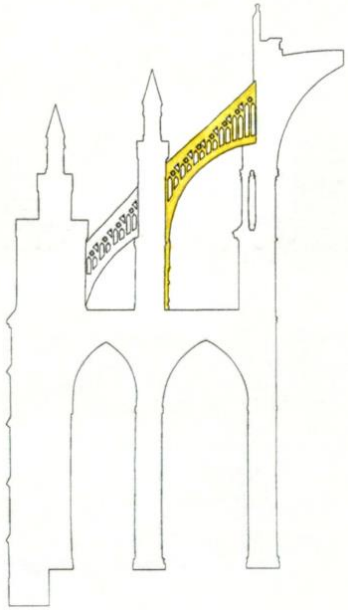


Figure 7.29 – Schematic Reference

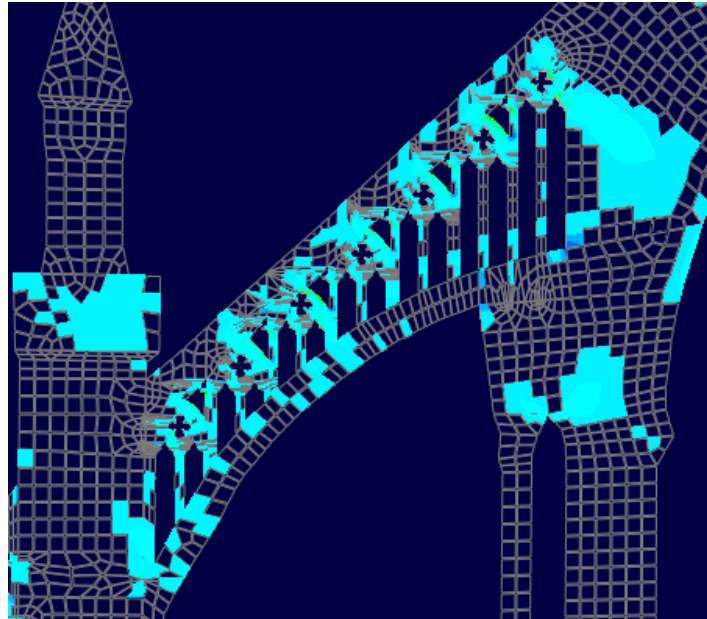


Figure 7.30 – Flying Buttress 1 of Cathédrale d'Amiens

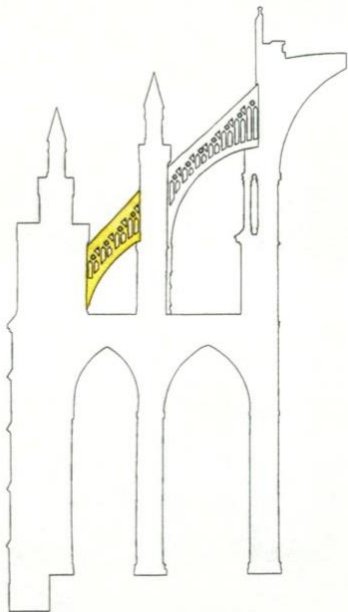


Figure 7.31 – Schematic Reference

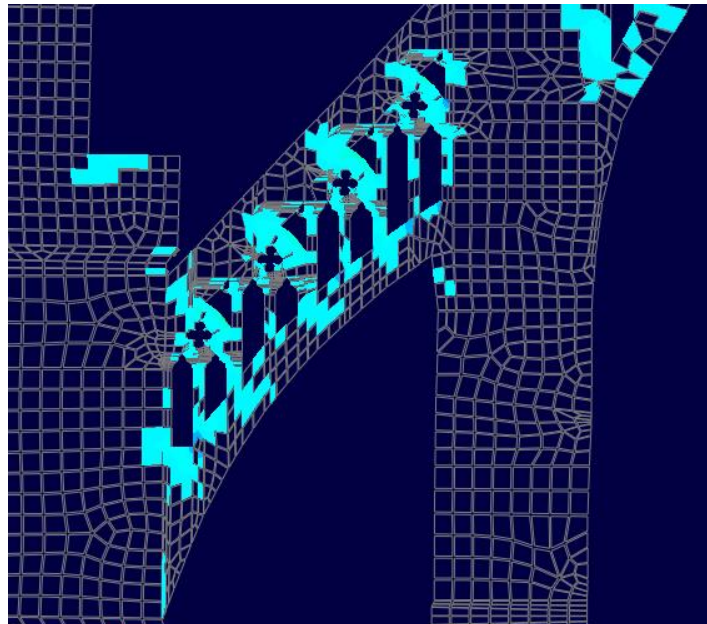


Figure 7.32 – Flying Buttress 2 of Cathédrale d'Amiens

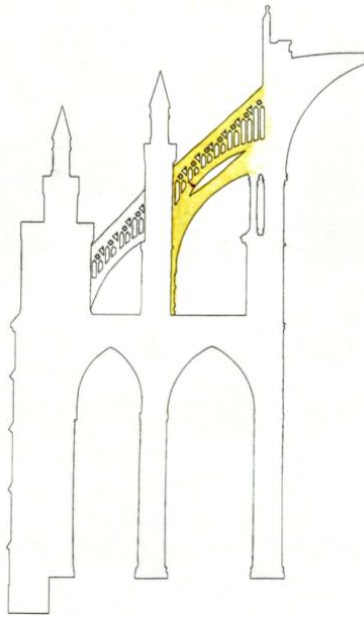


Figure 7.33 – Schematic Reference

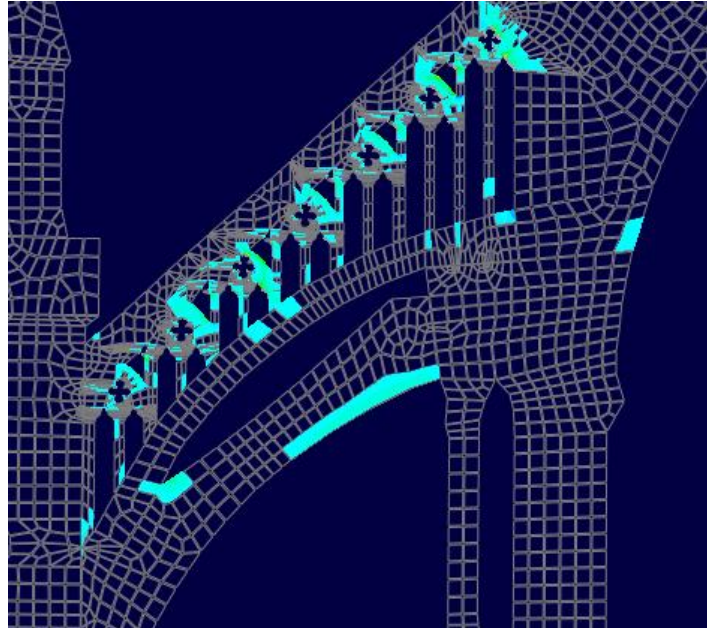


Figure 7.34 – Flying Buttress 1 & 3 of Cathédrale d'Amiens

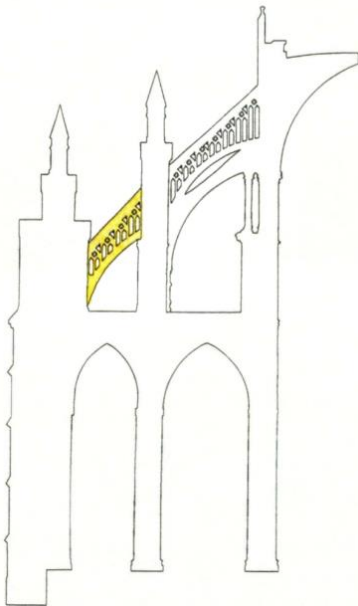


Figure 7.35 – Schematic Reference

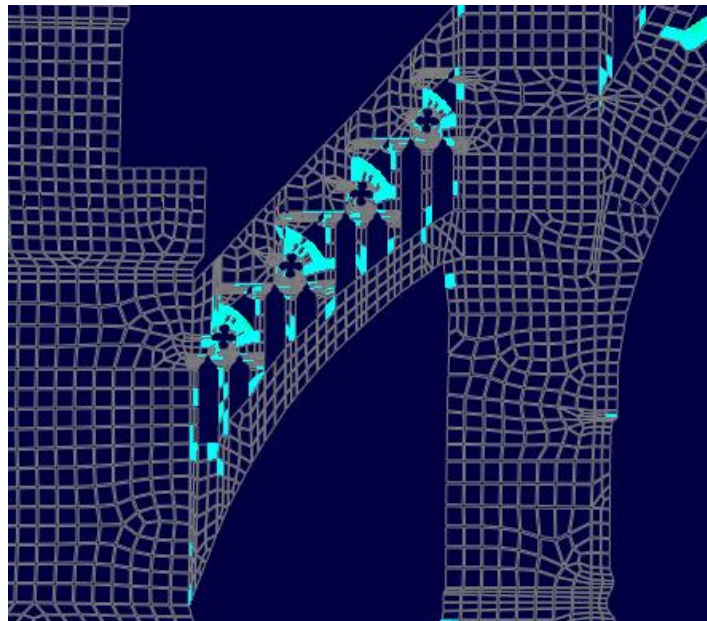


Figure 7.36 – Flying Buttress 2 of Cathédrale d'Amiens

7.3.3.2.1 areas vulnerable in tension

Tensile stress are indicated in light blue in **Figure 7.30**, **Figure 7.32**, **Figure 7.34** and **Figure 7.36** with the maximum principal stress range from 8.796×10^{-4} ton/cm² (1.251×10^{-2} ksi) to 6.206×10^{-3} ton/cm² (8.827×10^{-2} ksi). These figures are zoomed closely to their respected flying buttress elements indicated by the schematics on their left shaded in yellow (**Figure 7.29**, **Figure 7.31**, **Figure 7.33** and **Figure 7.35**). The stress renderings shown on the right side only show tensile stresses in order to easily identify the vulnerable regions of the masonry structure instead of displaying the entire stress ranges. As mentioned previously, **Appendix C**, p.91 – 96 and p.99 – 104 shows comprehensive stress renderings for Cathédrale d'Amiens from RAM Elements that contain complete stress ranges of the entire cross section profile with respect to minimum and maximum principal stresses, as well as the deflected shape of the profile section.

According to the cross section profile labeled as *état antérieur à 1497* (**Figure 7.30** and **Figure 7.32**), the tensile stresses of the first flying buttress appear to be heavily concentrated along the quatrefoil regions. The only possible explanation is the difference of compressive stress distributions along the extrados and the intrados. The compressive stress differential between the intrados and extrados causes the delicate quatrefoil regions to experience tension as a result. Similar distribution of tensile stresses appears along the quatrefoil regions for the second flying buttress as well.

For the cross section profile labeled as *état actuel* (**Figure 7.34** and **Figure 7.36**), the overall tensile stress distribution for the first and second flying buttresses still remain concentrated along the quatrefoil regions. However, the stresses are significantly less than its previous design state. The third flying buttress helps alleviate much of the tensile stress from the quatrefoil regions by creating another load path from the upper vaulted nave and roof. The third flying buttress causes the compressive stress differential between the intrados and extrados to be less in magnitude since a significant part of the thrust load is now directed to a more effective path. However, due to the low slope of the third flying buttress, it is expected for the lower region along the intrados to experience tensile stresses.

7.3.3.2.2 areas remaining in compression

The remaining regions that are not shaded in color (**Figure 7.30**, **Figure 7.32**, **Figure 7.34** and **Figure 7.36**) are regions that experience compression with values ranging from -3.547×10^{-3} ton/cm² (-5.045×10^{-2} ksi) to -8.463×10^{-4} ton/cm² (-1.203×10^{-2} ksi). For the remaining stress not indicated in color, **Appendix C** contains complete stress renderings of the entire profile section with colors corresponding to their respective stress ranges. Each stress range is indicated on the top right corner of each rendering.

Based on the original cross section design in **Figure 7.26**, the thrust loads solely transmit through the extrados and intrados regions of the first and second flying buttresses. The designers of the flying buttress system still carried the logic that the thrust loads traveled in a linear fashion to some degree. In addition, the solid segments that consist the extrados and intrados of the flying buttress lack sufficient rigidity to effectively transmit thrust loads without the interior delicate masonry units to give way to tension.

According to historical accounts, designers realized that the original flying buttress design was inadequate to effectively resist lateral loads from the upper vaulted nave when the columns and walls began to deform into an S shape. The decision to incorporate a third solid flying buttress was implemented in order to mitigate a structural failure. The addition of the third flying buttresses redistributes tension and compressive stresses. In fact, implementation of the third flying buttress caused the extrados and intrados of flying buttresses 1 and 2 remain more in compression than the previous design state.

8 Parametric studies

Several parametric studies have been conducted for all three cathedrals with regards to masonry mechanical properties, design geometry and load application to further understand how certain design parameters may affect stress distribution of the flying buttress system over other factors.

8.1 modulus of elasticity of limestone

The modulus of elasticity of limestone was manipulated in order to see if this mechanical property considerably affects member stress distribution, while keeping the rest of the mechanical properties and load application the same as **section 7.1**, **section 7.2** and **section 7.3**. A fictitious lower bound limit of 2.0×10^6 psi was chosen while the upper bound limit was taken as 5.4×10^6 psi.

Results have shown that changing the modulus of limestone within reasonable limits do not show any noticeable change with regards to tension stress distribution of all three cathedrals.

8.2 unit weight of limestone

The unit weight of limestone was another mechanical property manipulated in order to see if it noticeably affects member stress distribution, while keeping the rest of the mechanical properties and load application the same as **section 7.1**, **section 7.2** and **section 7.3**. A lower bound limit of 140 pcf was chosen while the upper bound limit was taken as 160 pcf.

Results have shown that the lower bound limit of the unit weight of limestone increased tensile stress areas for the Notre-Dame de Paris and Cathédrale d'Amiens, but no change in tensile stress distribution for Cathédrale Saint-Étienne, Bourges. However, the upper bound limit of the unit weight of limestone decreased tensile stress distribution for all three cathedrals.

8.3 inclination, span distance and thickness of flying buttress

According to a parametric study titled *Structure and Form of Early Gothic Flying Buttresses* by Nikolinakou, Tallon and Ochsendorf, twenty French flying buttresses were analyzed to determine the range of structural behavior with respect to flyer length, culée thickness, flyer (flying buttress) inclination and intrados curvature.

Their investigation summarized that an efficient flying buttress may be evaluated based on four primary factors:

- flying buttress experiencing a low minimum thrust magnitude, implying that the member is short or thick and has an intrados formed of an arc segment that resembles close to a quarter circle
- flying buttress having a minimum line of thrust that has a plateau at the head, which reduces the likelihood of sliding failure. These types of flying buttresses usually have an intrados arch center offset towards the main structure (clerestory wall) with a steeper angle (end of *culée*).
- the pier buttress experiencing a force oriented vertically, which increases stability. These types of flying buttresses also have an intrados arch center offset towards the clerestory wall with a steeper angle (end of *culée*).
- supports designed to withstand large horizontal movements. These types of design are found for shorter and thicker flying buttresses.

The conclusions from Nikolinakou, Tallon and Ochsendorf's study is aligned to the results based on the stress models of the three cathedrals analyzed. The inclination, span distance and the thickness of the ends of the flying buttresses behaved closely from the findings of this previous study.

8.4 omitting quatrefoil regions of flying buttress of Cathédrale d'Amiens

The entire interior region located between the intrados and extrados ribs were removed in order to see how much the quatrefoil design contributes to the overall structural behavior of the flying buttress. Only the *état intérieur à 1497* profile was considered in order to see the overall structural behavior at its extreme condition without the aid of the solid flying buttress (flying buttress 3).



**Figure 8.1 – Cathédrale d'Amiens
Without Quatrefoil Regions**

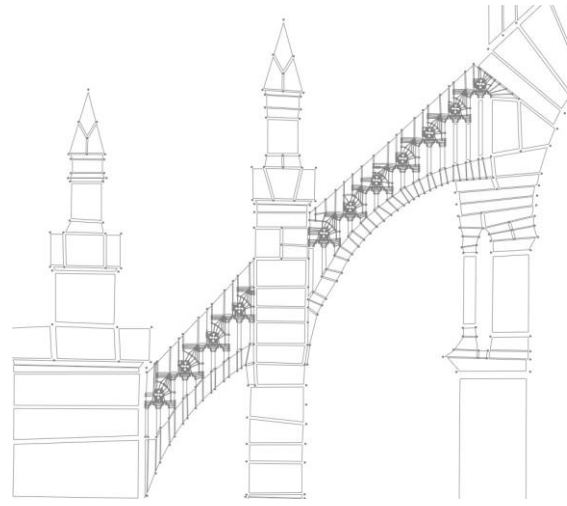


**Figure 8.2 – Cathédrale d'Amiens
With Quatrefoil Regions**

Using the same mechanical properties and load application as **section 7.3**, results have shown that the ribs of the extrados and intrados of flying buttress 2 remain mostly in compression. The ribs of the extrados and intrados for flying buttress 1 behave differently than flying buttress 2. The bottom region of the extrados rib experience tension, whereas the top region experiences compression. This behavior closely resembles like a simply supported beam with the self-weight of beam contributing the moment stresses shown in **Figure 8.1**. The top region of the intrados rib for flying buttress 1 experiences a more concentrated tensile region in a similar location as the original design.

Based on the results, the interior quatrefoil region serves to stabilize the intrados and extrados ribs indicated in **Figure 8.2**. The weight of the quatrefoil region helps the thrust lines to remain within the profile of the intrados rib. The quatrefoil region also serves to support the extrados rib in order to transfer tensile stress from the rib to the quatrefoil region. For this particular flying buttress design, the quatrefoil geometry serves both as crucial structural and architectural elements.

8.5 changing magnitude of lateral load

The magnitude of the horizontal load applied at the keystone was modified in order to see substantial change in member stress distribution. The magnitudes of the loads investigated were

5 tonnes, 10 tonnes, 15 tonnes and 20 tonnes while keeping the stone mechanical properties the same as **section 7.1**, **section 7.2** and **section 7.3**.

Results have shown that there were small noticeable changes with regards to the tensile stress distribution as the load decreased incrementally by 5 tonnes. However, the changes in stress distribution were not substantially different in comparison to the results based on the original design parameters.

9 Results and Conclusion

The following section reinforces how and why a certain design performs better than other designs. Results and commentary are presented for each Gothic structure analyzed within the defined assumptions and idealizations made for the two-dimensional stress analysis. Furthermore, the results indicate which flying buttress design performs the most effective or least effective among analyzed. An effective design is considered to be a system that remains mostly in compression while economizing the amount of stone used to resist or effectively transmit lateral loads. **Figure 9.1**, **Figure 9.2** and **Figure 9.3** only show stress regions in tension in order to easily distinguish areas in tension and compression. Lastly, recommendations are provided for further research in hopes to refine this investigation by considering other imperative design parameters when modeling, comparing and analyzing other flying buttress designs.



Figure 9.1 – Tensile Stress Distribution of Notre-Dame de Paris

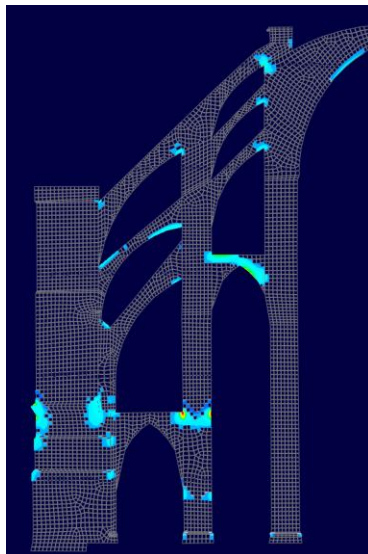


Figure 9.2 – Tensile Stress Distribution of Cathédrale Saint-Etienne, Bourges

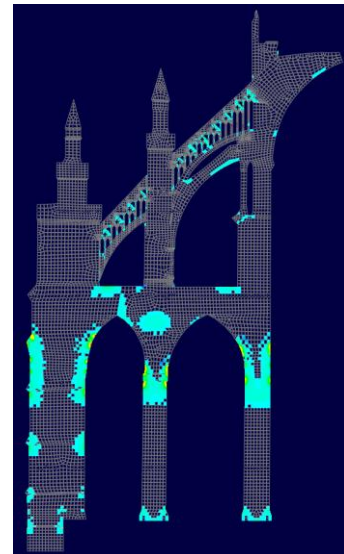


Figure 9.3 – Tensile Stress Distribution of Cathédrale d'Amiens

9.1 most effective design

The most effective design among the three cathedrals analyzed is Cathédrale Saint-Etienne, Bourges. The design of the flying buttress system effectively accommodated to the thrust lines based on the inverted catenary curve by positioning buttress that would capture the thrust loads of adjacent structure members above. In addition, designing the flying buttress with a steeper slope demonstrated that the Gothic member was successful in keeping the masonry units in compression.

9.2 least effective design

The least effective design is the Cathédrale d'Amiens. In spite of its impressive architectural embellishments, the voids that create the quatrefoil geometry (shown in **Figure 9.4**) caused virtually the entire interior of the flying buttresses incredibly vulnerable to tensile stresses. The flying buttresses were not able to sufficiently transmit thrust loads solely through the intrados and extrados regions. Even with the addition of the third flying buttress, the intricate quatrefoil design still remains vulnerable in tension.

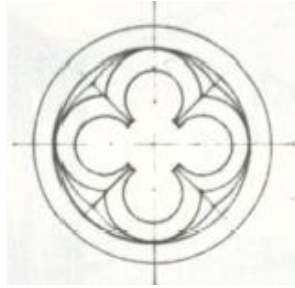


Figure 9.4 – Quatrefoil Design

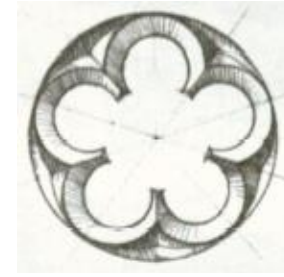


Figure 9.5 – Cinqfoil Design

Images courtesy of Francis D. K. Chang, *A Visual Dictionary of Architecture (2nd Ed.)*; John Wiley & Sons, Inc.

9.3 discussion of results

Since the Notre-Dame de Paris was one of the first Gothic structures to incorporate the flying buttress, the overall profile of the structure appears to be relatively massive compared to the slender Cathédrale Saint-Étienne and Cathédrale d'Amiens. Again, such uncertainty of the thrust load behavior caused designers to be conservative in their design practices. It is remarkably

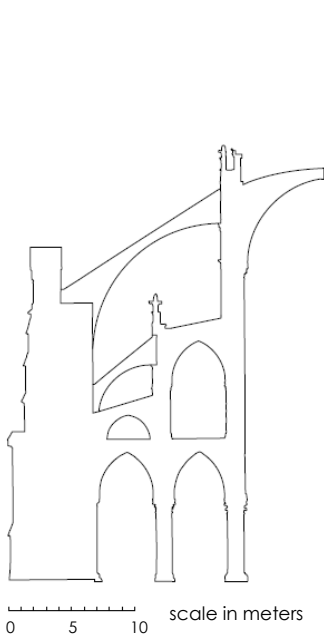


Figure 9.6 – Profile of Notre-Dame de Paris



Figure 9.7 – Profile of Cathédrale Saint-Étienne, Bourges

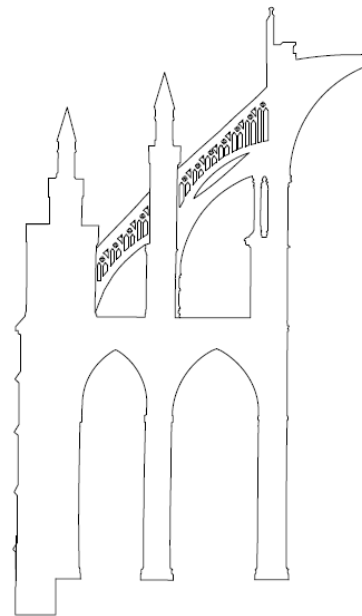


Figure 9.8 – Profile of Cathédrale d'Amiens

impressive that the primary exterior buttress is able to span across 10 meters (32.8 ft) while resisting thrust loads from the high vault. This implies that longer distances require greater force for the stones to retain its arch shape without the masonry units slipping. This also exerts larger forces on their supporting elements (Nikolinakou, Tallon & Ochsendorf), which may be an issue with regards to slipping or overturning failure on the supporting elements. This explains the massive thickness of the exterior buttress in Notre-Dame de Paris. In addition, the smaller flying buttress and the arch above the outer aisle only shows that the designer improvised during the construction process when the interior columns began to bow outward. Furthermore, the slope of the exterior flying buttress is relatively low compared to the other two cathedrals. From an engineering standpoint, if the designer understood the catenary thrust behavior, material cost and savings would be significant in relation to the cross sections of the other cathedrals.

For the cathedral Saint-Étienne, Bourges, the obvious design differences with respect to the Notre-Dame de Paris is the number of flying buttresses distributed evenly above both inner and outer aisles, the relative slender shape of the flying buttresses, the span difference, and a slightly steeper slope. The only noticeable design parameters between the cathedrals of Bourges and Paris are the flying buttress with no interior geometric voids. Cathédrale Saint-Étienne performs more effectively with regards to transmitting thrust loads, while achieving height and the delicate appearance than the Notre-Dame de Paris. The Gothic style is more refined and effectively demonstrated by the Cathédrale Saint-Étienne, Bourges.

Lastly, the Cathédrale d'Amiens does have much more of an elaborate and delicate appearance than the previous cathedrals mentioned. It is also substantially taller than the other two structures. However, the designer's emphasis on height and the intricate design of the flying buttress system came at a potentially devastating cost when the inadequacies of the extrados and intrados became ineffective to resist thrust loads from the high vault. However, the slope of the flying buttress are steeper than the ones from Paris and Bourges. Unfortunately, the delicate voids in the flying buttresses of Amiens show that this is the most ineffective way to transfer thrust loads. **Figure 9.6, Figure 9.7** and **Figure 9.8** are to scale in relation to each other.

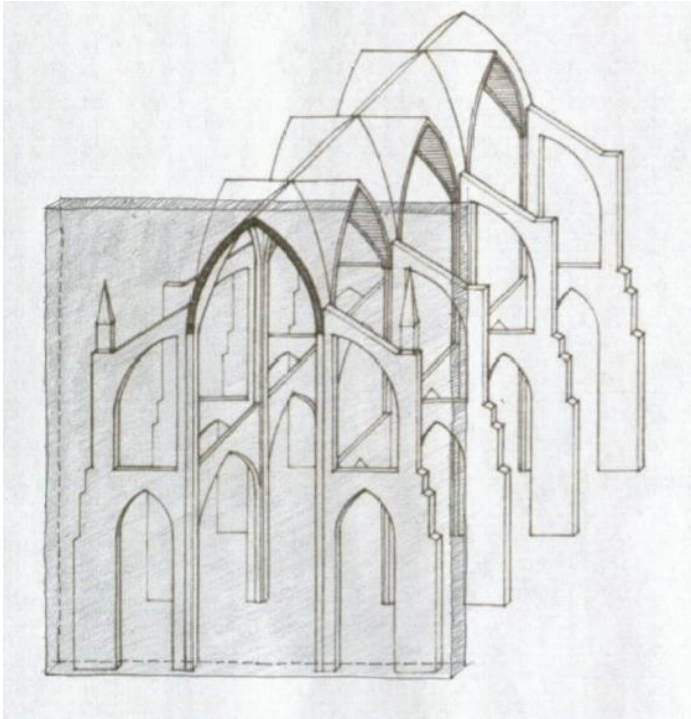


Figure 9.9 – Section View of Nave and Flying Buttress System

Image courtesy of Francis D. K. Chang, *A Visual Dictionary of Architecture* (2nd Ed.); John Wiley & Sons, Inc.

geometrical design, as shown in **Figure 9.9** and **Figure 9.10**. Modeling the entire Gothic structure in such detail would be an enormous and tedious endeavor since there are limited cross section and elevation drawings that would cover the entire Gothic structure. In addition, the lack of understanding the integration of the roof structure to the masonry superstructure poses a great challenge on how to accurately idealize lateral loads to the flying buttress system.

The shaded plane shown in **Figure 9.9** shows how the two-dimensional profile was extracted from a three-dimensional structural schematic of a typical Gothic cathedral.

9.4 limitations

There were several limitations that hindered the investigation from producing refined and realistic results. The two-dimensional analysis did not allow the stress distributions to transmit along the third dimensional axis. The model did not take into precise account of the intricate geometries (refer to **Figure 9.9**) of the columns and piers since the members are not perfectly circular or nicely rectangular throughout a particular structural element. Moreover, the regions of the upper vaulted nave are treated to have the same thickness for the two-dimensional analysis. In reality, the shells and the ribs of the upper vaulted nave would have to be analyzed three-dimensionally due to its inherent

9.5 recommendations for further research

Suggestions to perfect the modeling process could be an endless endeavor since there are so many unknown factors with regards to Gothic structures constructed centuries ago.

The main factor worth investigating is accurately modeling the brick and mortar joints within the flying buttress system. The current model shown is inaccurate in the sense that the convenience of creating shells that respected the section profile took priority than constructing shells in relation to the masonry unit and mortar joint. Most shells may account for several masonry units acting in unity. For future analysis, creating in shells as masonry units depicted from the architectural cross sections may yield more realistic results with regards to the interaction between masonry units within the flying buttress. In addition, determining the exact mechanical properties of stone and mortar used for construction would be ideal for this detailed investigation. Testing would need to be performed such as non-destructive testing (NDT). According to a report titled *Nondestructive Testing of Historic Structures* (2001) by Livingston, one non-destructing testing method for masonry structures is penetrating radiation. This approach may be time consuming depending on the density and thickness of the masonry, but NDT is a great alternative since it does not compromise the architectural or structural integrity of heritage structures. Another alternative to obtain authentic data for masonry properties is to determine sites of ancient quarries used for the construction of cathedrals from historical records, if possible.

Moreover, ancient builders also tried economize on building materials by using infill in cavities of piers, walls and columns. This may skew results if certain structural members were idealized entirely as masonry units when or if there exists a cavity filled with cementitious material with crushed stone or aggregate. If substantial effort is going to be made to such accuracy, locating cavities within certain structural members might be worth investigating.

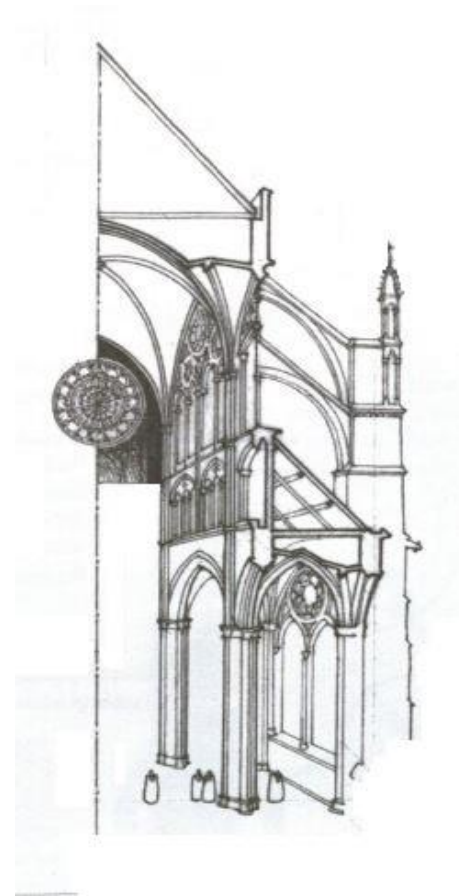


Figure 9.10 – Section View of Aisle and Nave

Image courtesy of Francis D. K. Chang, *A Visual Dictionary of Architecture* (2nd Ed.); John Wiley & Sons, Inc.

In addition, understanding the construction timeline of these ancient structures may provide a deeper understanding of how a structure behaves today. Critical events in history such as major wars, weather events and design changes may give insightful information rather than analyzing the structure without any historical context as load paths may have shifted from such change from its original intent. Moreover, such restoration efforts may have used different materials which may surprise analysts due to different mechanical properties (Roca, Cervera, Gariup and Pela, 2010).

Previous research has been conducted according to *Experiments in Gothic Structure* (1982) by Robert Mark where photoelastic modeling was used to determine stress distributions of cross sections of Gothic cathedrals. The weights were positioned strategically and scaled to simulate wind pressures based on the following equation:

$$p = \frac{1}{2} \rho \cdot V^2 \cdot C \cdot G \quad (9.1)$$

where p = wind pressure

ρ = mass density of air, taken as 0.135 kg-s/m⁴

V = wind velocity

C = variable, non-dimensional coefficient related to building form

G = gust effect factor

The data with respect to all of these variables mentioned above are known for the Cathédrale d'Amiens. However, the derivation for these values are not shown such as the gust effect factor, which would be difficult to accurately apply wind loads to the Notre-Dame de Paris and Cathédrale Saint-Etienne, Bourges. The wind pressure equation is referenced from *Wind Effects on Structures: An Introduction to Wind Engineering* (1978) by Simiu and Scanlan.

Wind pressures can also be derived using Equation 27.3-1 and Equation 27.4-1 from the ASCE 7-10 Code (American Society of Civil Engineers – Minimum Design Loads for Buildings and Other Structures). An external source must be used to obtain the basic wind speeds of Western Europe.

As mentioned before, the pursuit of perfecting and idealizing models can be endless. The endeavor of understanding Gothic structures is fascinating, even though there are numerous challenges in creating models that resemble close to reality. Unfortunately, there will never be a generation that will ever create something even close to what the Gothic builders have accomplished. In many ways, there is a global sense of responsibility given to the current generation of engineers and architects to understand and maintain something profound. The

Gothic builders realized that not only have they tried to reach incredible heights, but they have also managed to reach an invisible dimension that will exist all throughout humanity. This investigation was to show which regions were vulnerable to tensile stresses in order to provide effective solutions for historic preservation efforts. The ulterior motive of this study is to help researchers embark on a trajectory that discovers original solutions and apply them to practice in greater precision and detail.

References

- "Amiens, Cathédrale Notre-Dame." Mapping Gothic France. Web. 14 Feb. 2016.
- "Bourges, Cathédrale Saint-Étienne." Mapping Gothic France. Web. 14 Feb. 2016.
- "Paris, Cathédrale Notre-Dame." Mapping Gothic France. Web. 14 Feb. 2016.
- "Vénération De La Sainte Couronne D'Epines." Notre-Dame De Paris. Web. 14 Feb. 2016.
- Allen, E., Zalewski, W., & Michel, N. (2010). Form and forces: Designing efficient, expressive structures (pp. 219-231). Hoboken, New Jersey: John Wiley & Sons.
- Ball, P. (2008). Universe of Stone - A Biography of Chartres Cathedral (pp. 47-48). New York: HarperCollins.
- Barrallo, J., & Sanchez-Beitia, S. (n.d.). Mathematical Models of Gothic Structures (Rep.). San Sebastian.
- Ching, F. D. (2008). Building Construction Illustrated (4th ed.) (pp. 2.25, 5.20). Hoboken, New Jersey: John Wiley & Sons.
- Ching, F. D. (2012). A Visual Dictionary of Architecture (2nd ed.) (pp. 4-6, 28-29, 280-293). Hoboken, New Jersey: John Wiley & Sons.
- Clark, William W., and Robert Mark. "The First Flying Buttresses: A New Reconstruction of the Nave of Notre-Dame De Paris." The Art Bulletin 66.1 (1984): 47-65. Print.
- Coefficients of Linear Thermal Expansion. (n.d.). Retrieved February 17, 2016, from http://www.engineeringtoolbox.com/linear-expansion-coefficients-d_95.html
- Cultrone, G., Sebastián, E., & Huertas, M. (2004, December 11). Forced and natural carbonation of lime-based mortars with and without additives: Mineralogical and textural changes [Scholarly project]. In Universidad De Granada. Retrieved February 29, 2016, from http://www.ugr.es/~grupo179/pdf/Cultrone_05b.pdf
- Erdogmus, E., Boothby, T. E., & Smith, E. B. (2009). Structural Appraisal of the Florentine Gothic Construction System (Rep.).

FAQ. (n.d.). Retrieved February 17, 2016, from <https://limestonesymposium.org/faq>
Gençtürk B., & Kiliç, S. (2006). Assessment of Historic Masonry Arch Bridges Using the Discrete Finite Elements Method (Tech.).

Gercek, H. (2006). Poisson's ratio values for rocks. *International Journal of Rock Mechanics & Mining Sciences*, 1-13. Retrieved February 6, 2016.

Heyman, J. (1995). *The Stone Skeleton - Structural Engineering of Masonry Architecture* (pp. 12-19, 88-106). Cambridge: Cambridge University Press.

Huerta, S. (2001). *Mechanics of masonry vaults: The equilibrium approach* (pp. 47-70, Publication). Guimarães.

Huerta, S. (2010). The safety of masonry buttresses. *Proceedings of the Institution of Civil Engineers* (pp. 3-24). Retrieved February 6, 2016.

Indiana Limestone Handbook (22nd ed.). (n.d.). Indiana Limestone Institute of America.

Livingston, R. A. (2001). *Nondestructive Testing of Historic Structures* (pp. 249-271, Tech.). Kluwer Academic.

Lourenço, P. B. (2002). *Computations of historical masonry constructions* (Rep.). Guimarães.

Mark, R. (Ed.). (1993). *Architectural Technology up to the Scientific Revolution* (pp. 8-10, 106-122). Cambridge, Massachusetts: MIT Press.

Mark, Robert. *Experiments in Gothic Structure* (pp. 18-25). Cambridge, MA: MIT, 1982. Print.

Nikolinakou, M. A., Tallon, A. J., & Ochsendorf, J. A. (2005). Structure and Form of Early Gothic Flying Buttresses (Vol. 9, pp. 1191-1217, Tech. No. 9-10).

Philippe Block et al., Real-time limit analysis of vaulted masonry buildings, *Computers and Structures* (2006), doi:10.1016/j.compstruc.2006.08.002

Roca, P., Cervera, M., Gariup, G., & Pela, L. (2010). *Structural Analysis of Masonry Historical Construction. Classical and Advanced Approaches* (pp. 300-325, Tech.). Barcelona: CIMNE. Retrieved February 6, 2016.

Sahlin, S. (1971). Stability of concentrically loaded masonry walls. In *Structural Masonry* (pp. 52-56). Englewood Cliffs, New Jersey: Prentice-Hall. Tschoepe, R. (2016). The Short Course on Historic Mortar. *The Old House Journal*.

Simiu, E., & Scanlan, R. H. (1978). Relation of Wind Pressure over Slender Buildings to Wind Velocities. In *Wind Effects on Structures: An Introduction to Wind Engineering* (pp. 161-163). John Wiley & Sons.

Varma, M., Jangid, R. S., & Ghosh, S. (2010). Thrust Line Using Linear Elastic Finite Element Analysis for Masonry Structures (Vol. 133-134, pp. 503-508, Publication). *Trans Tech*.

Viola, E., Panzacchi, L., & Tornabene, F. (2004). Structural Analysis of Historical Masonry Arches. In *Restoration, Recycling and Rejuvenation Technology for Engineering and Architecture Application* (pp. 358-369). Rome: Aracne. Retrieved February 2, 2015.

Appendix A – Computations and Assumptions

Poisson's ratio

The mechanical properties of stone masonry was determined by observing values used from previous research similar in nature and other scientific sources. Based on a scientific literature review titled *Poisson's ratio values for rocks* (2006) by H. Gercek, the poisson's ratio of limestone had a range from 0.1 to 0.33. In addition, a study titled *Vaulting of Narbonne Cathedral* (2011) by A. Nichols, V. Paul and J. Nichols used a value of 0.25 for poisson's ratio for limestone. Based on these two points of comparison, a value of 0.25 was used for poisson's ratio for this study.

Unit weight of limestone

For an approximated value of unit weight of limestone, three sources were compared in determining an accurate value. According to limestonesymposium.org, the website specified the unit weight of limestone to be approximately 150 pcf. Another source titled *Vaulting of Narbonne Cathedral* (2011) by A. Nichols, V. Paul and J. Nichols used a value of 150 pcf as well. However, the Indiana Limestone Institute states a value of 144 pcf. For this research, a value of 150 pcf was used for this study.

Coefficient of thermal expansion

According to engineeringtoolbox.com, the coefficient of thermal expansion was taken to be 8×10^{-6} m/m-K (4.4×10^{-6} in/in-F). Another resource by Indiana Limestone Institute states a range of 2.4×10^{-6} in/in-F to 3.0×10^{-6} in/in-F. This value was required in order to satisfy mechanical properties needed for analysis by RAM Elements. However, this value is disregarded since stresses due to temperature differentials do not fall within the parameters of this study.

Modulus of elasticity

The *Indiana Limestone Handbook* (22nd Edition) was referenced in determining the value of the modulus of elasticity of structural limestone which ranged from a minimum value of 3,300,000 to a maximum value of 5,400,000 psi. Since the exact modulus of elasticity of limestone is unknown for any of the cathedrals, the lower bound value of 3,300,000 psi was used for the modulus of elasticity of limestone.

Computation of lateral load

Loads are only permitted in klf (kips per lineal foot) in RAM Elements for shells. Therefore, the thickness of the vaulted nave was taken for each of the cathedrals. The thickness of the cathedrals are as follows:

➤ Notre-Dame de Paris	0.849 m (33.4 in.)
➤ Cathédrale Saint-Étienne, Bourges	1.128 m (44.4 in.)
➤ Cathédrale d'Amiens	0.941 m (37.0 in.)

In addition, the reaction was solved at the keystone for each cathedral by idealizing the nodes as a roller in the z-direction (vertical direction) with no superimposed loads. The reaction of the cathedrals are as follows:

➤ Notre-Dame de Paris	16.77 tonnes (36.97 k)
➤ Cathédrale Saint-Étienne, Bourges	65.26 tonnes (143.87 k)
➤ Cathédrale d'Amiens	30.90 tonnes (68.12 k)

In order to keep the majority of the modeling parameters constant for the sake of consistency and simplicity, the load was applied in the horizontal direction at the keystone. Another reason was due to the lack of information with regards to roof construction and the framing connection to the masonry structure. The website, mappinggothic.org, did provide photos of the roofing frame for some cathedrals. Furthermore, the photos did not convey in detail how the roof frame was connected to the masonry superstructure and whether if the roof frame was supported only supported at the ends without an intermediate support.

20 tonne (44 k) load was used to determine the horizontal thrust for all three cathedrals. This value was referenced from *the Stone Skeleton – Structural Engineering of Masonry Architecture* (1995) by Jacques Heyman. The thrust value mentioned by Heyman does not specify what percentage of the 20 tonne load is from structural self-weight and/or wind effects. A sustained horizontal thrust of 20 tonnes was referred for the Cathédrale d'Amiens. The same value was applied for the Notre-Dame de Paris and the Cathédrale Saint-Étienne, Bourges since the Cathédrale d'Amiens is the tallest structure with the largest span (in transverse direction) which would carry the largest load of the three structures.

The lateral loads used for each of the cathedrals were the summation of the 20 tonnes plus the horizontal reactions solved by RAM Elements divided by the thickness of the keystones, which resulted in the following:

- Notre-Dame de Paris 43.28 tonnes/m (29.1 klf)
- Cathédrale Saint-Etienne, Bourges 75.58 tonnes/m (50.7 klf)
- Cathédrale d'Amiens 54.06 tonnes/m (36.4 klf)

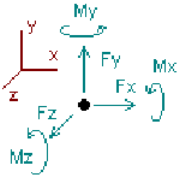
Horizontal Reactions of Keystones



Current Date: 2/17/2016 9:04 PM
Units system: Metric
File name: C:\Users\226-\Desktop\RAM cathedral models\20 tonnes\notre-dame de paris.etz\

Analysis result

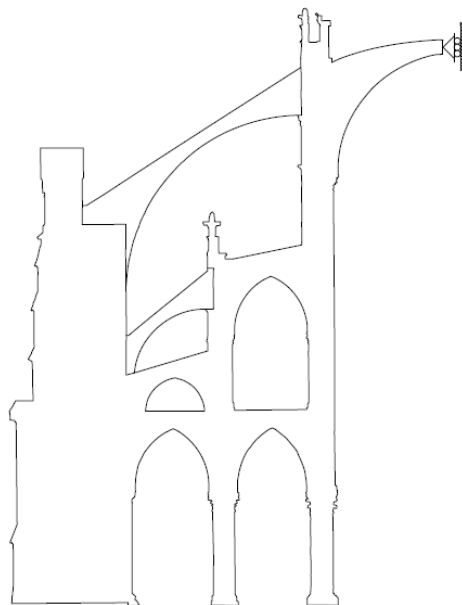
Reactions



Direction of positive forces and moments

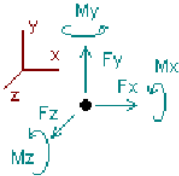
Node	Forces [Ton]			Moments [Ton*m]		
	FX	FY	FZ	MX	MY	MZ
Condition DL=Dead Load						
140	-10.61281	0.00000	0.00000	0.00000	0.00000	0.00000
228	-6.16015	0.00000	0.00000	0.00000	0.00000	0.00000
SUM	-16.77296	0.00000	0.00000	0.00000	0.00000	0.00000

Notre-Dame de Paris



Analysis result

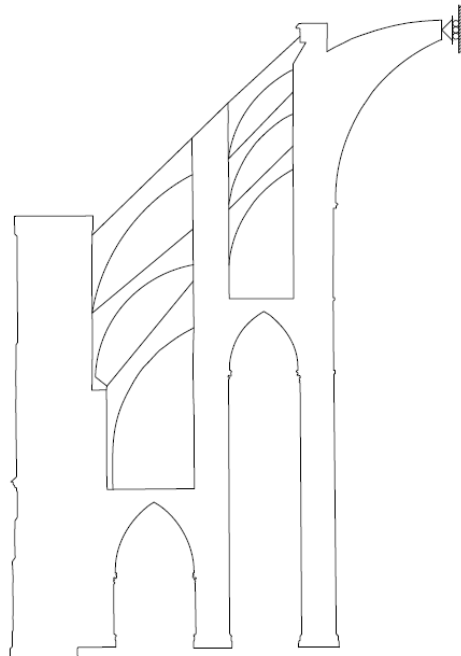
Reactions



Direction of positive forces and moments

Node	Forces [Ton]			Moments [Ton*m]		
	FX	FY	FZ	MX	MY	MZ
Condition DL=Dead Load						
1	-47.45594	0.00000	0.00000	0.00000	0.00000	0.00000
2	-17.80463	0.00000	0.00000	0.00000	0.00000	0.00000
SUM	-65.26058	0.00000	0.00000	0.00000	0.00000	0.00000

Cathédrale Saint-Etienne, Bourges



Analysis result

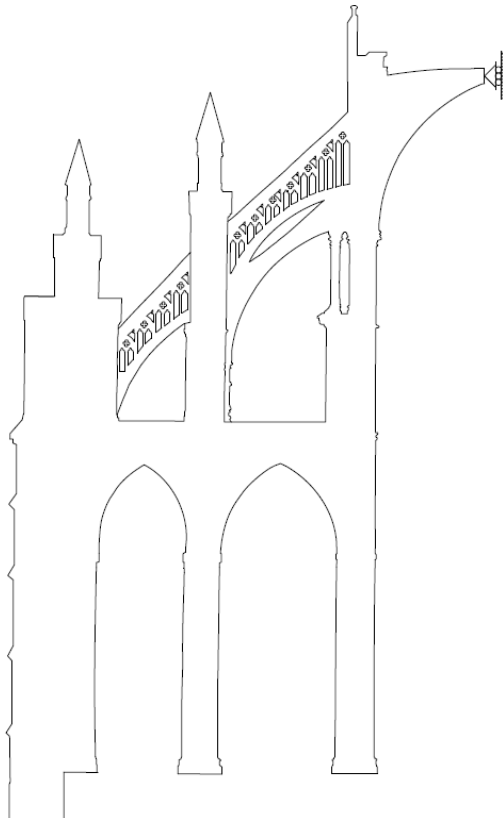
Reactions



Direction of positive forces and moments

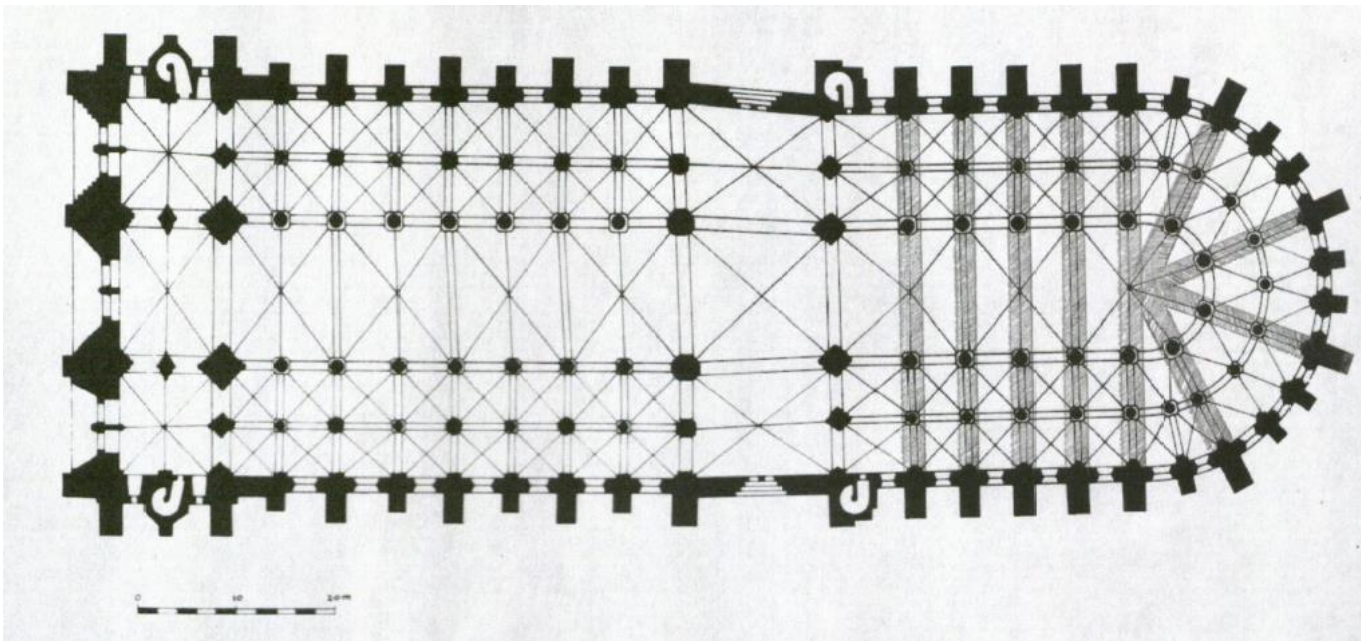
Node	Forces [Ton]			Moments [Ton*m]		
	FX	FY	FZ	MX	MY	MZ
Condition DL=Dead Load						
432	-21.36033	0.00000	0.00000	0.00000	0.00000	0.00000
4338	-9.54916	0.00000	0.00000	0.00000	0.00000	0.00000
SUM	-30.90949	0.00000	0.00000	0.00000	0.00000	0.00000

Cathédrale d'Amiens



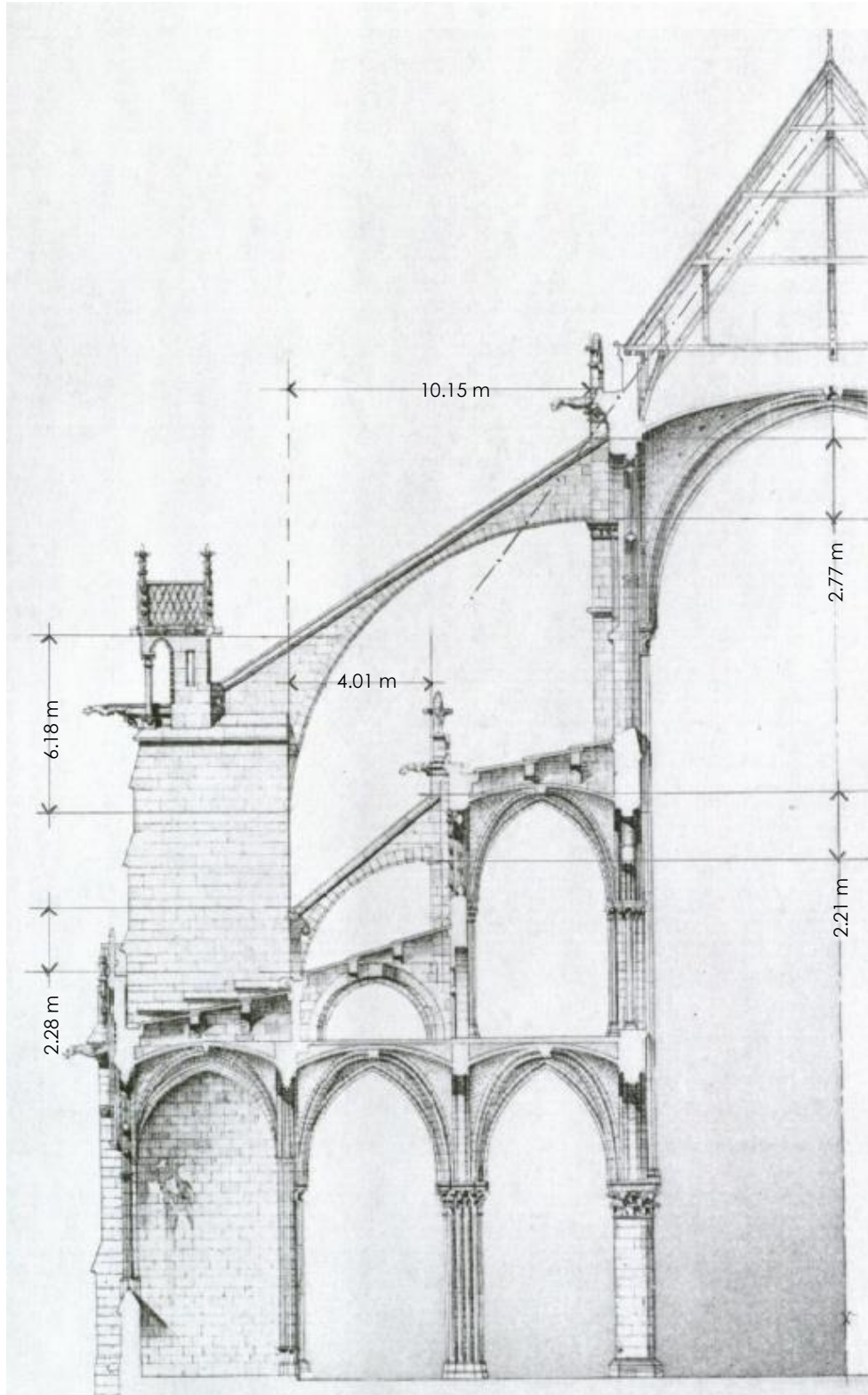
Appendix B – Architectural Drawings

The following images are in reference to **section 7.1.2**, **section 7.2.2** and **section 7.3.2** in detail for Notre-Dame de Paris, Cathédrale Saint-Étienne, Bourges and Cathédrale d'Amiens.



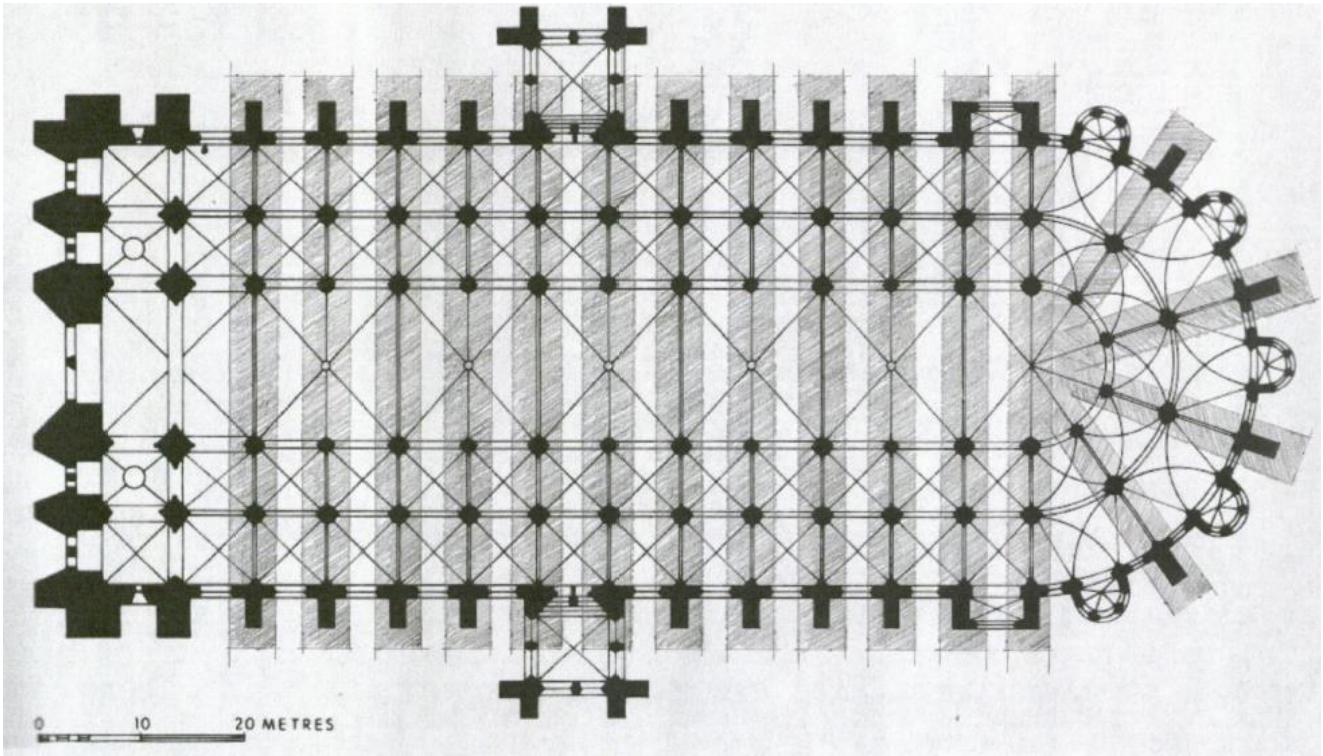
Plan View of Notre-Dame de Paris

Image courtesy of mappinggothic.org, Media Center for Art History, Department of Art History and Archaeology, Trustees of Columbia University



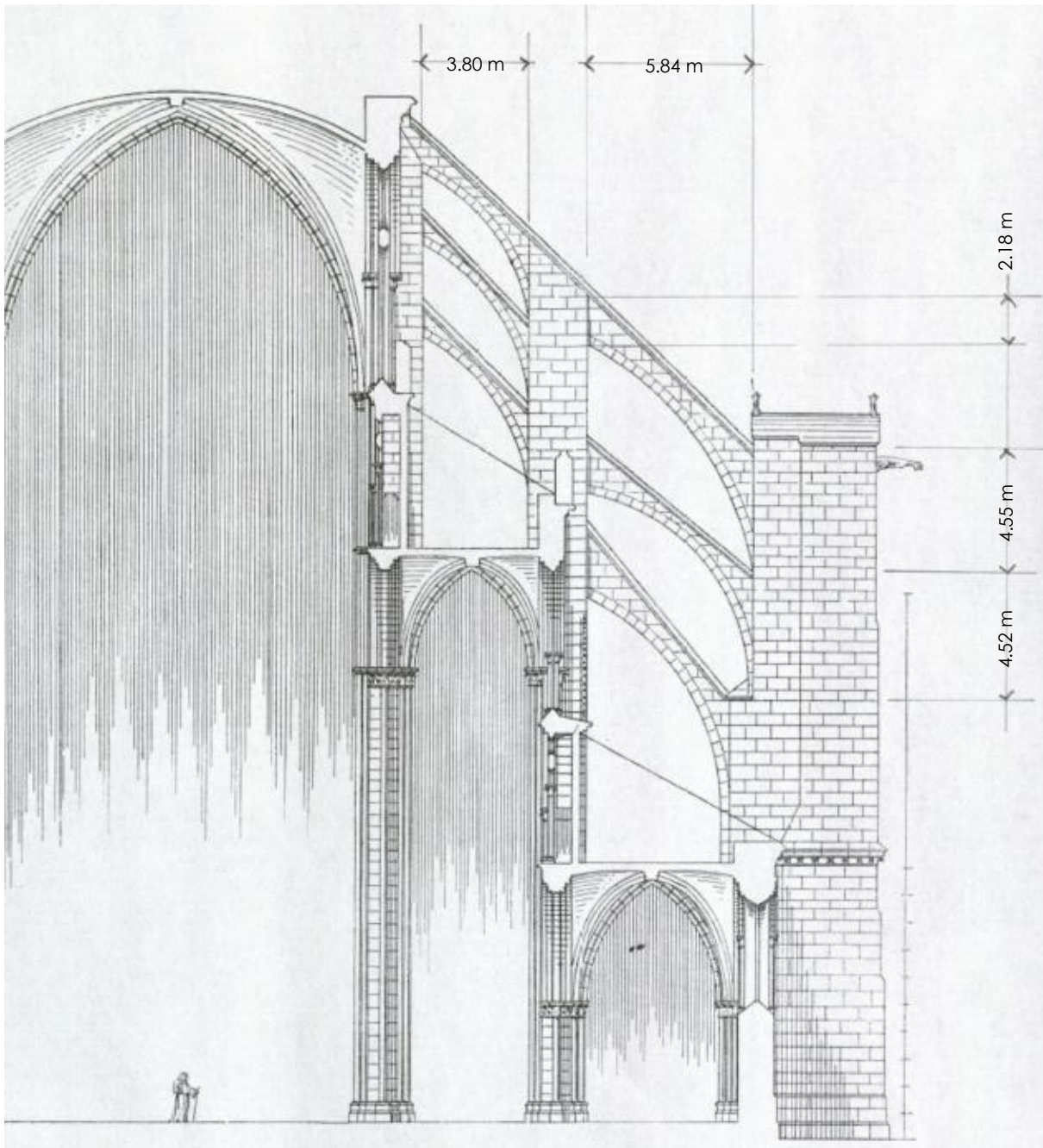
Cross Section of Notre-Dame de Paris

Image courtesy of mappinggothic.org, Media Center for Art History, Department of Art History and Archaeology, Trustees of Columbia University



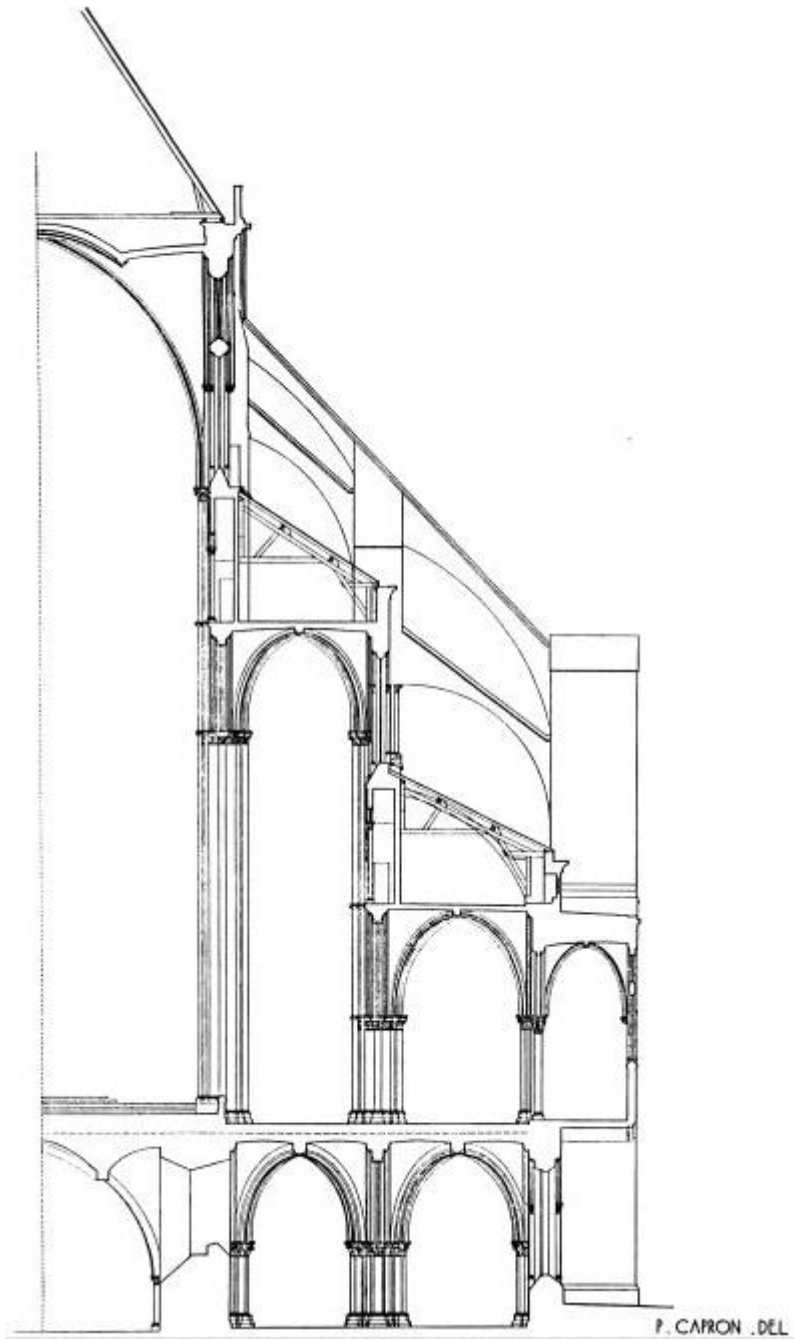
Plan View of Cathédrale Saint-Étienne, Bourges

Image courtesy of mappinggothic.org, Media Center for Art History, Department of Art History and Archaeology, Trustees of Columbia University



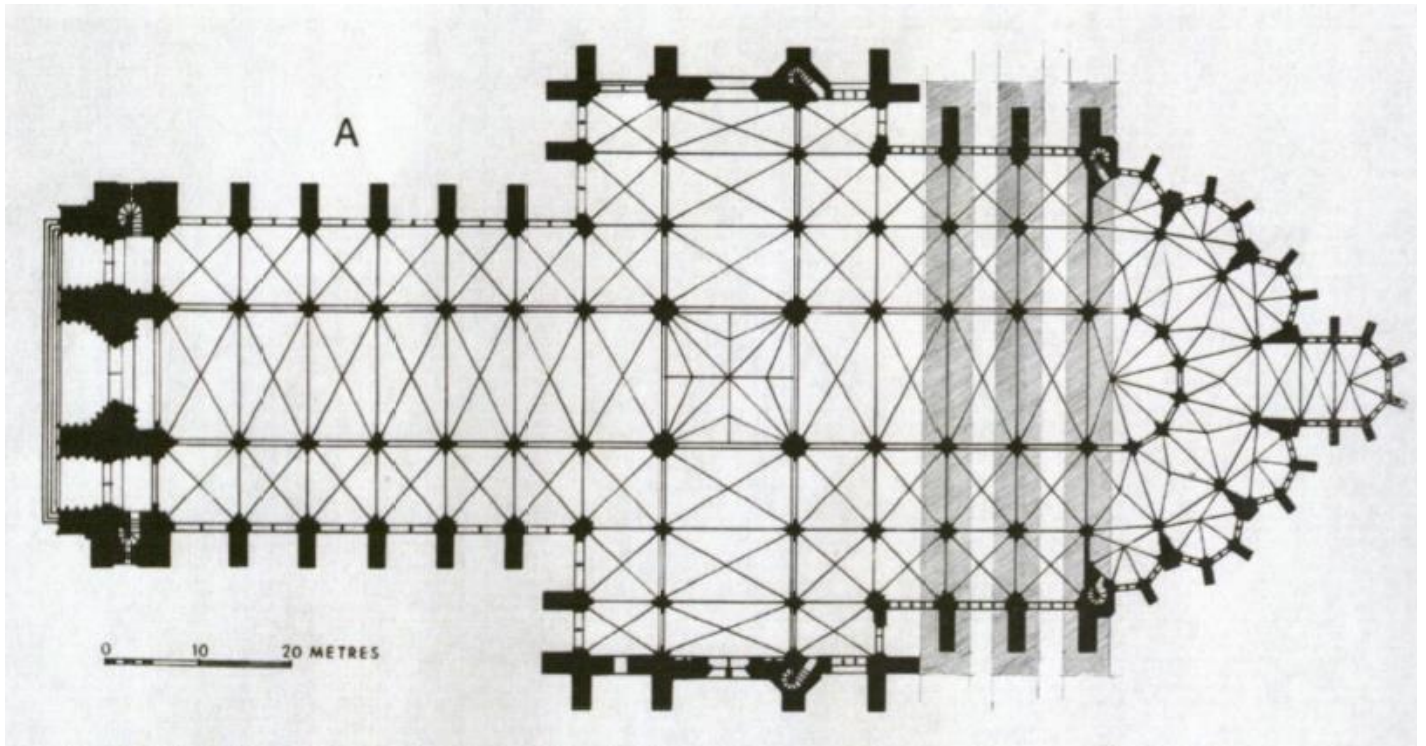
**Cross Section of Cathédrale Saint-Étienne, Bourges
(not constructed in reality)**

Image courtesy of mappinggothic.org, Media Center for Art History, Department of Art History and Archaeology, Trustees of Columbia University



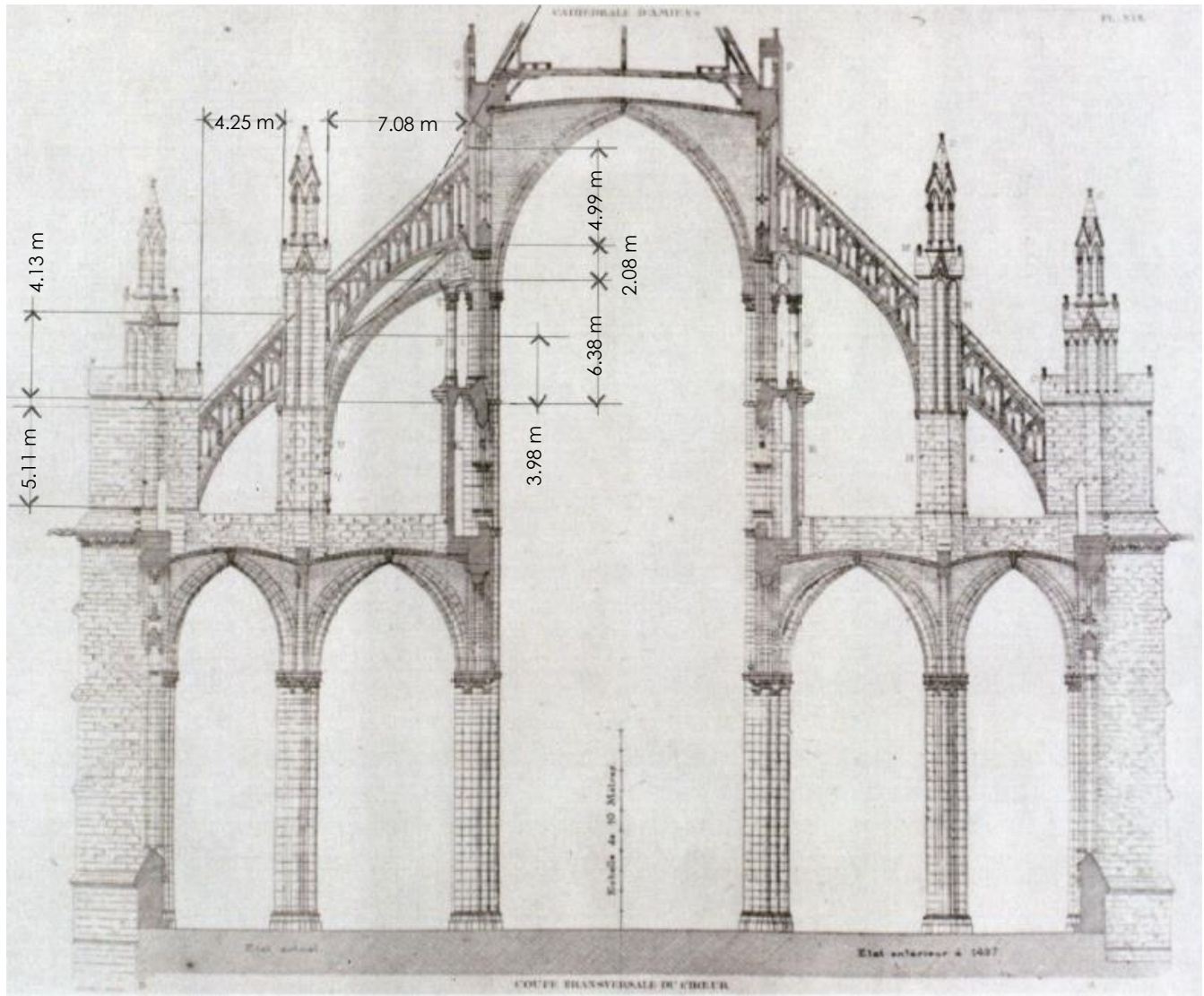
**Cross Section of Cathédrale Saint-Étienne, Bourges
(constructed in reality)**

Image courtesy of mappinggothic.org, Media Center for Art History, Department of Art History and Archaeology, Trustees of Columbia University



Plan View of Cathédrale d'Amiens

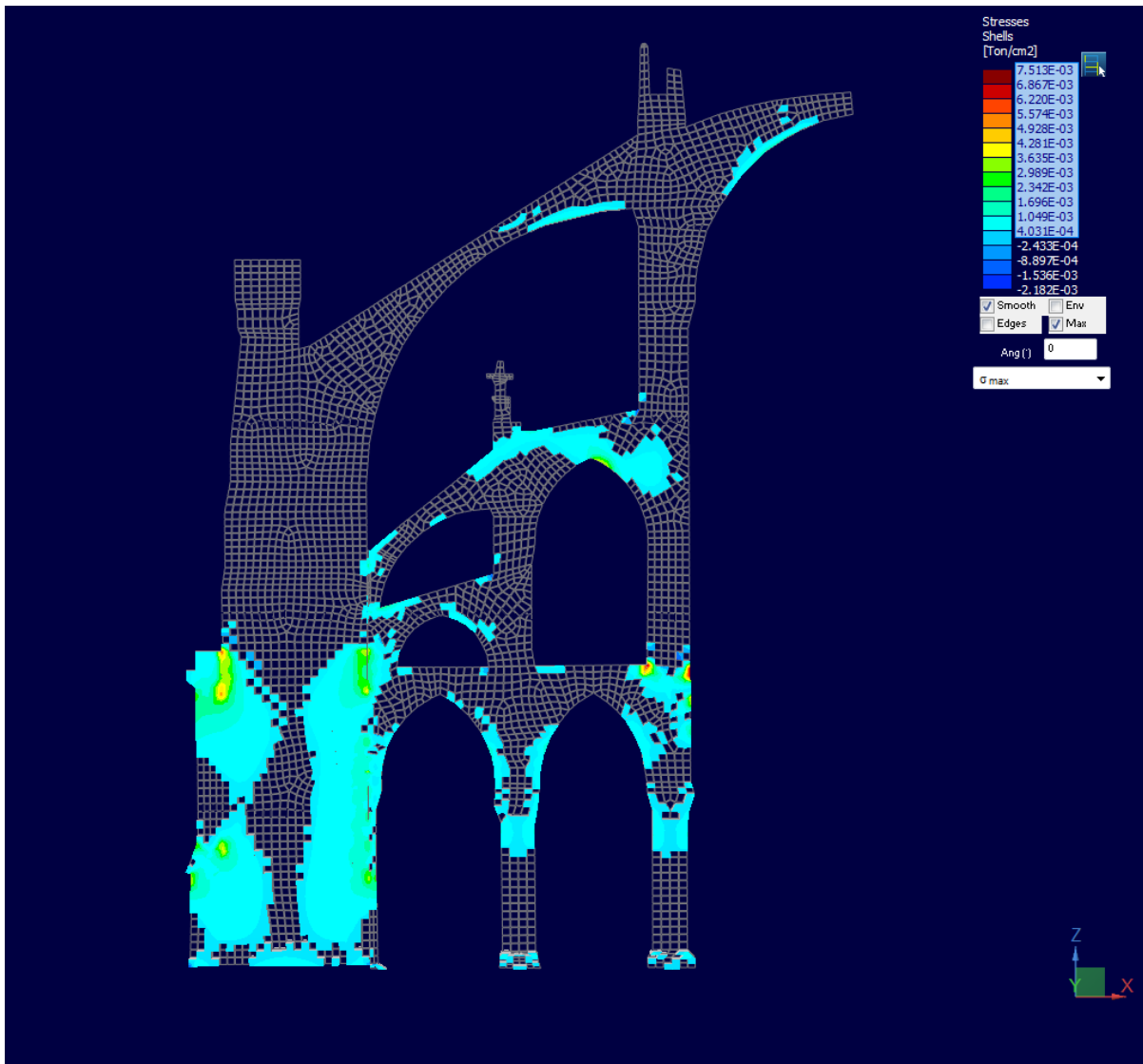
Image courtesy of mappinggothic.org, Media Center for Art History, Department of Art History and Archaeology, Trustees of Columbia University



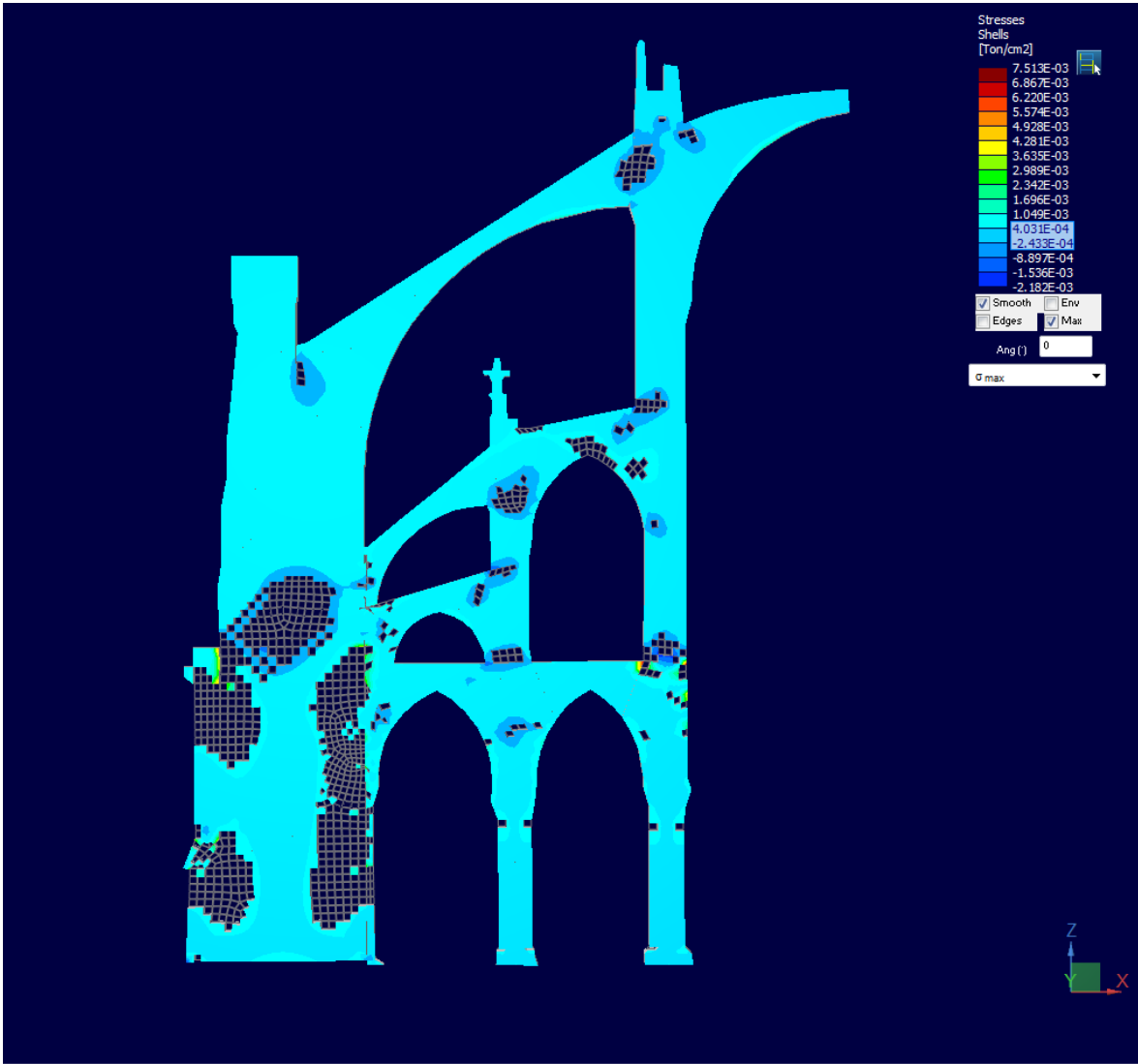
Cross Section of Cathédrale d'Amiens

Image courtesy of mappinggothic.org, Media Center for Art History, Department of Art History and Archaeology, Trustees of Columbia University

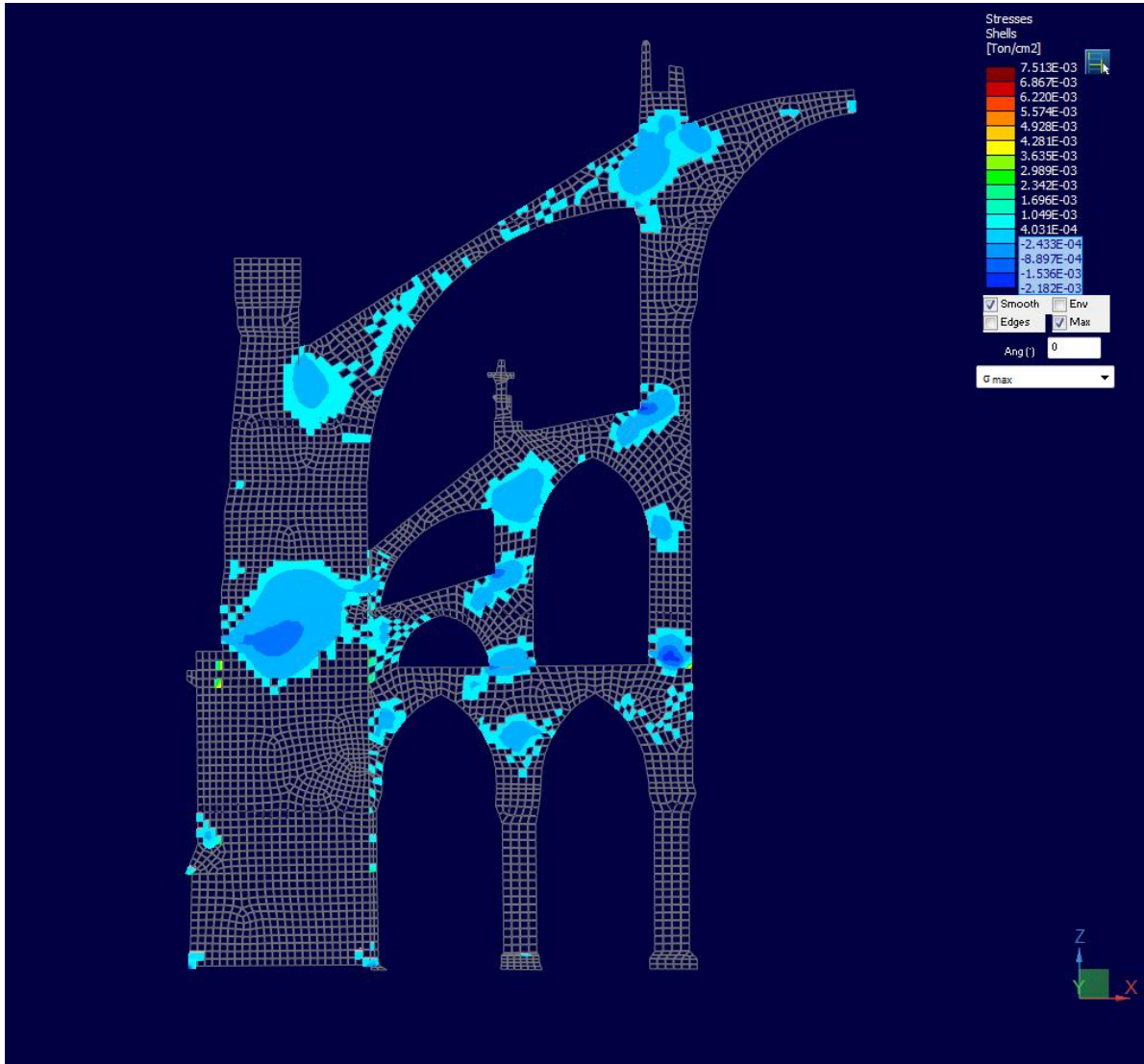
Appendix C – Model Renderings



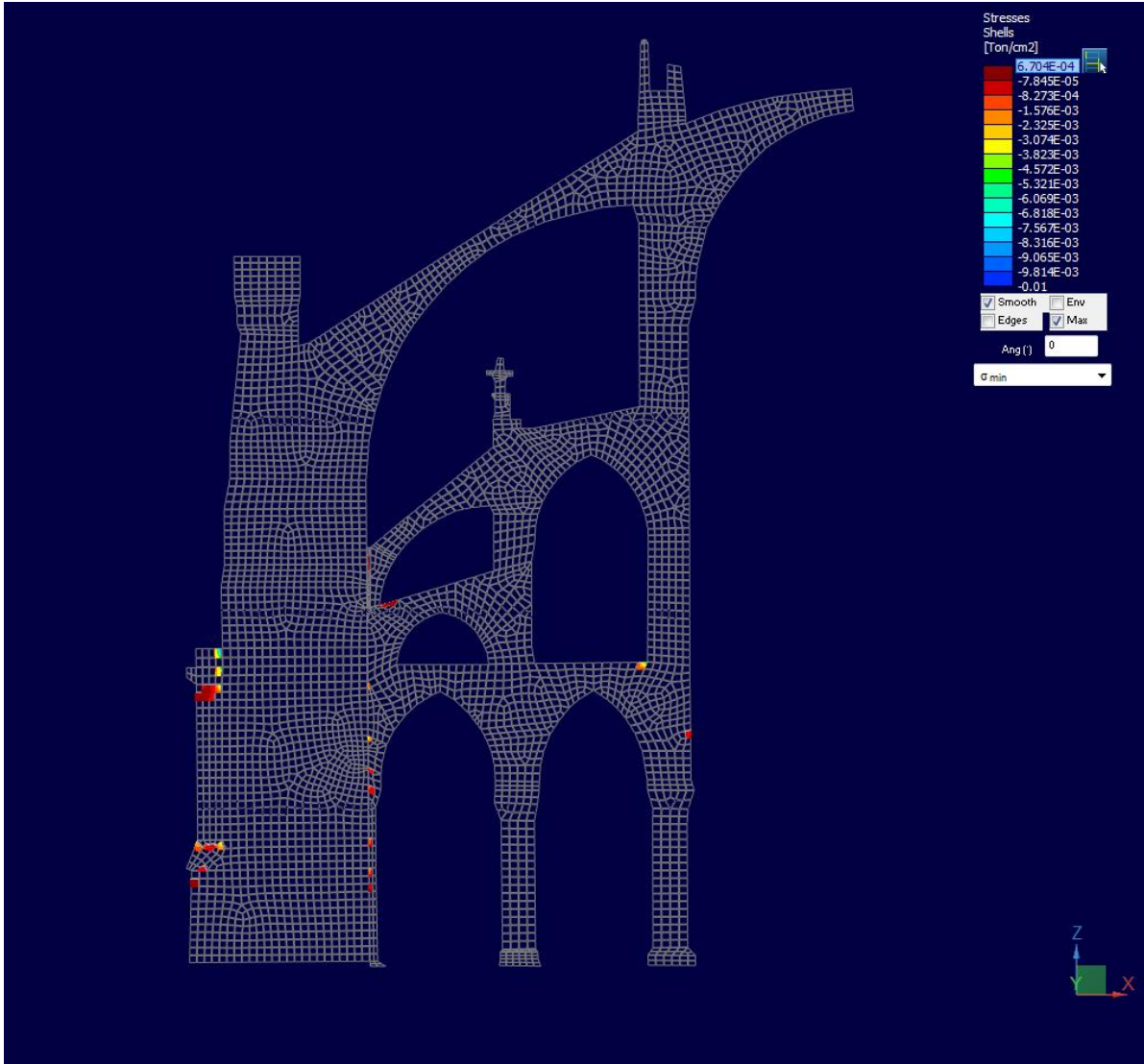
Maximum Principal Stresses ($4.031 \times 10^{-4} \sim 7.513 \times 10^{-3}$ ton/cm²) of Notre-Dame de Paris



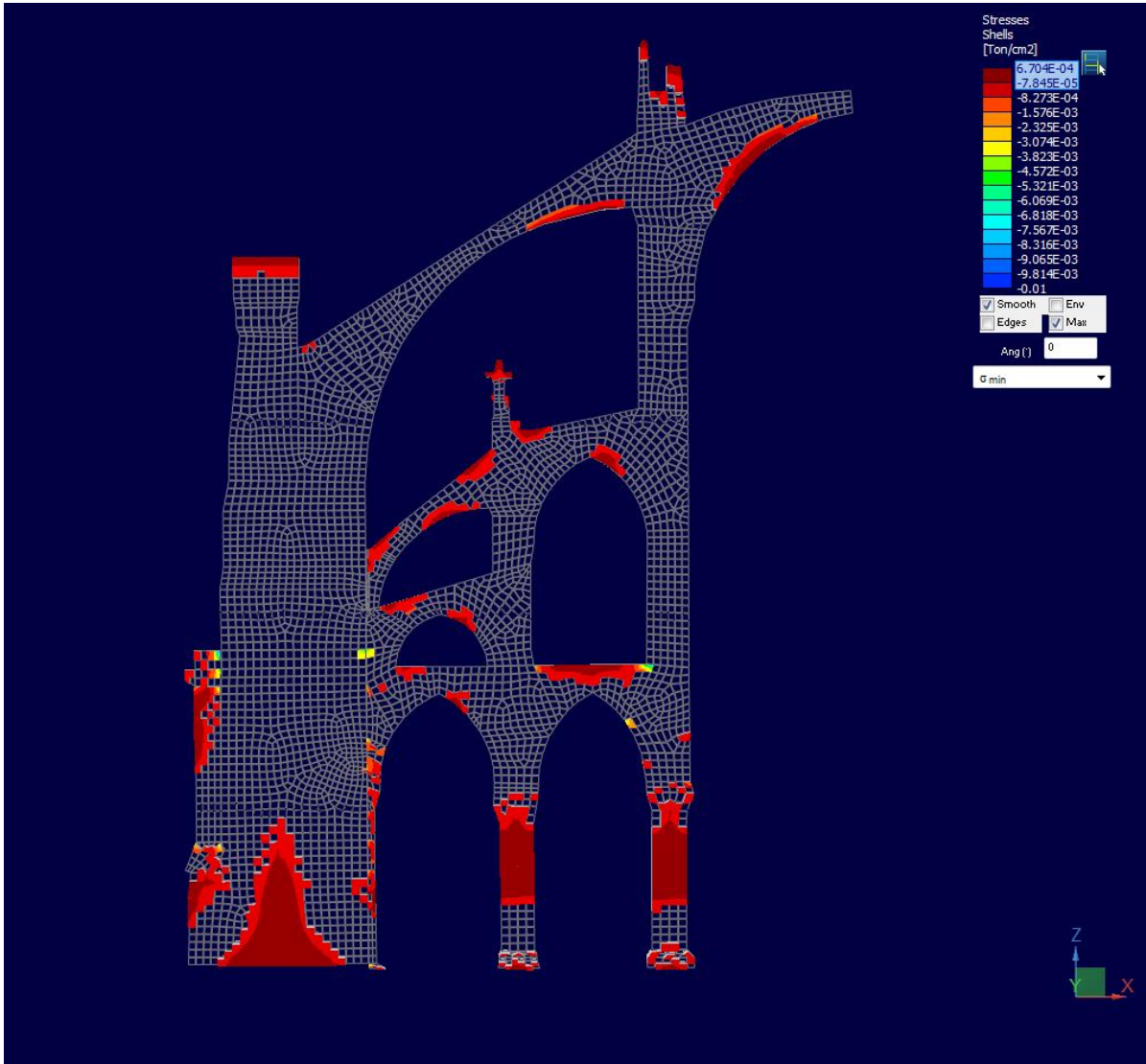
Maximum Principal Stresses ($4.031 \times 10^{-4} \sim -2.433 \times 10^{-4}$ ton/cm²) of Notre-Dame de Paris



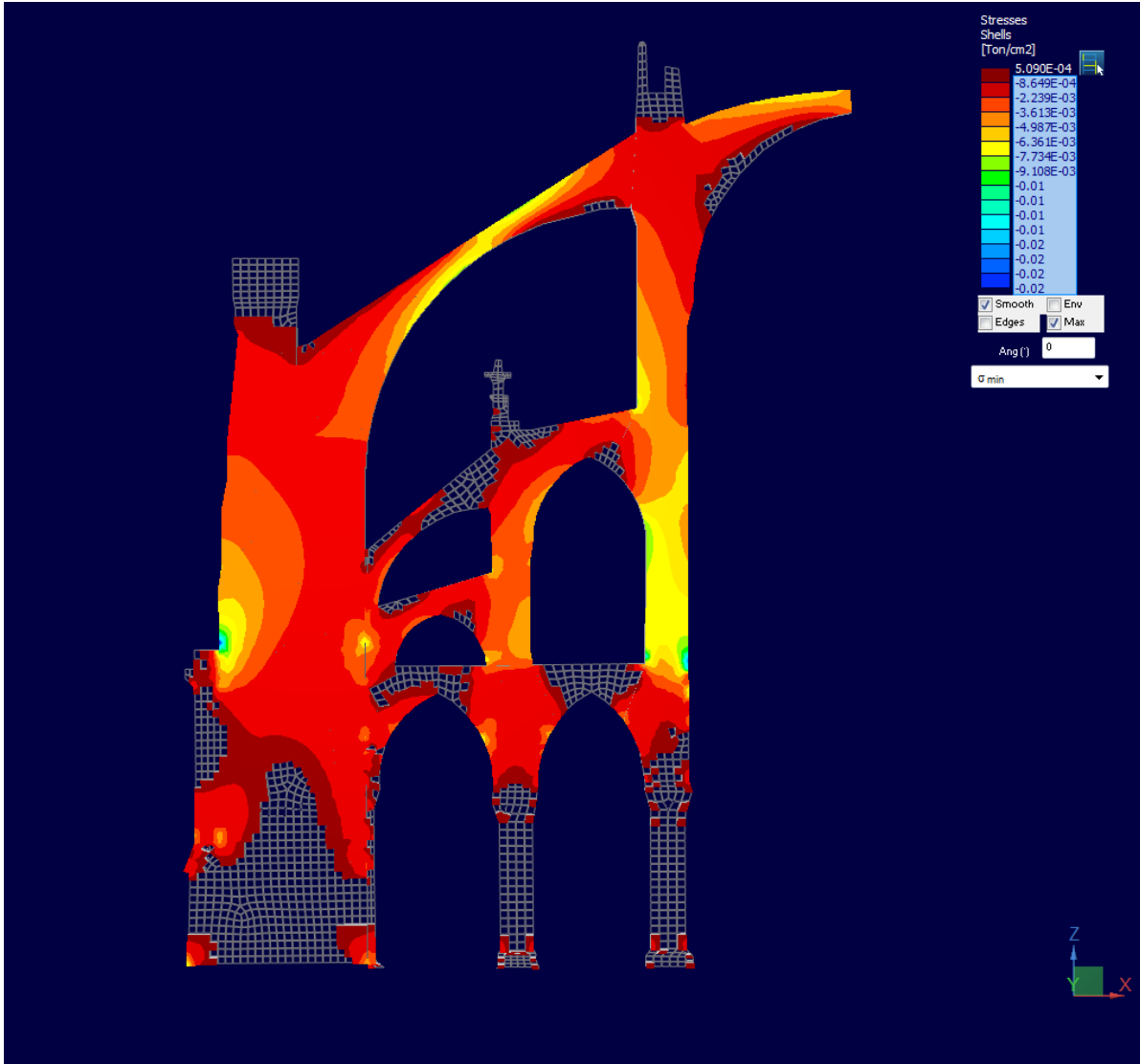
Maximum Principal Stresses ($-2.182 \times 10^{-3} \sim -2.433 \times 10^{-4}$ ton/cm²) of Notre-Dame de Paris



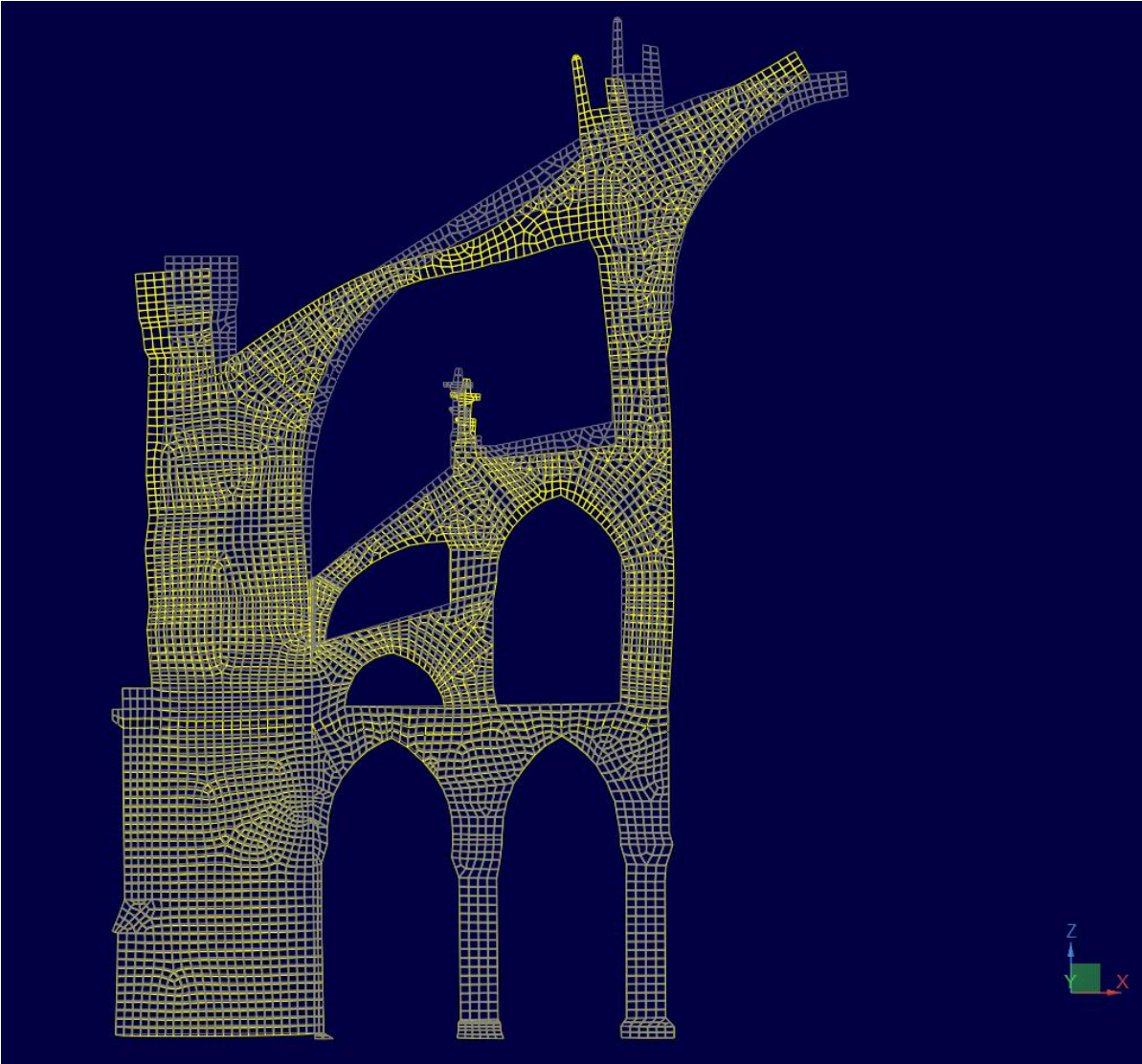
Minimum Principal Stresses (6.704×10^{-4} ton/cm²) of Notre-Dame de Paris



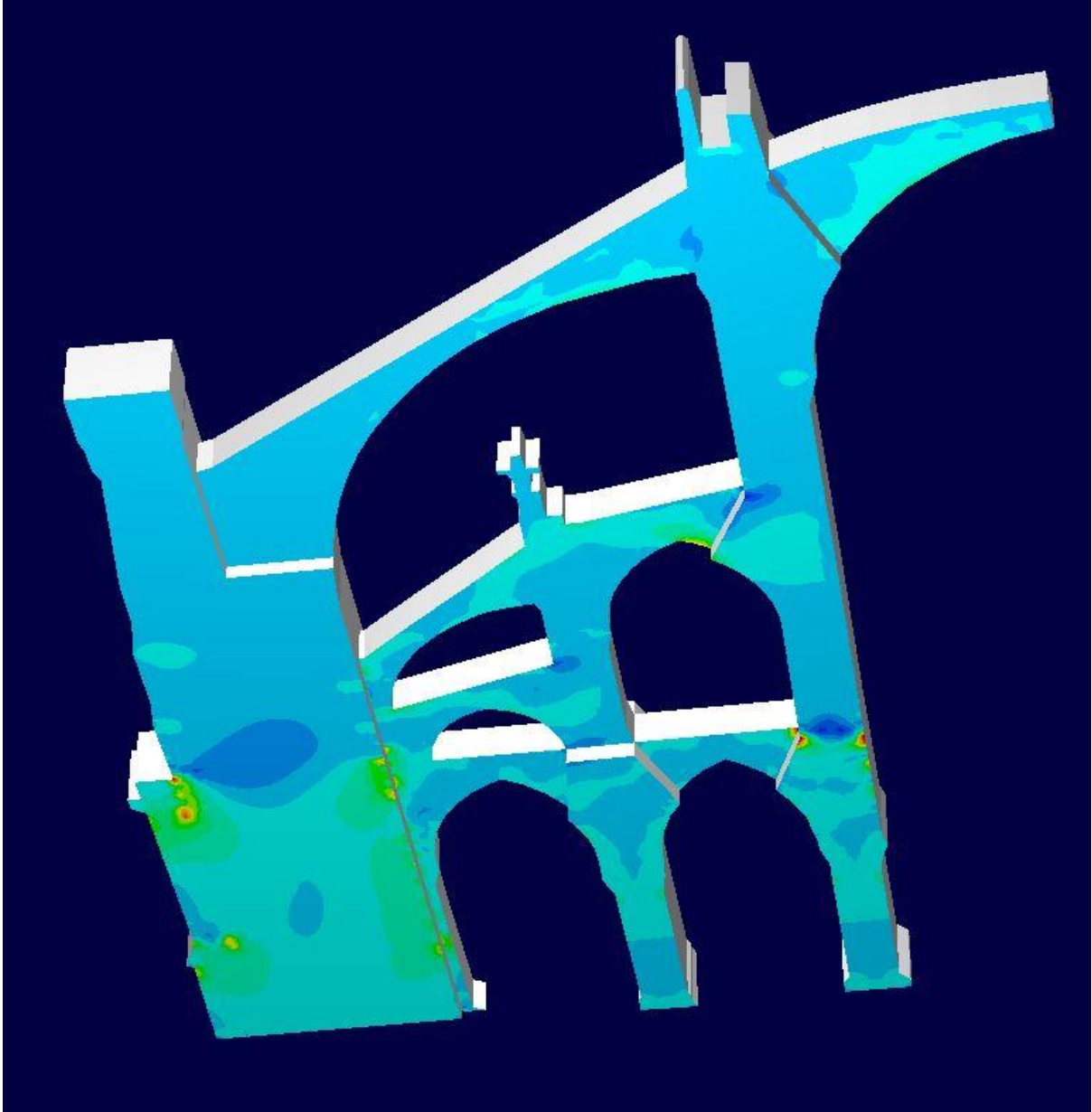
Minimum Principal Stresses ($-7.845 \times 10^{-5} \sim 6.704 \times 10^{-4}$ ton/cm²) of Notre-Dame de Paris



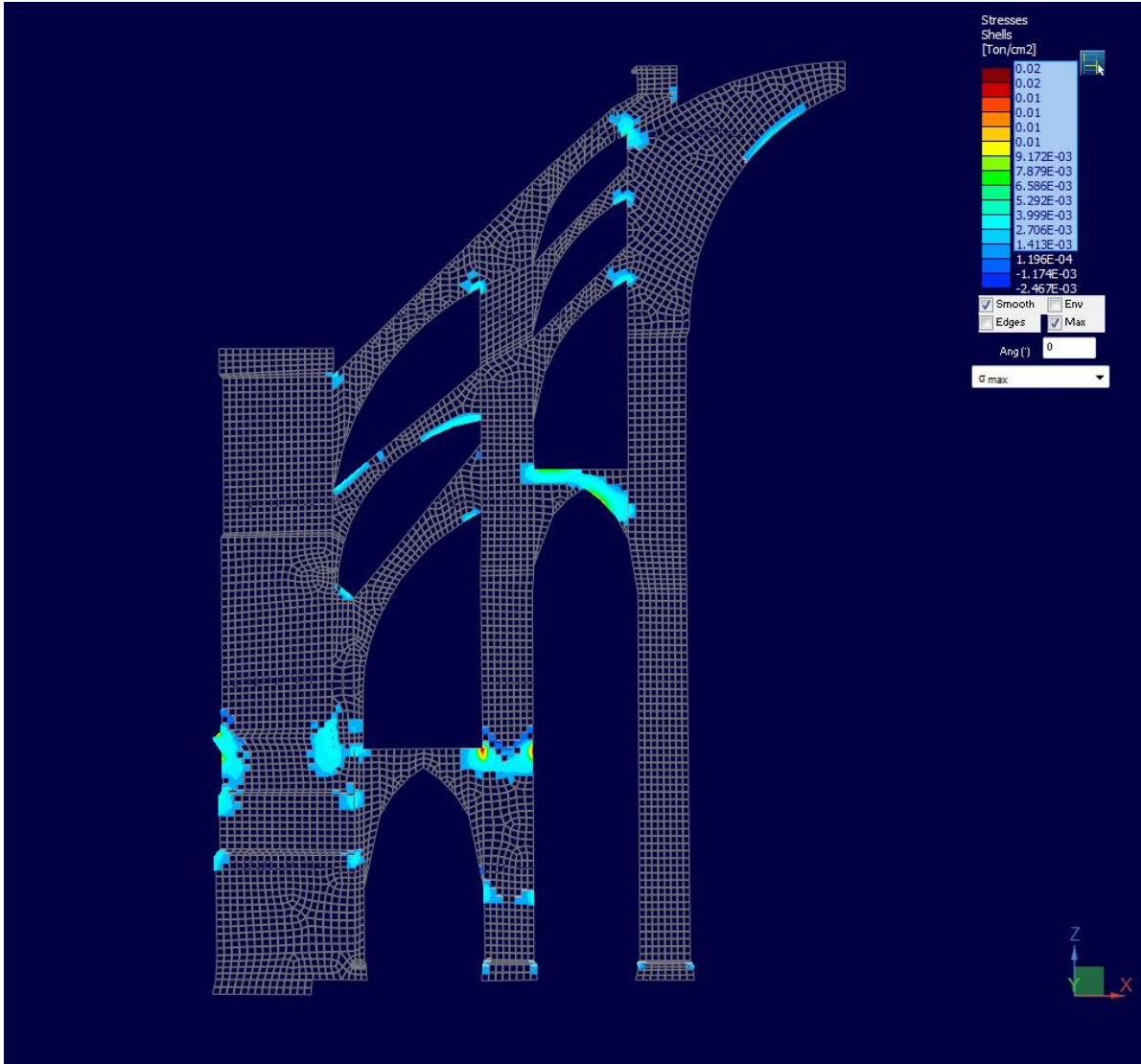
Minimum Principal Stresses (-0.02 ~ -8.649x10⁻⁴ ton/cm²) of Notre-Dame de Paris



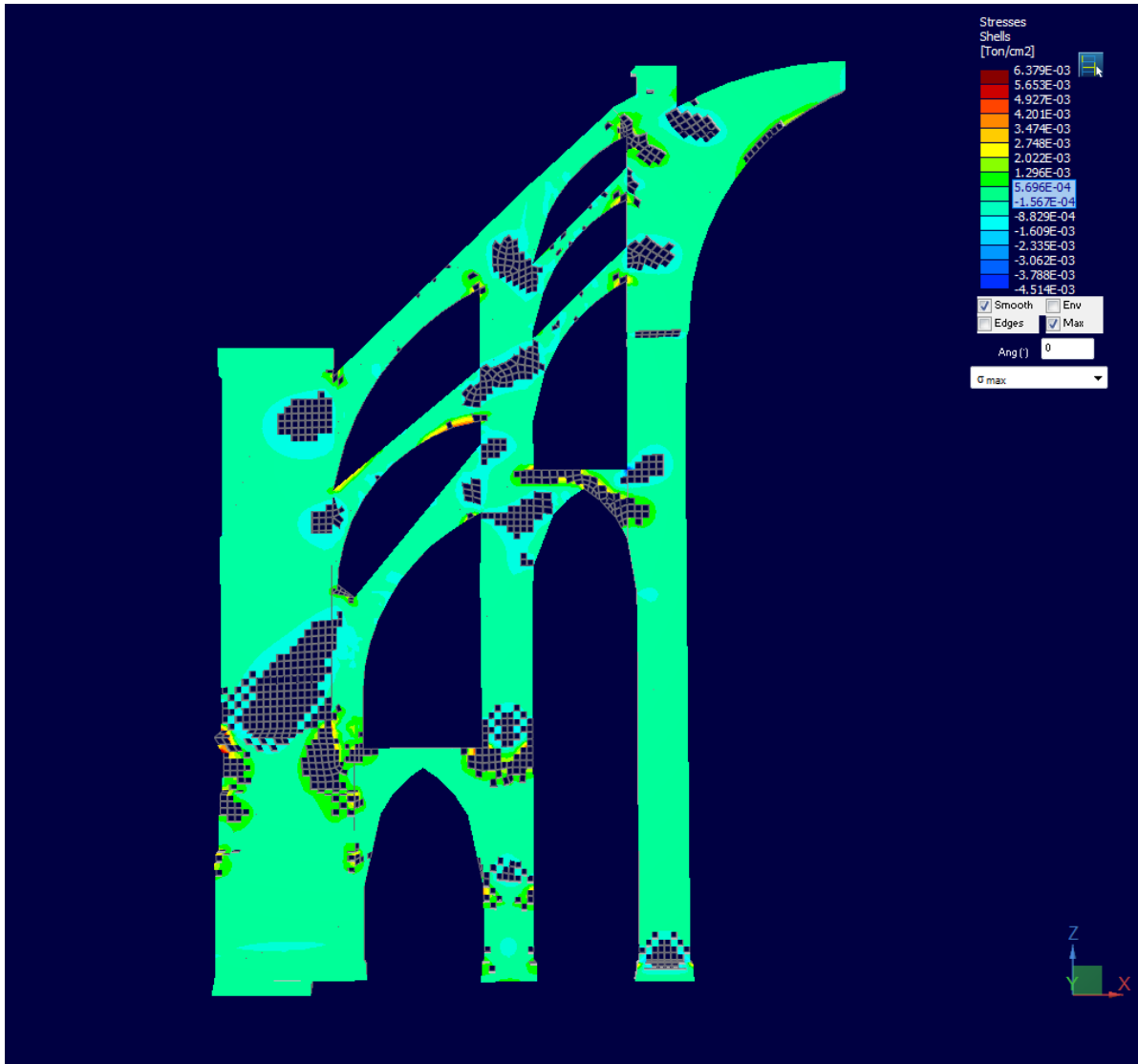
Projected Cross Section Profile Deflection of Notre-Dame de Paris



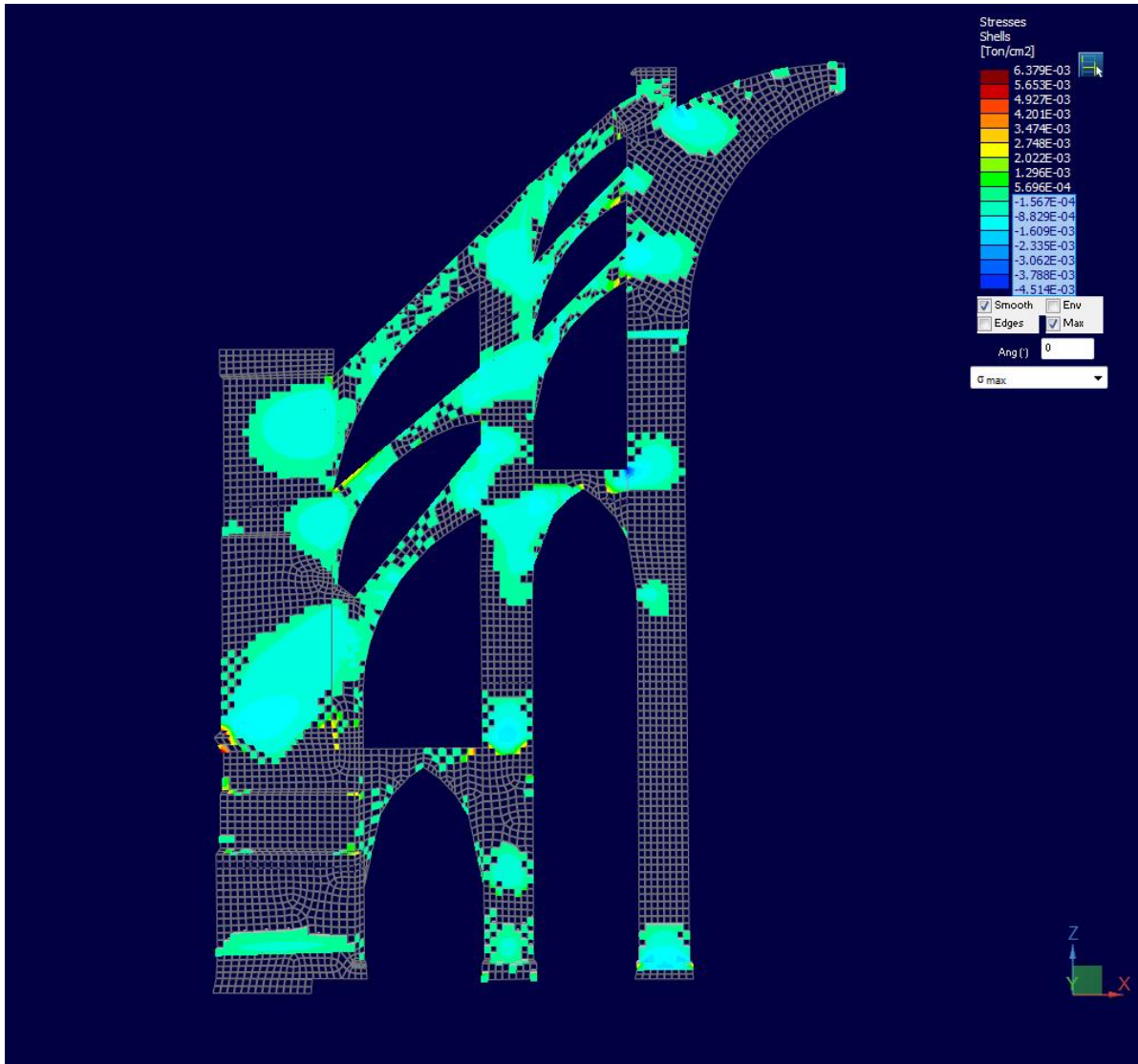
Profile of varying thicknesses of Notre-Dame de Paris



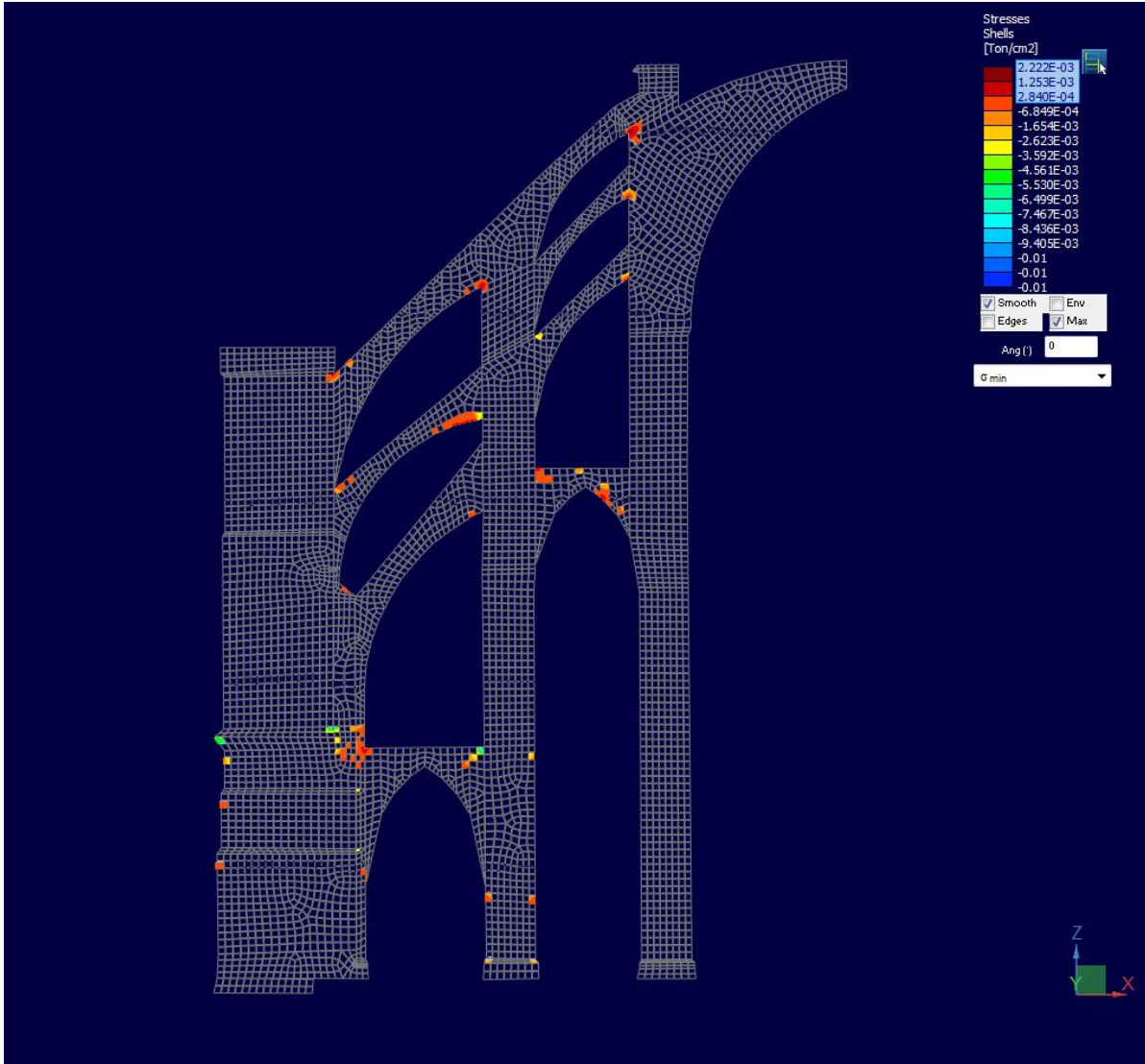
Maximum Principal Stresses ($1.413 \times 10^{-3} \sim 0.02$ ton/cm²) of Cathédrale Saint-Etienne, Bourges



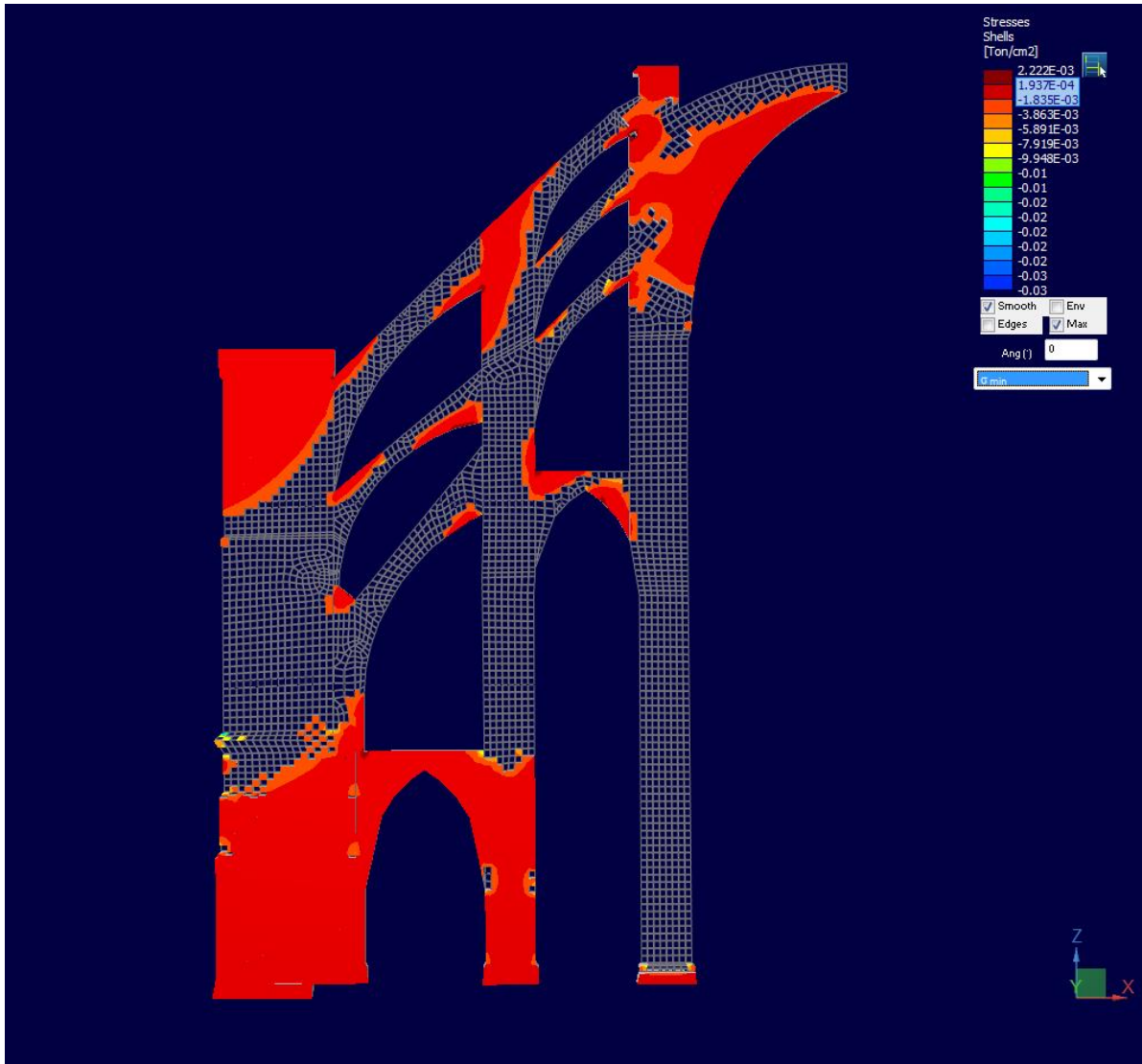
Maximum Principal Stresses ($-1.567 \times 10^{-4} \sim 5.696 \times 10^{-4}$ ton/cm²) of Cathédrale Saint-Etienne, Bourges



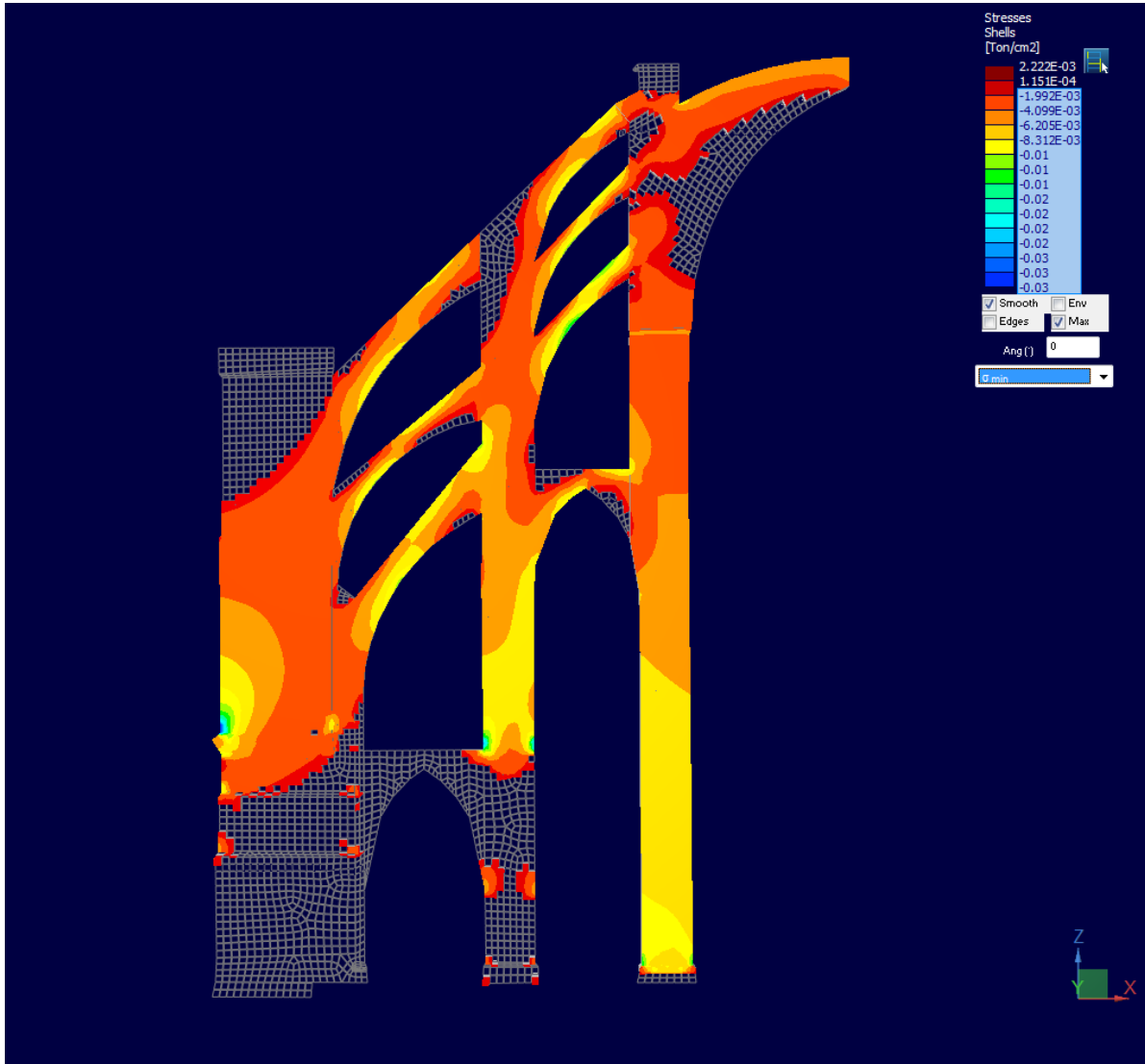
Maximum Principal Stresses ($-4.514 \times 10^{-3} \sim -1.567 \times 10^{-4}$ ton/cm²) of Cathédrale Saint-Etienne, Bourges



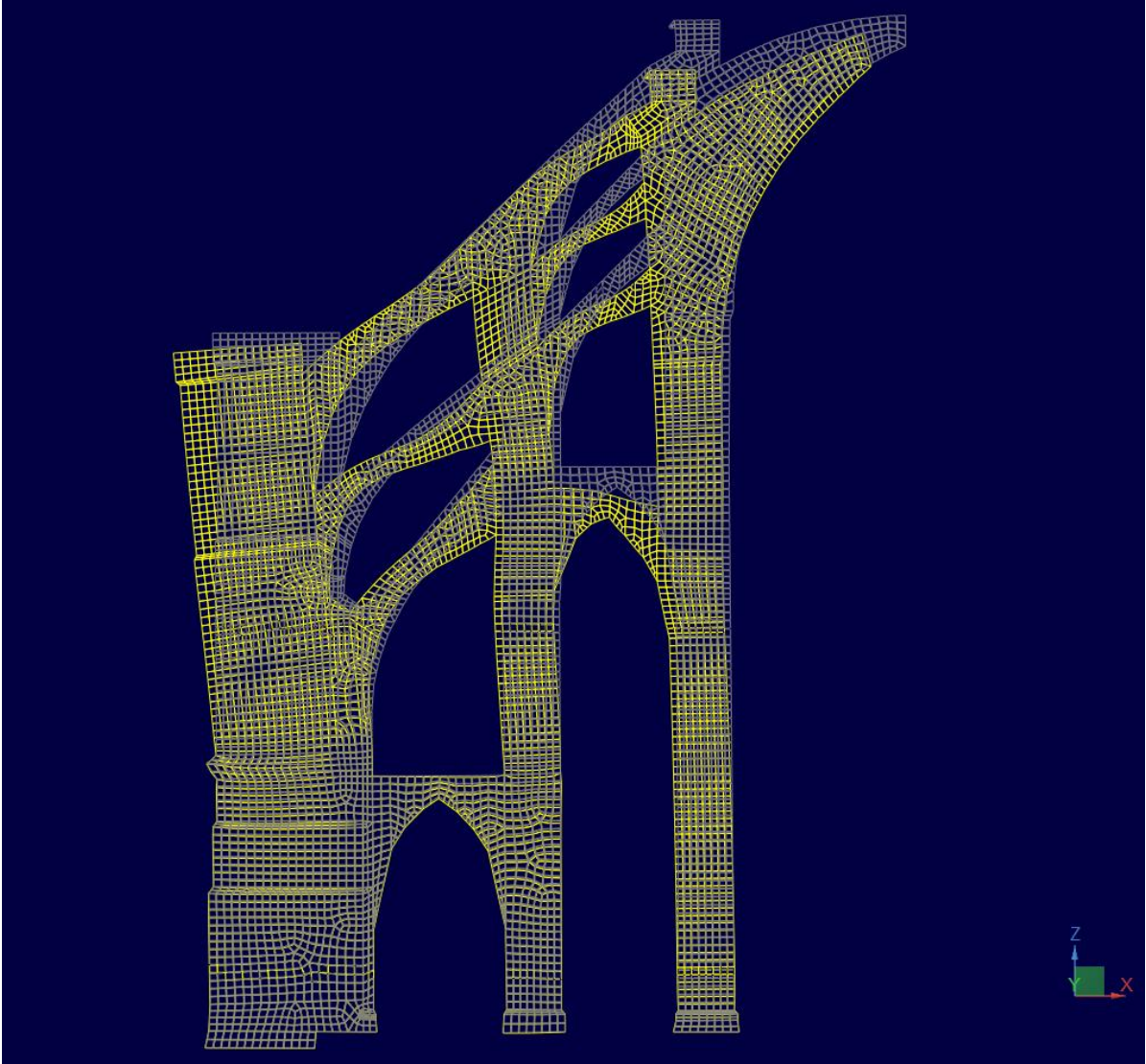
Minimum Principal Stresses ($2.840 \times 10^{-4} \sim -2.222 \times 10^{-3}$ ton/cm²) of Cathédrale Saint-Etienne, Bourges



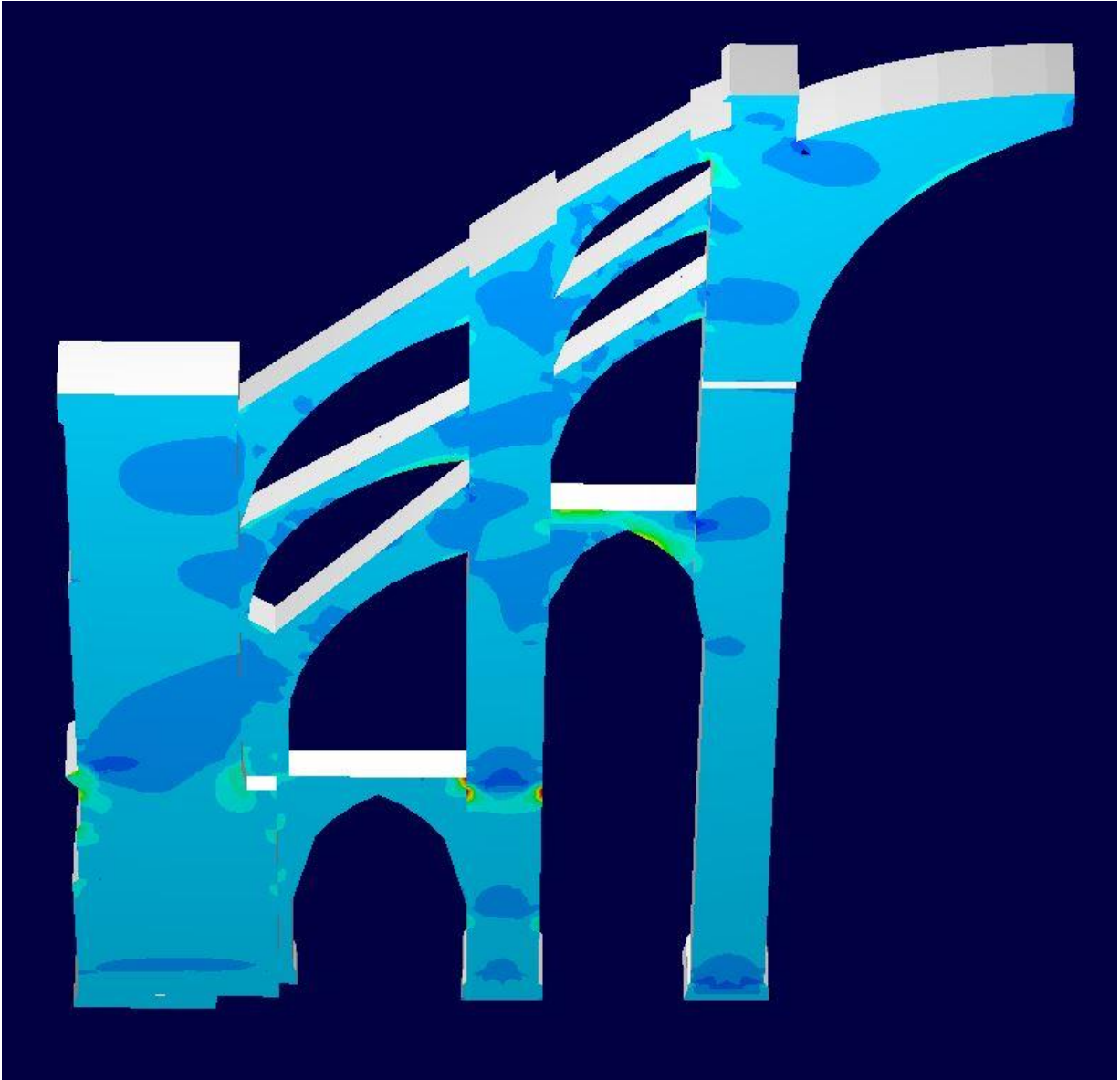
Minimum Principal Stresses ($-1.835 \times 10^{-3} \sim 1.937 \times 10^{-4}$ ton/cm²) of Cathédrale Saint-Etienne, Bourges



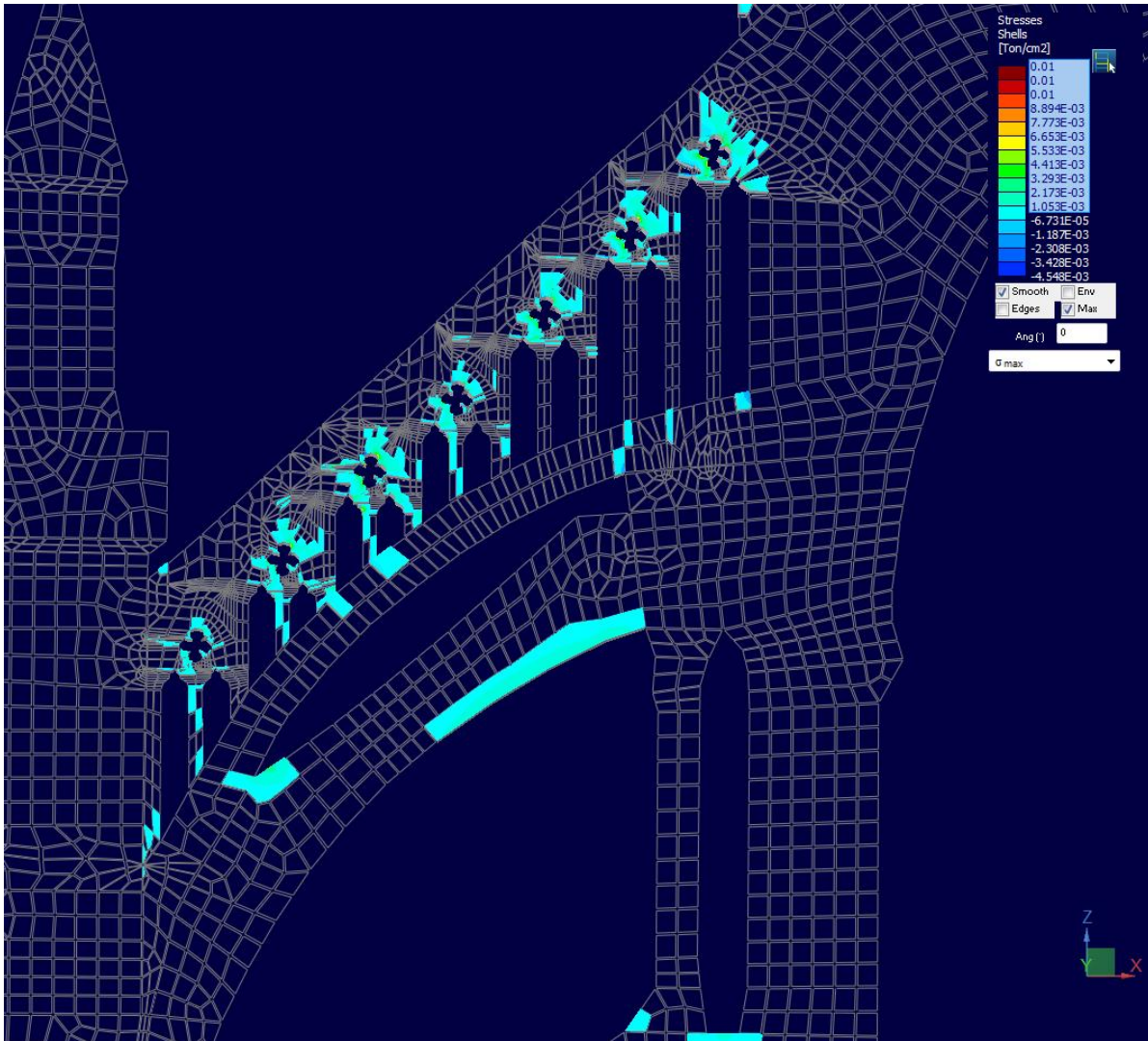
Minimum Principal Stresses ($-0.03 \sim -1.992 \times 10^{-3}$ ton/cm²) of Cathédrale Saint-Etienne, Bourges



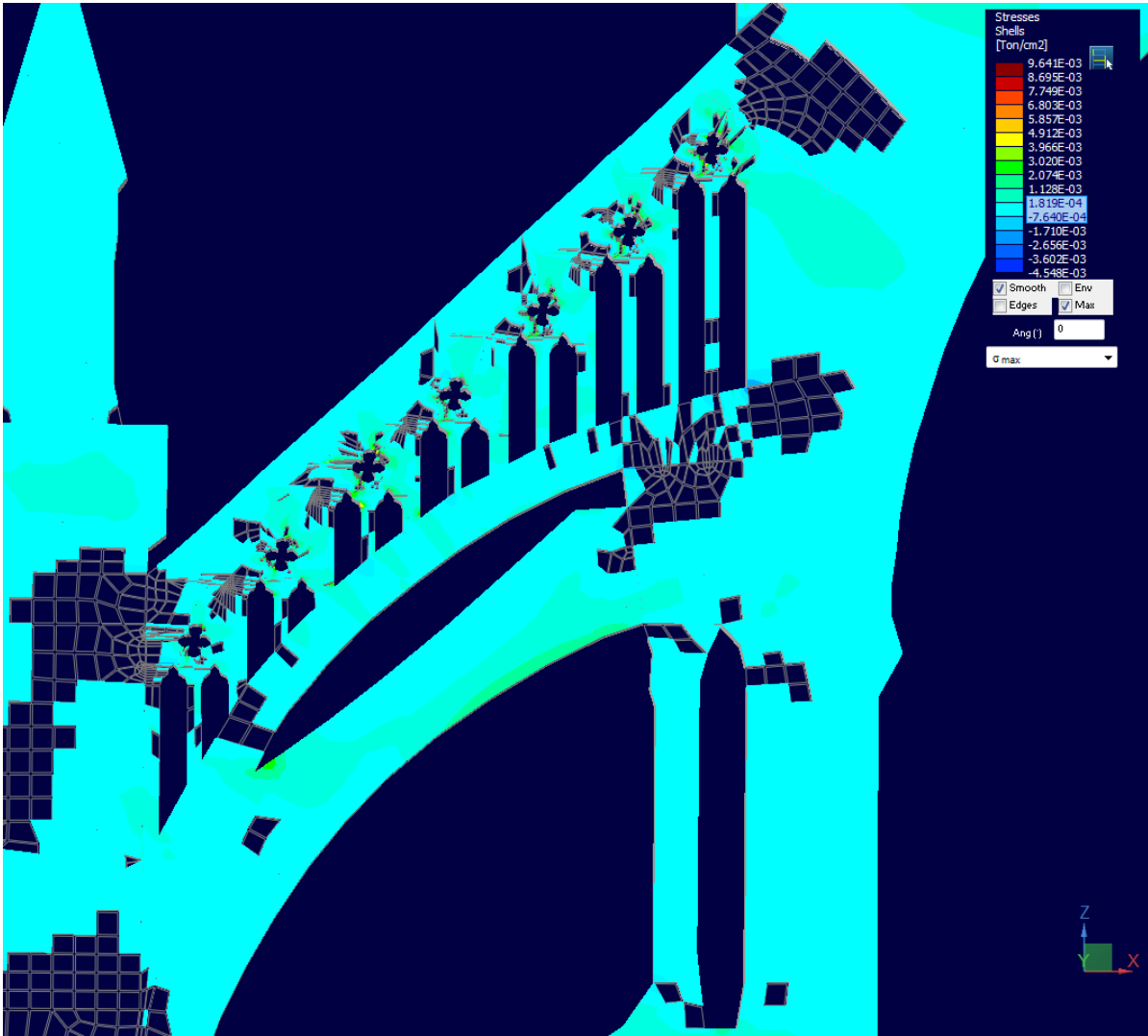
Projected Cross Section Profile Deflection of Cathédrale Saint-Etienne, Bourges



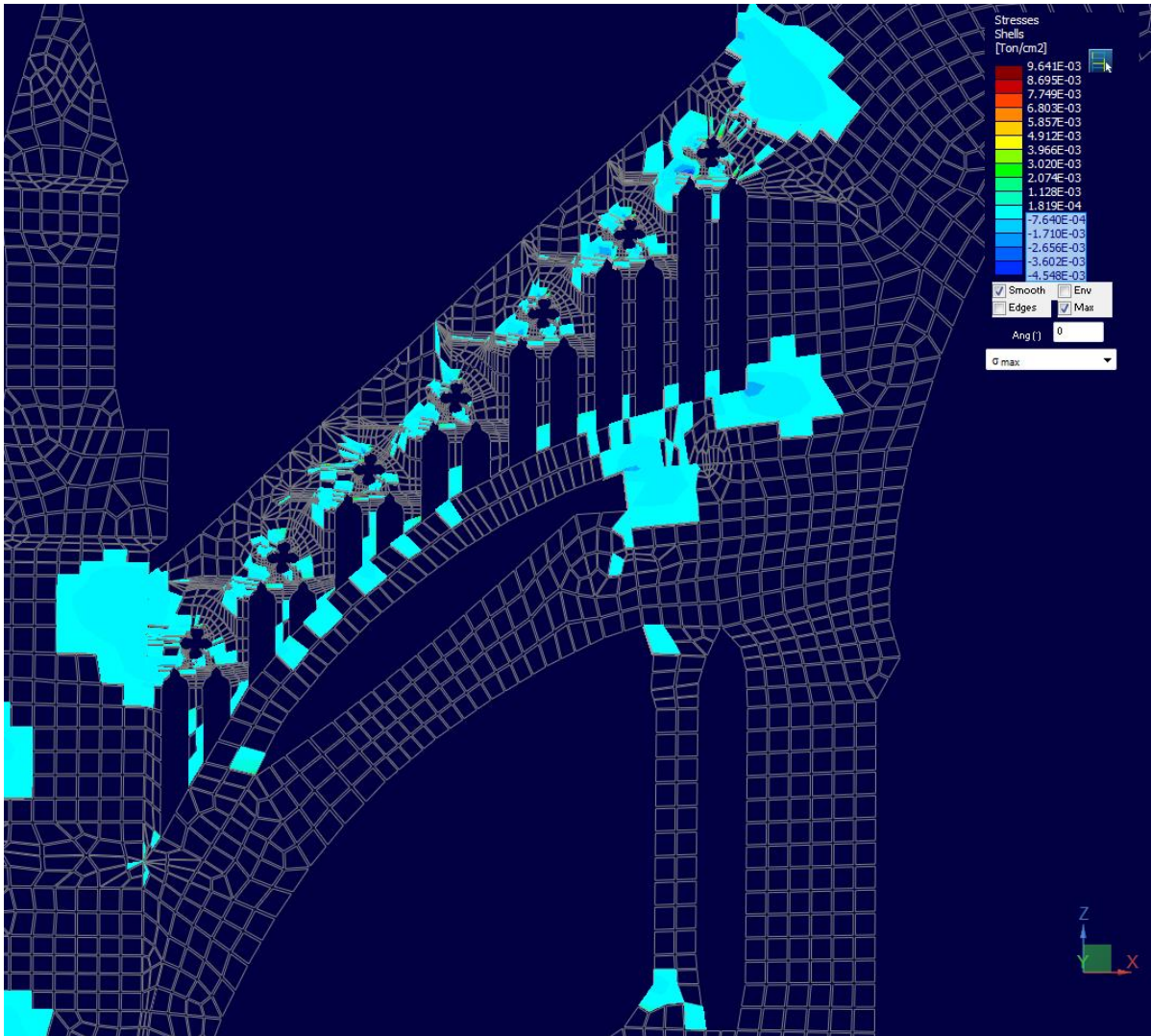
Profile of varying thicknesses of Cathédrale Saint-Étienne, Bourges



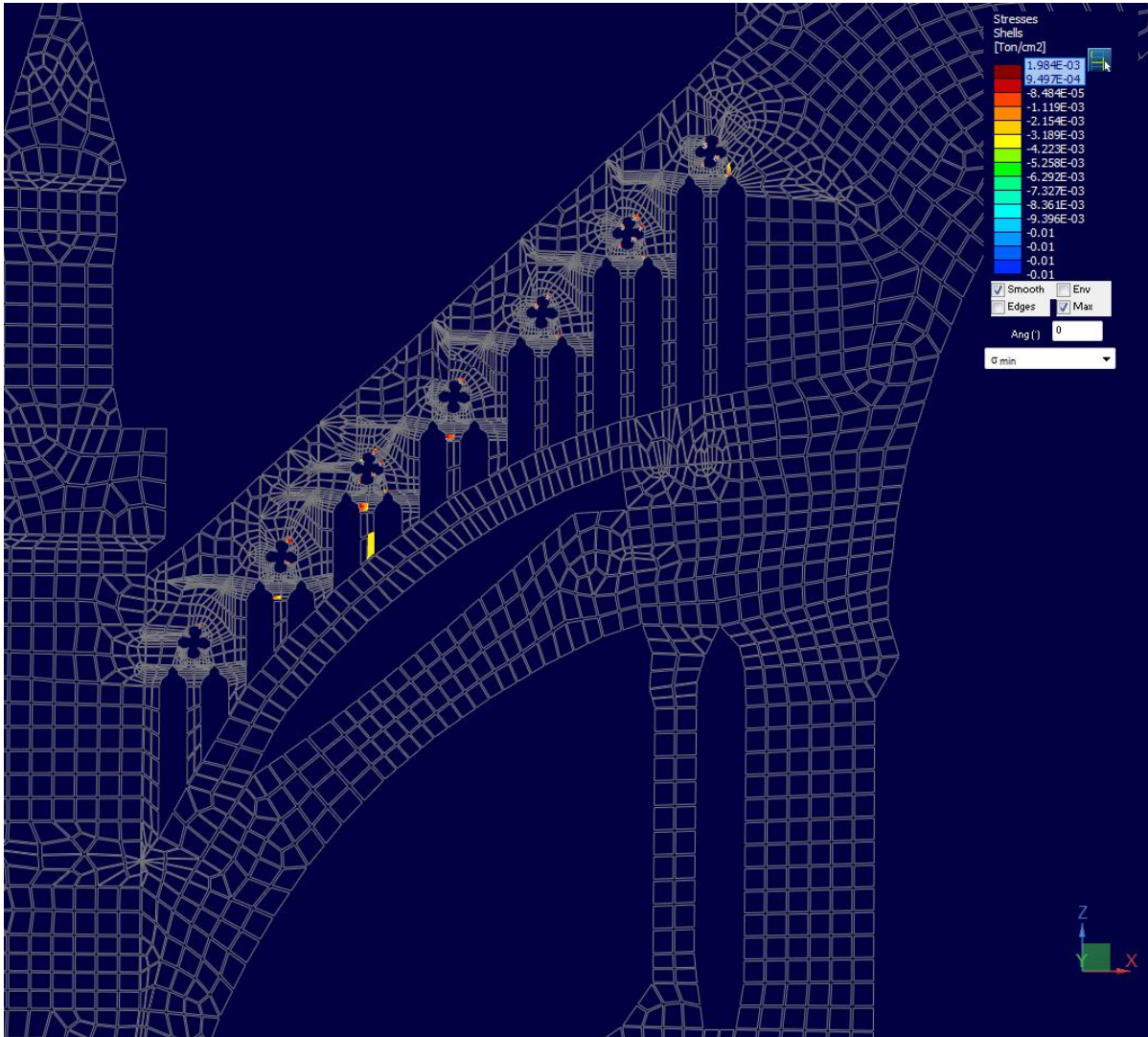
Maximum Principal Stresses ($1.053 \times 10^{-3} \sim 0.01$ ton/cm²) of Cathédrale d'Amiens (état actuel) of Flying Buttress 1 and 3



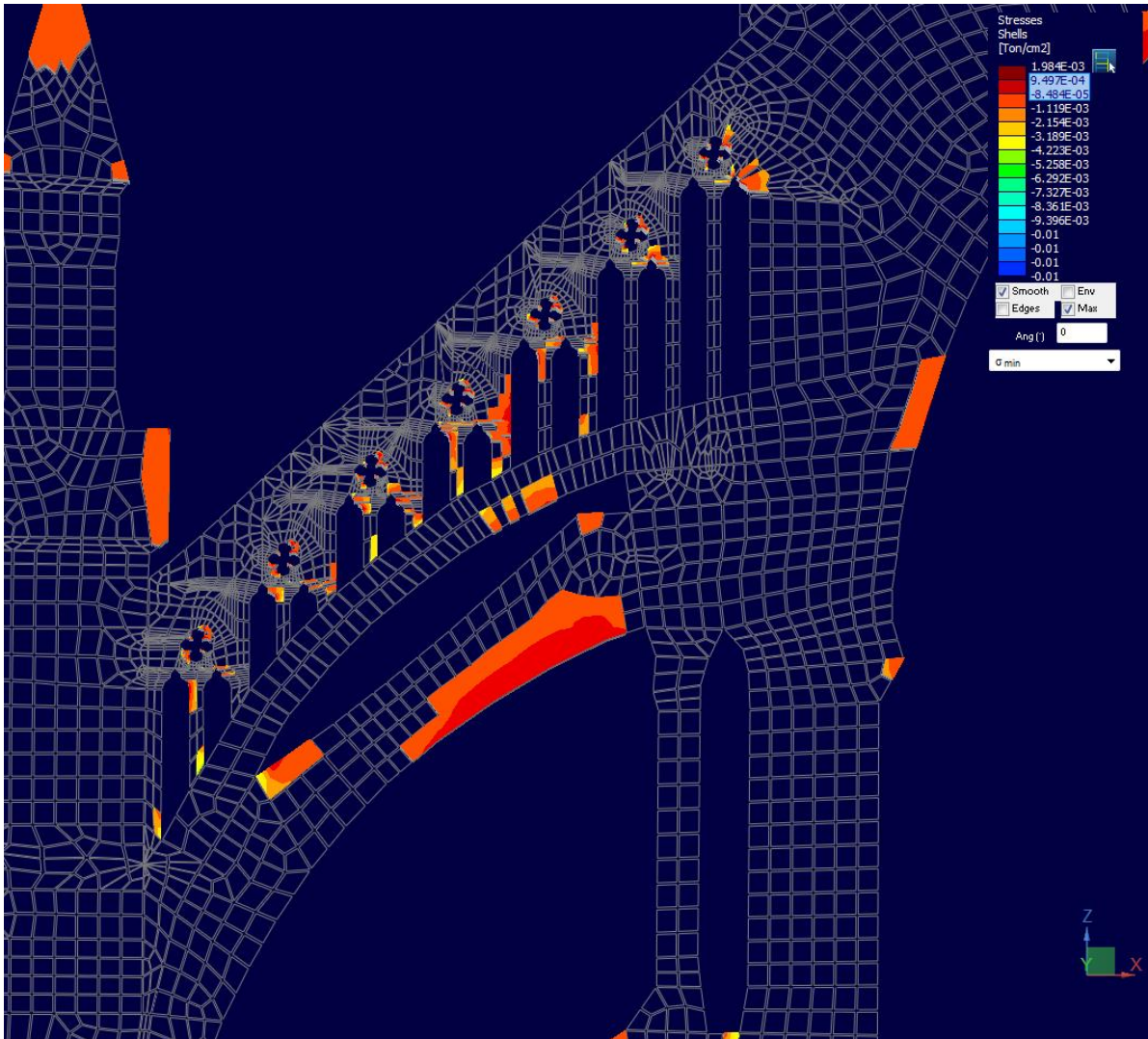
Maximum Principal Stresses ($-7.640 \times 10^{-4} \sim 1.819 \times 10^{-4}$ ton/cm²) of Cathédrale d'Amiens (état actuel) of Flying Buttress 1 and 3



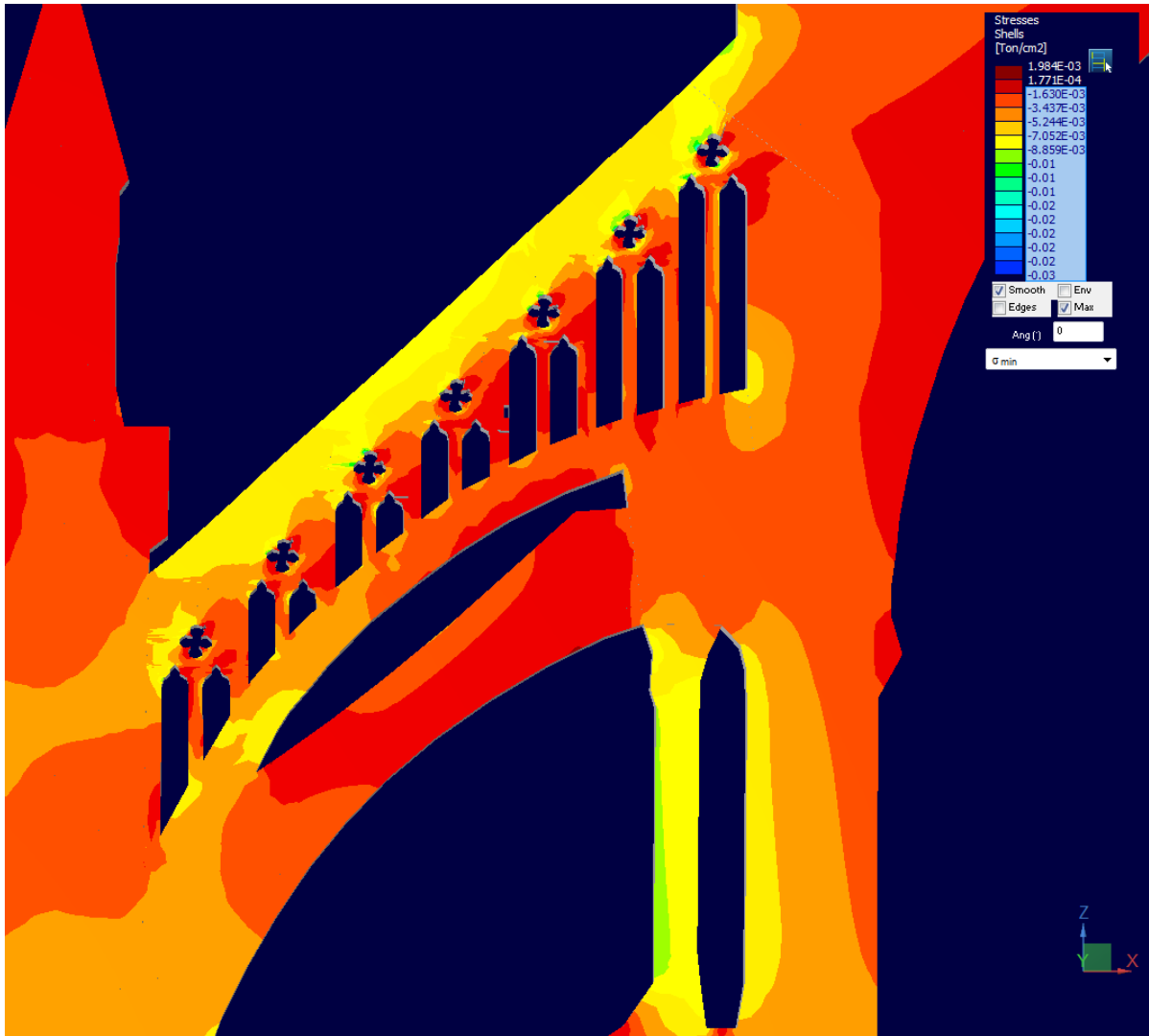
Maximum Principal Stresses ($-4.548 \times 10^{-3} \sim -7.640 \times 10^{-4}$ ton/cm²) of Cathédrale d'Amiens (état actuel) of Flying Buttress 1 and 3



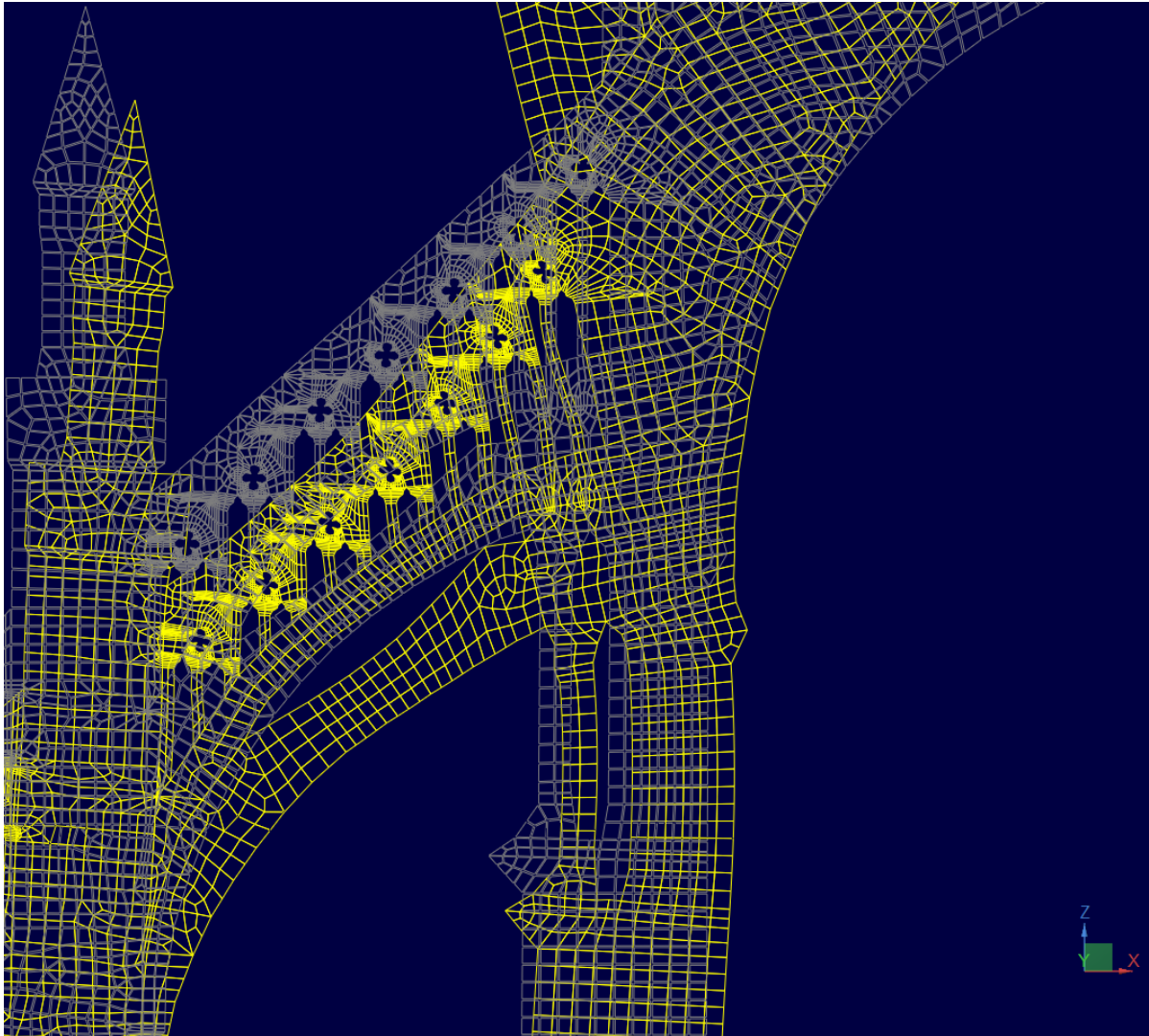
Minimum Principal Stresses ($9.497 \times 10^{-4} \sim 1.984 \times 10^{-3}$ ton/cm²) of Cathédrale d'Amiens (état actuel) of Flying Buttress 1 and 3



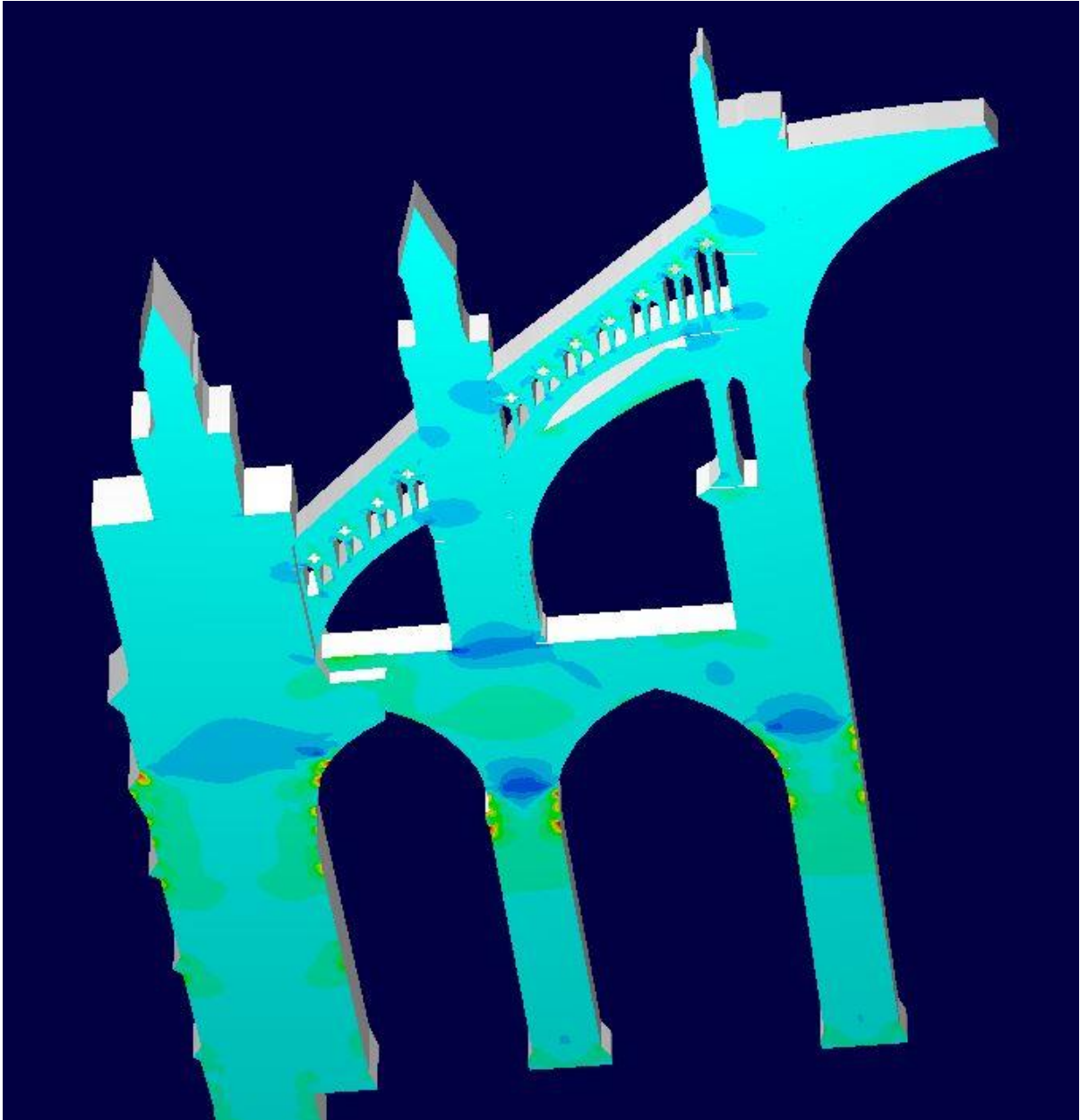
Minimum Principal Stresses ($-8.484 \times 10^{-5} \sim 9.497 \times 10^{-4}$ ton/cm²) of Cathédrale d'Amiens (état actuel) of Flying Buttress 1 and 3



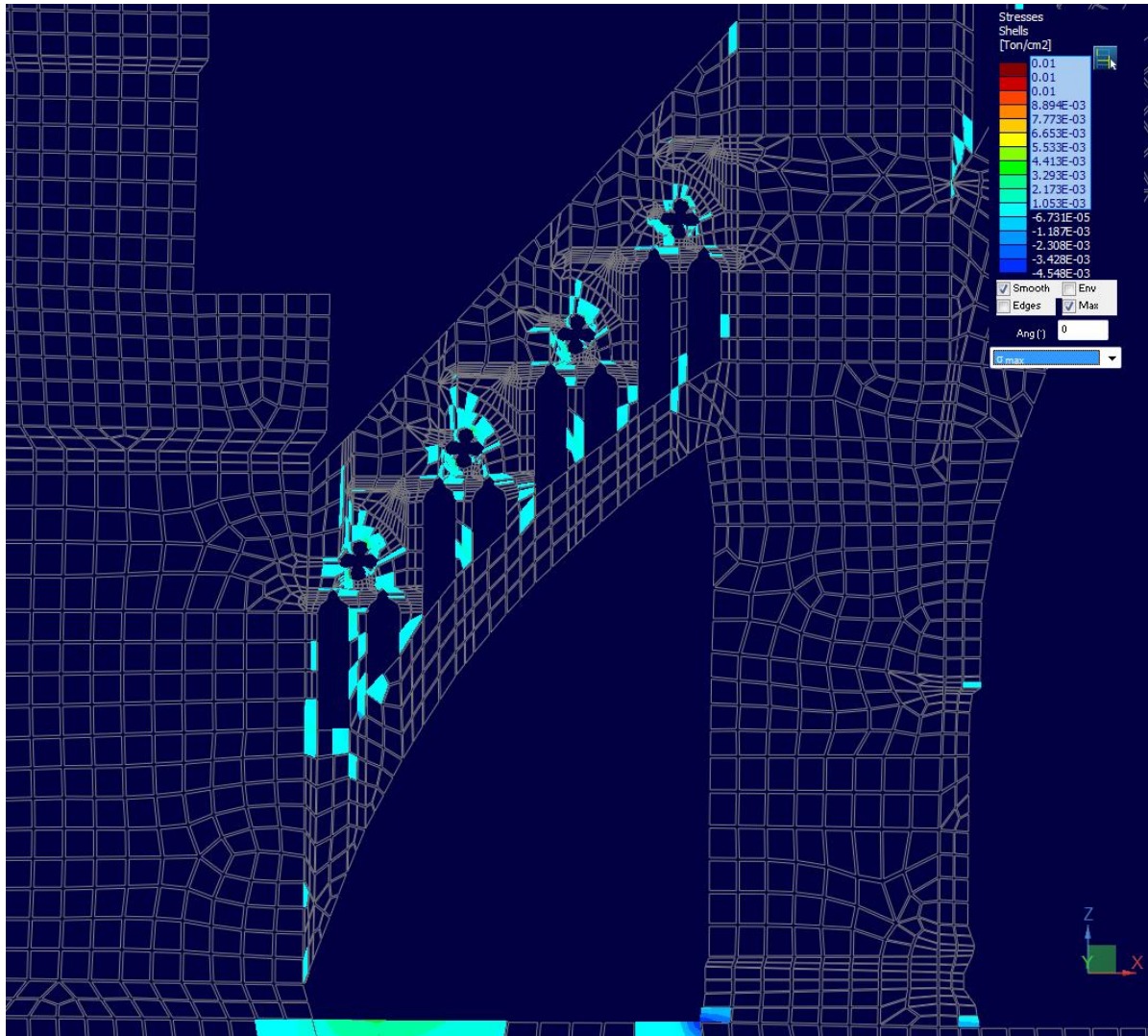
Minimum Principal Stresses (-0.02 ~ -1.630x10⁻³ ton/cm²) of Cathédrale d'Amiens (état actuel) of Flying Buttress 1 and 3



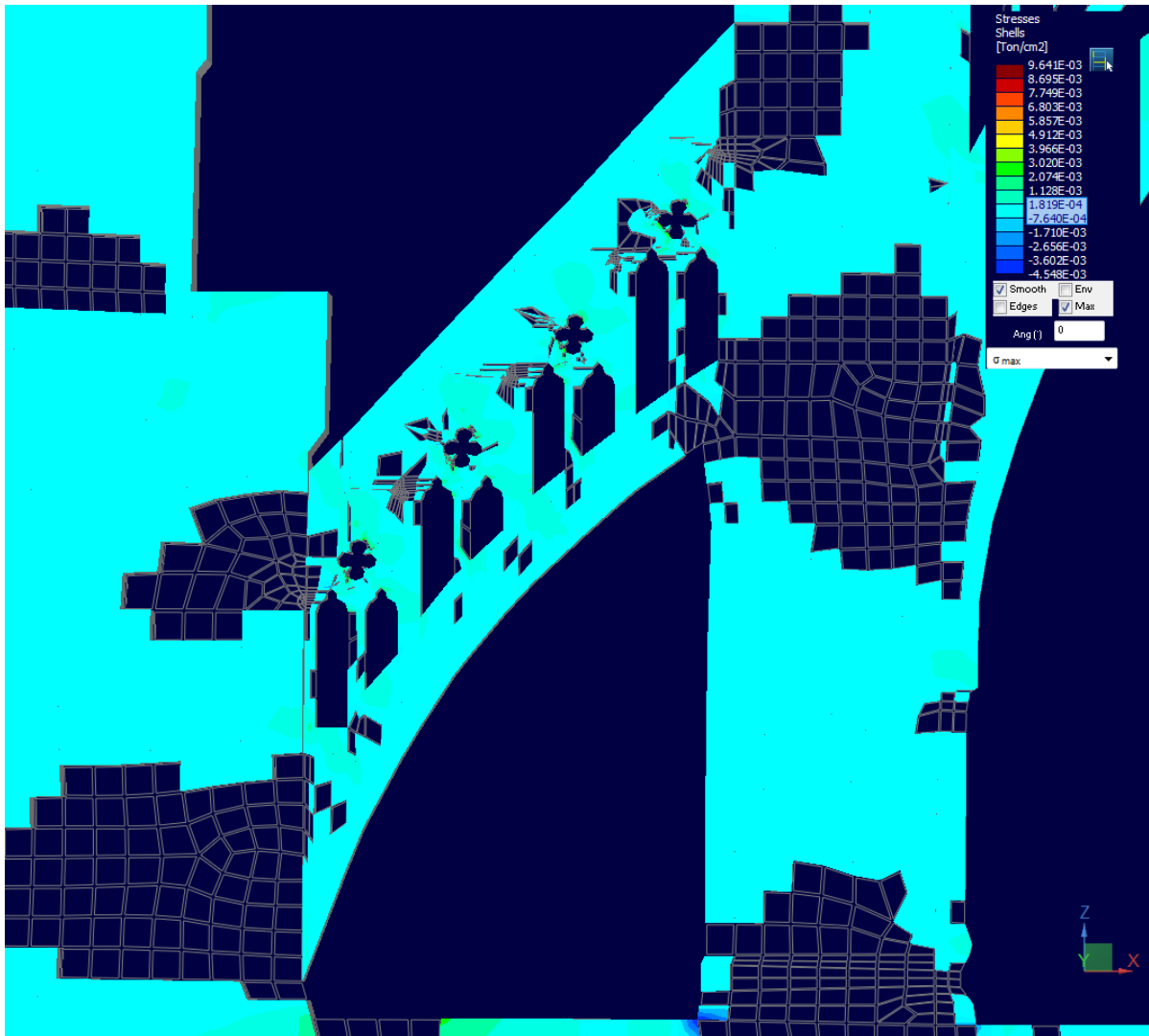
**Projected Cross Section Profile Deflection of Cathédrale d'Amiens (état actuel)
of Flying Buttress 1 and 3**



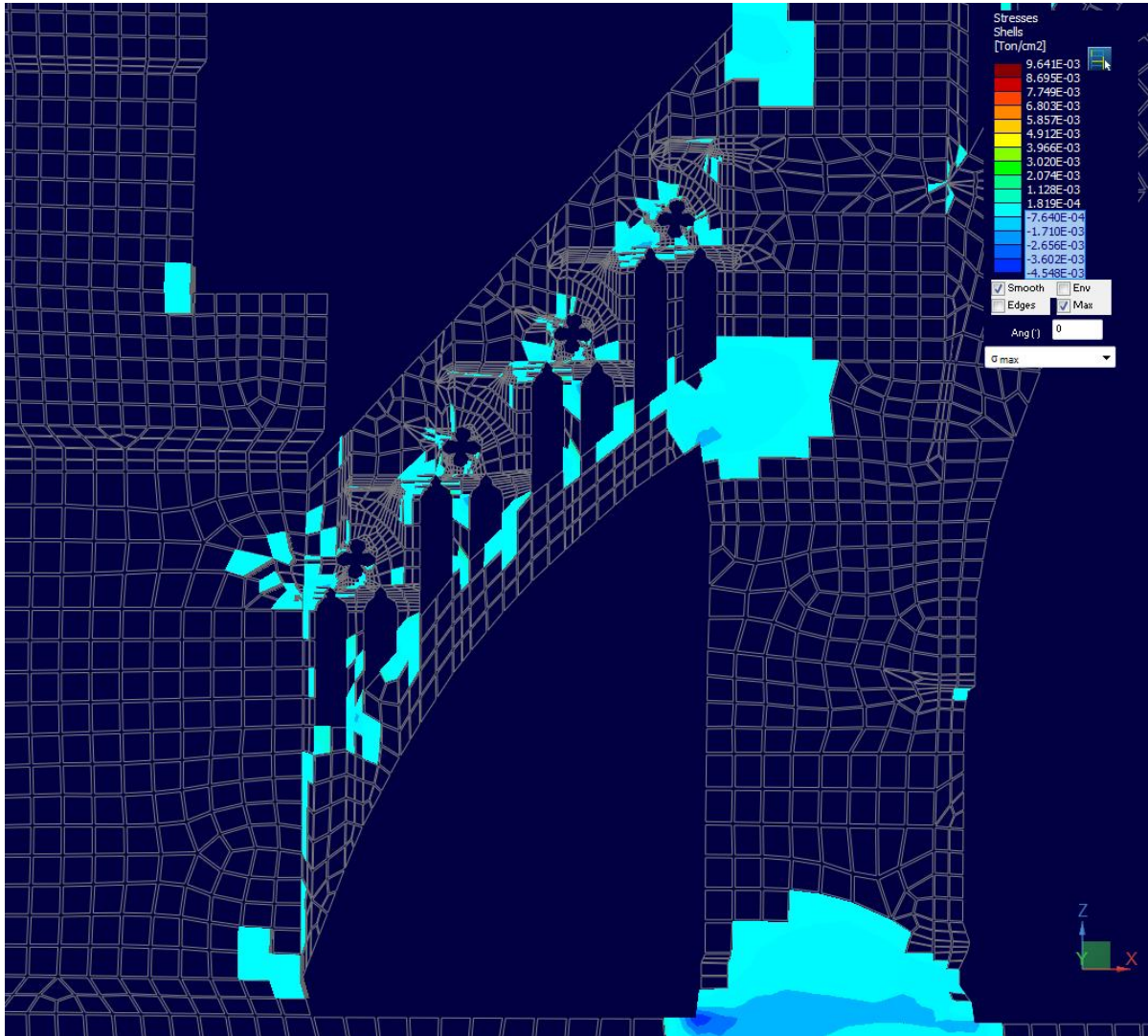
Profile of varying thicknesses of Cathédrale d'Amiens



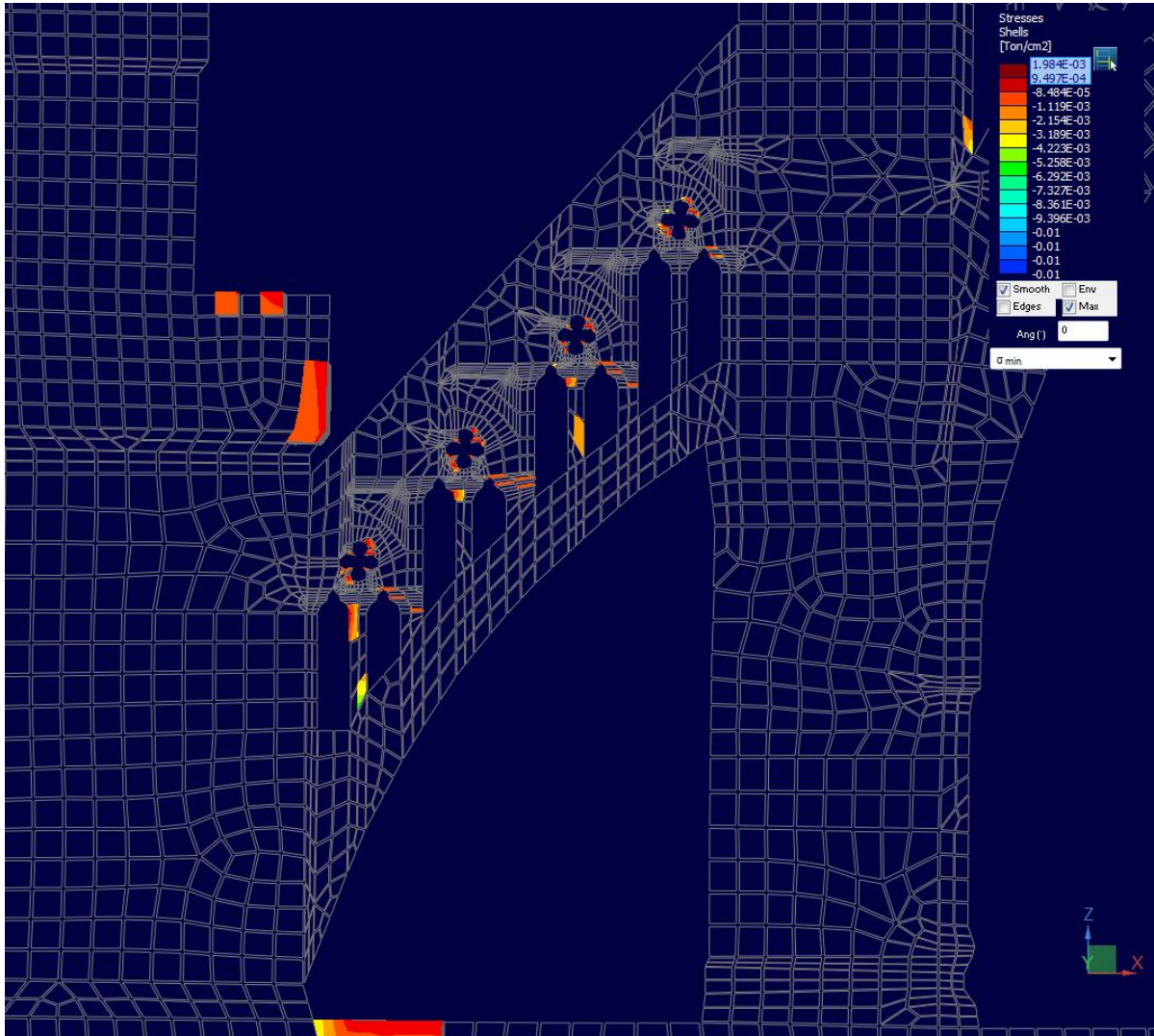
Maximum Principal Stresses ($1.053 \times 10^{-3} \sim 0.01$ ton/cm²) of Cathédrale d'Amiens (état actuel) of Flying Buttress 2



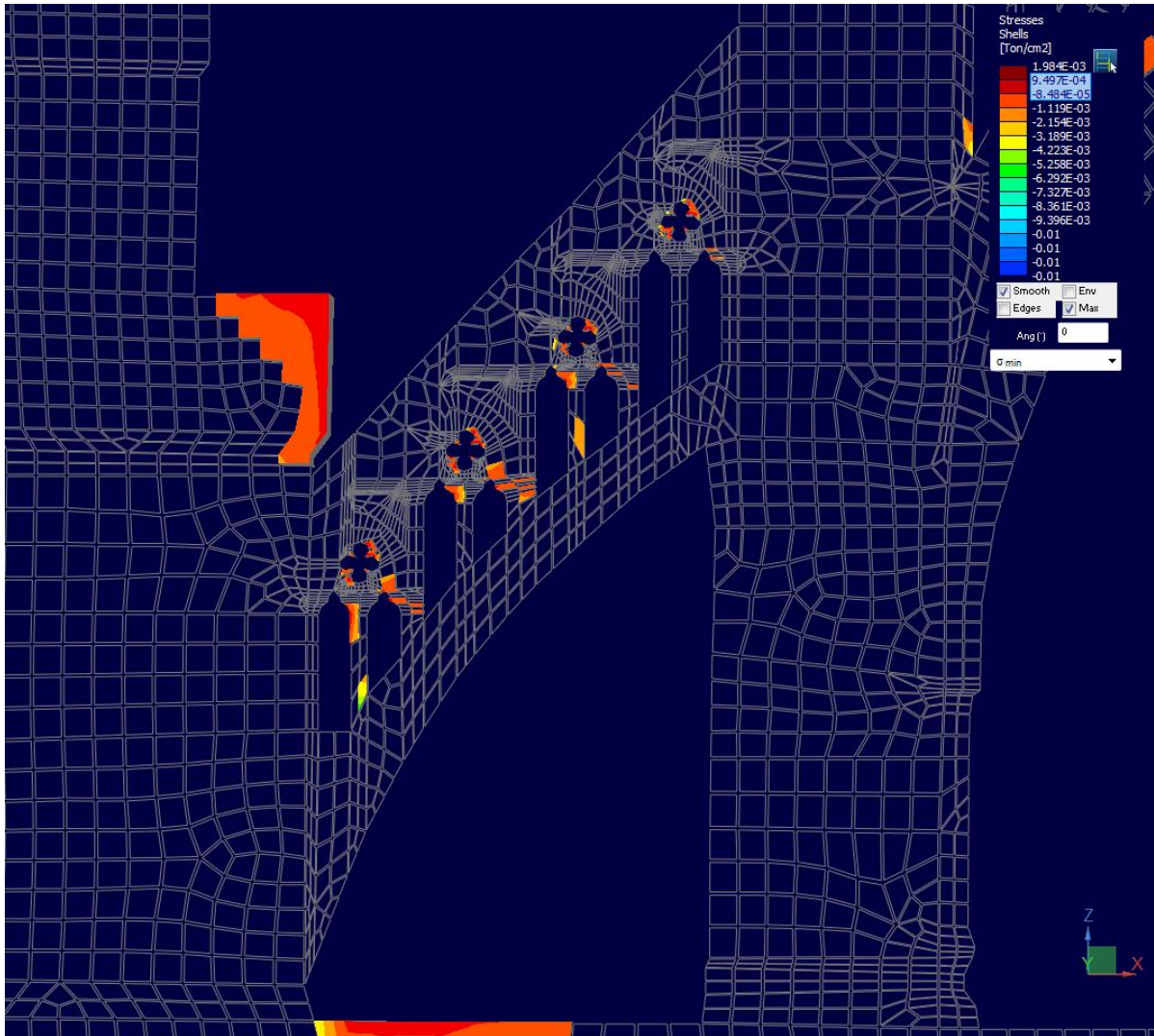
Maximum Principal Stresses ($-7.640 \times 10^{-4} \sim 1.819 \times 10^{-4}$ ton/cm²) of Cathédrale d'Amiens (état actuel) of Flying Buttress 2



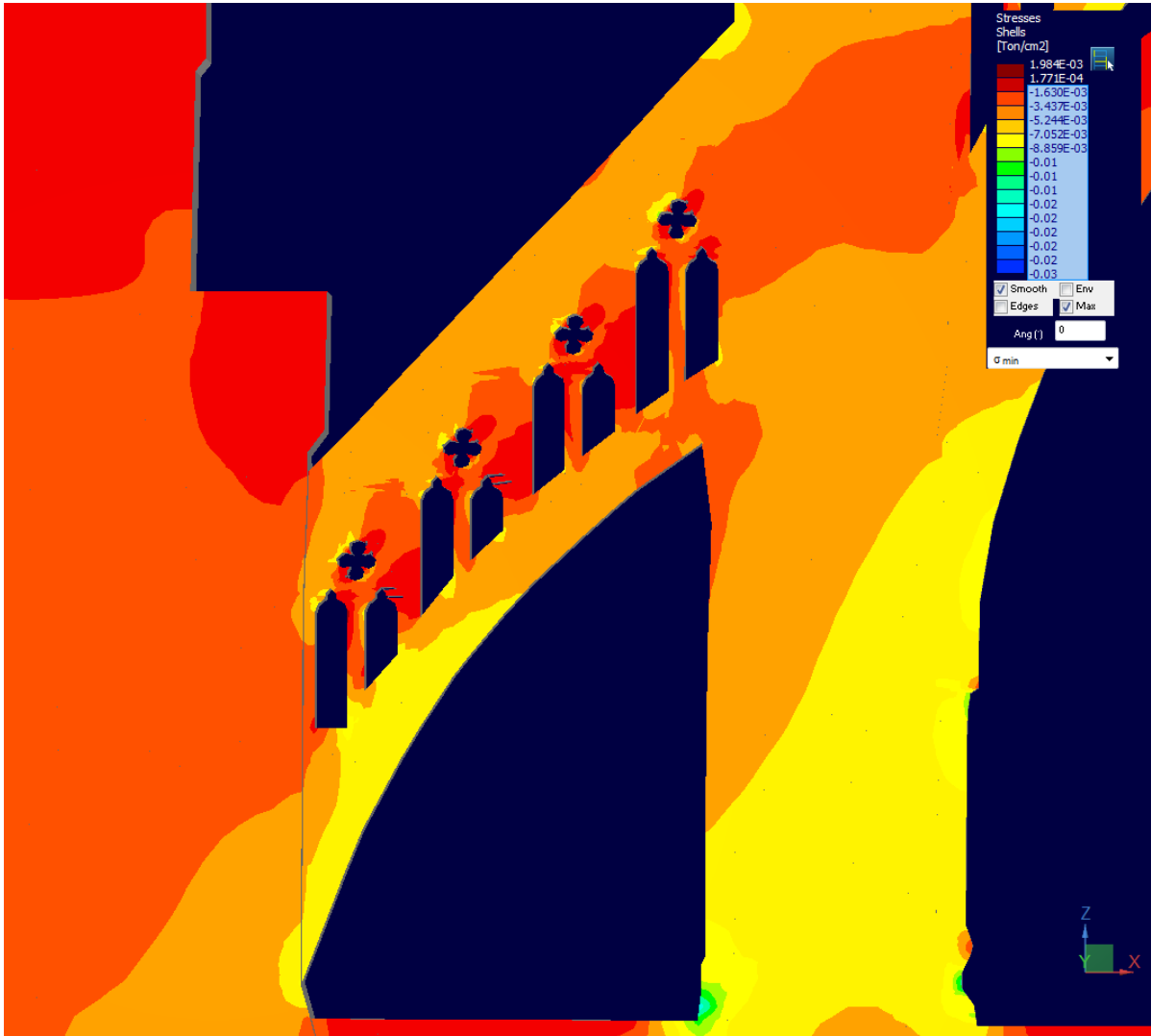
Maximum Principal Stresses ($-4.548 \times 10^{-3} \sim -7.640 \times 10^{-4}$ ton/cm²) of Cathédrale d'Amiens (état actuel) of Flying Buttress 2



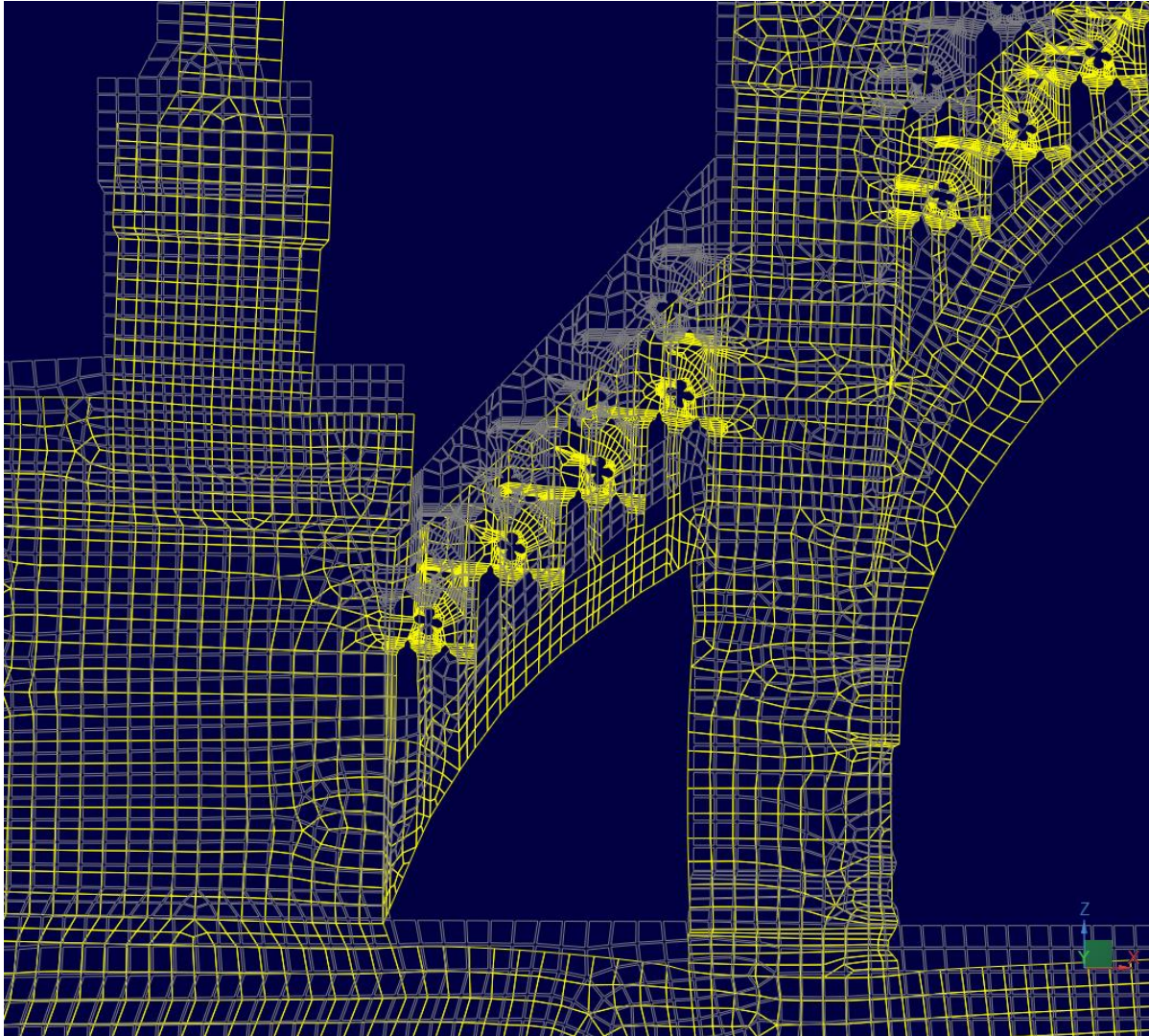
Minimum Principal Stresses ($9.497 \times 10^{-4} \sim 1.984 \times 10^{-3}$ ton/cm²) of Cathédrale d'Amiens (état actuel) of Flying Buttress 2



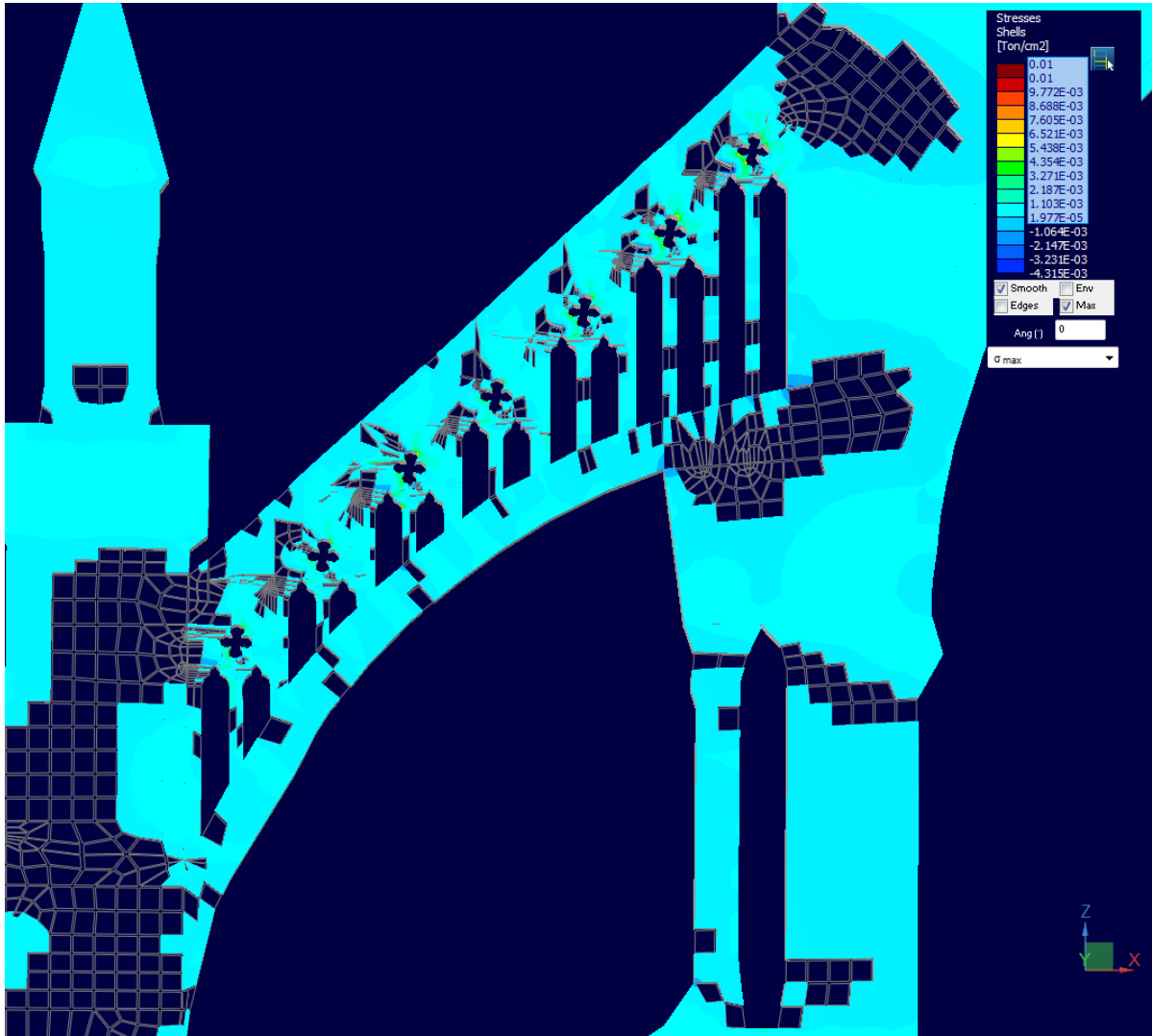
Minimum Principal Stresses ($-8.484 \times 10^{-5} \sim 9.497 \times 10^{-4}$ ton/cm²) of Cathédrale d'Amiens (état actuel) of Flying Buttress 2



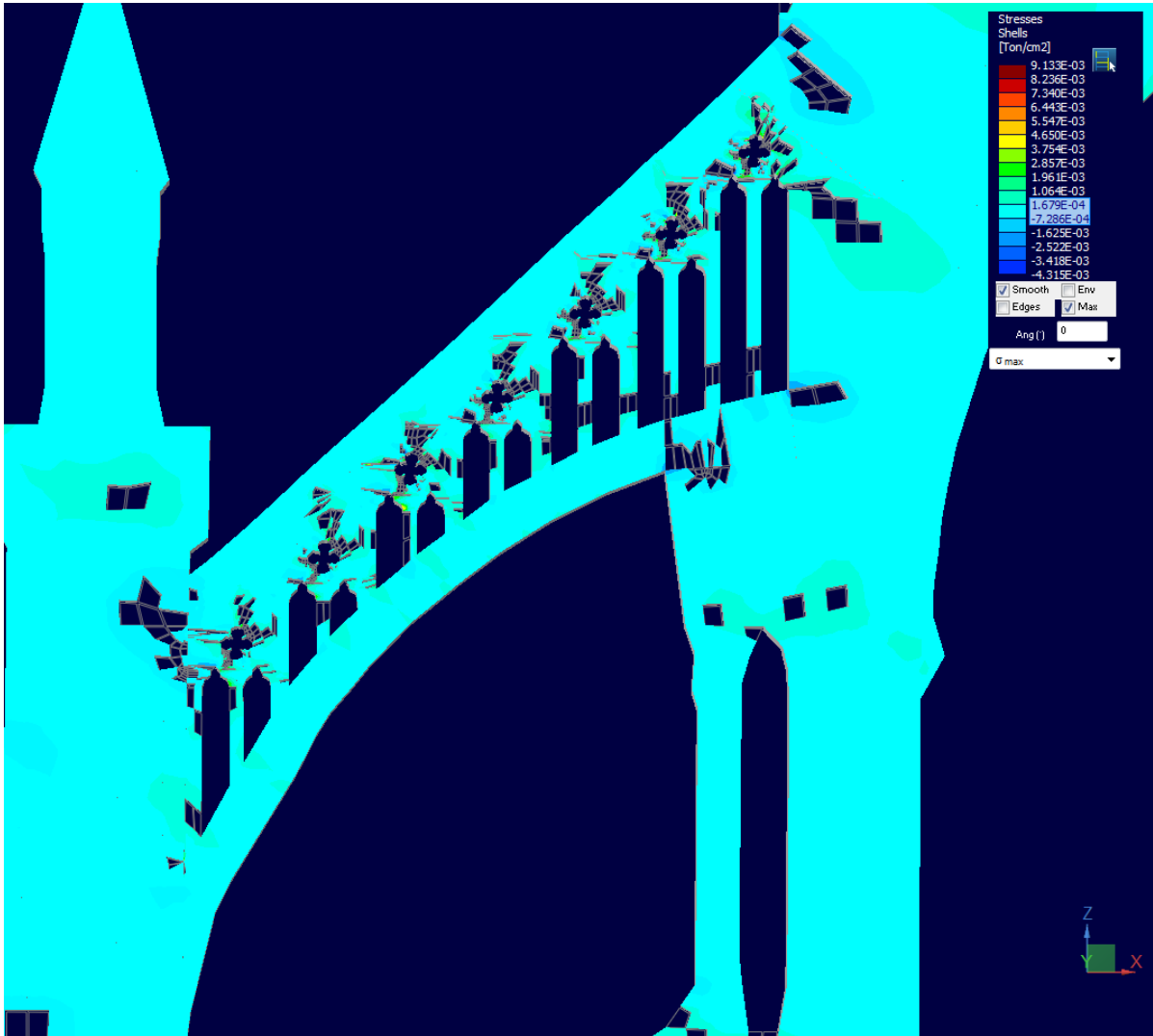
Minimum Principal Stresses ($-0.02 \sim -1.630 \times 10^{-3}$ ton/cm²) of Cathédrale d'Amiens (état actuel) of Flying Buttress 2



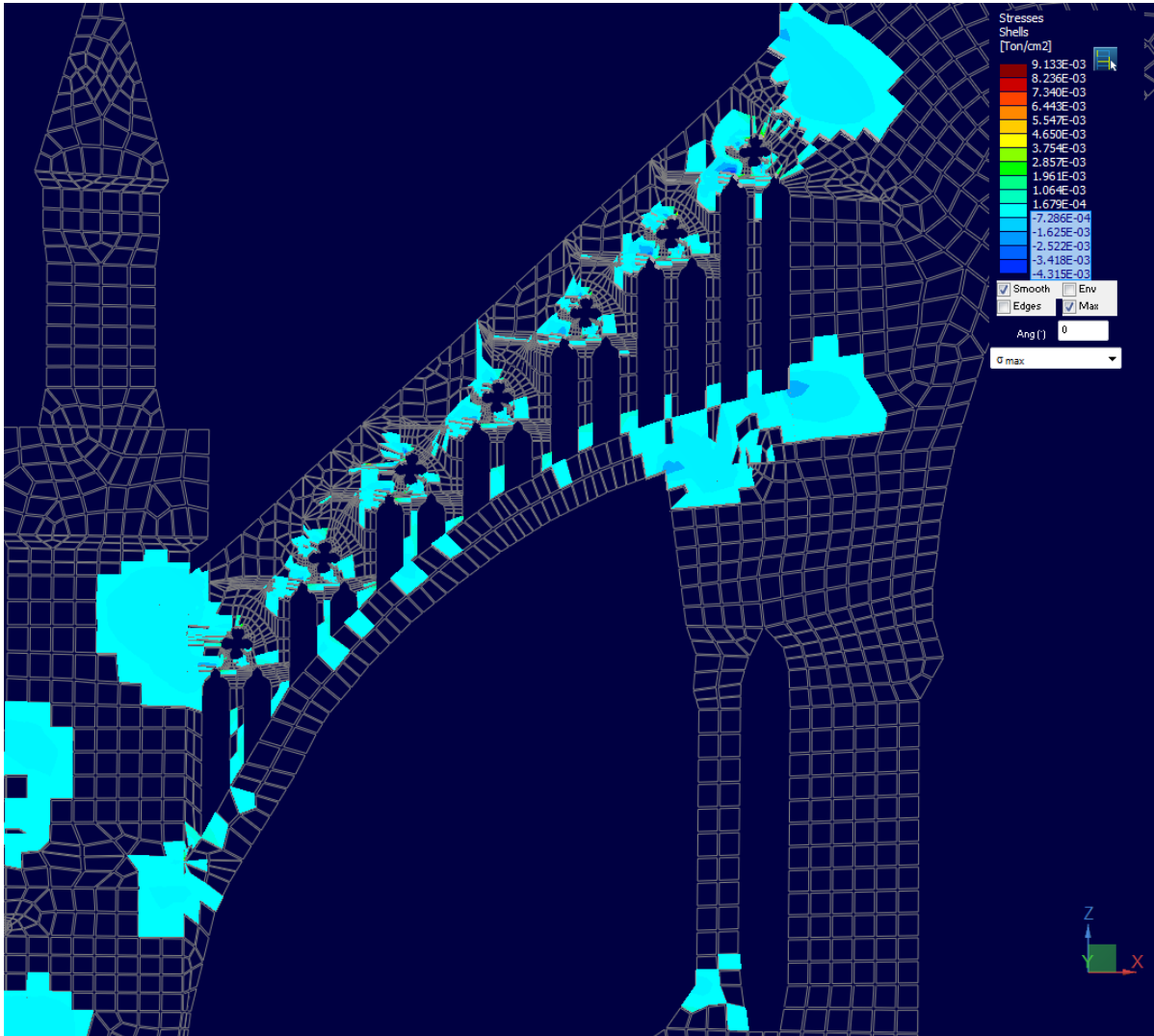
**Projected Cross Section Profile Deflection of Cathédrale d'Amiens (état actuel)
of Flying Buttress 2**



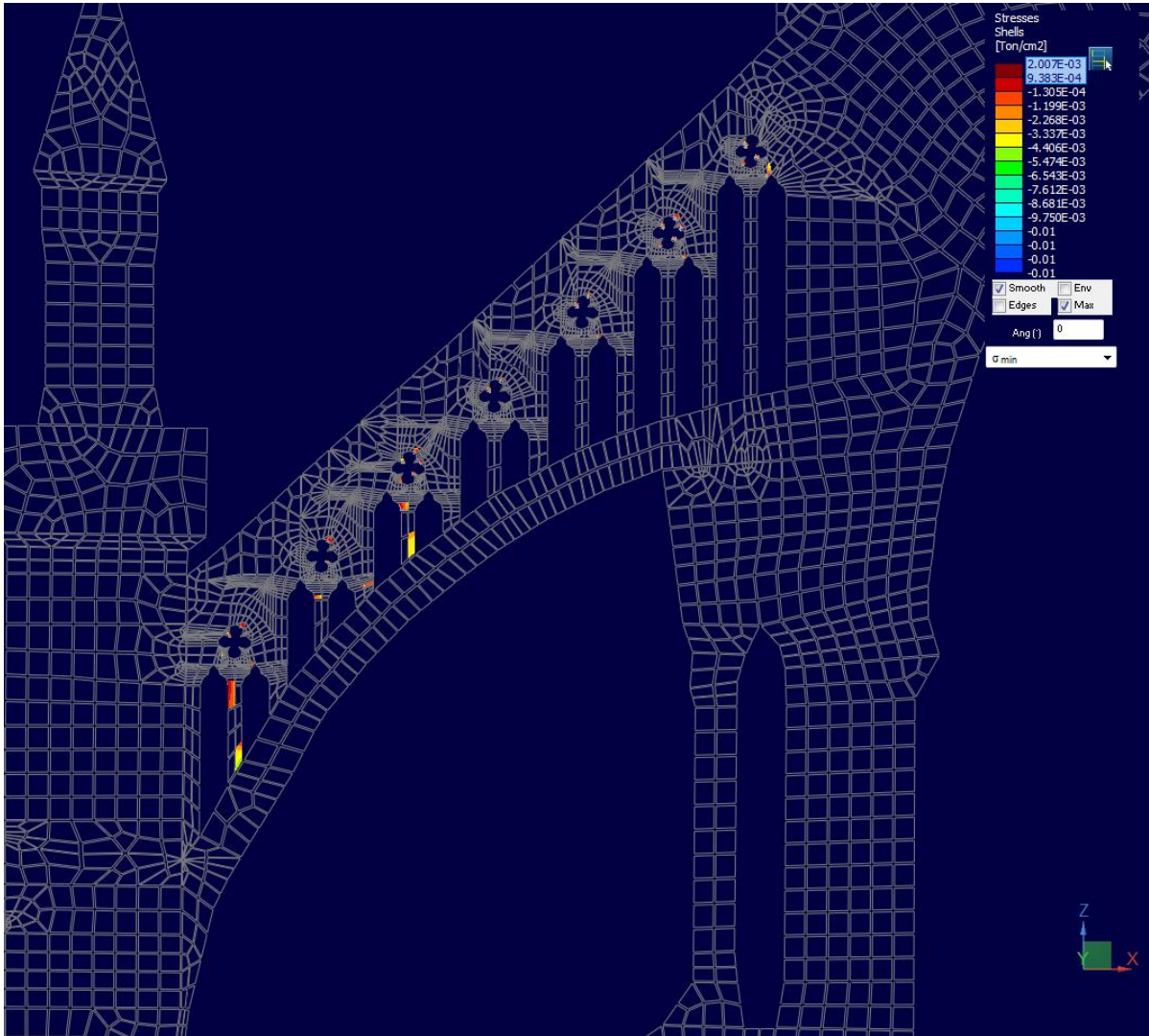
Maximum Principal Stresses ($1.977 \times 10^{-5} \sim 0.01 \text{ ton/cm}^2$) of Cathédrale d'Amiens (état antérieur à 1497) of Flying Buttress 1



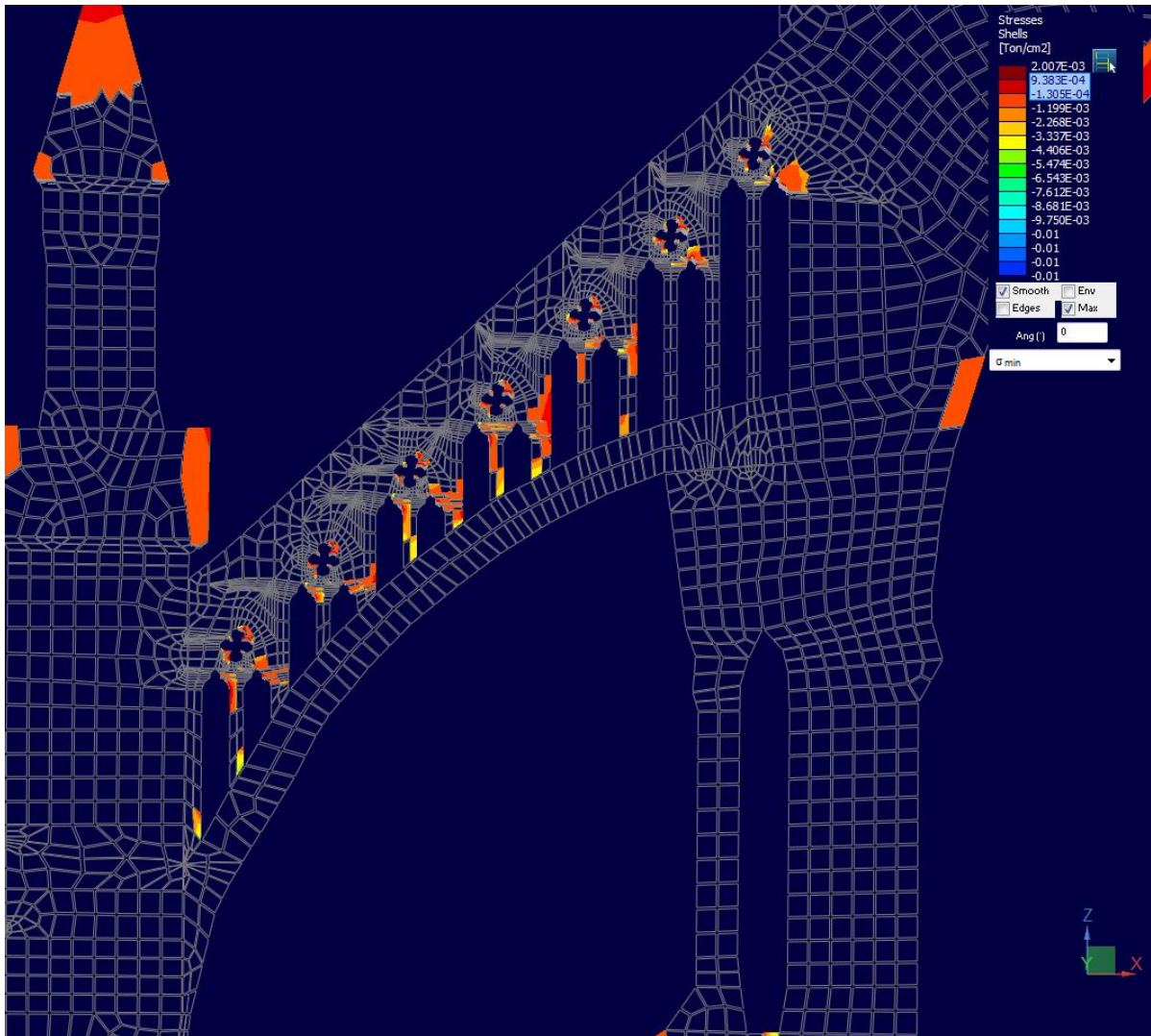
Maximum Principal Stresses ($-7.286 \times 10^{-4} \sim 1.679 \times 10^{-4}$ ton/cm²) of Cathédrale d'Amiens (état antérieur à 1497) of Flying Buttress 1



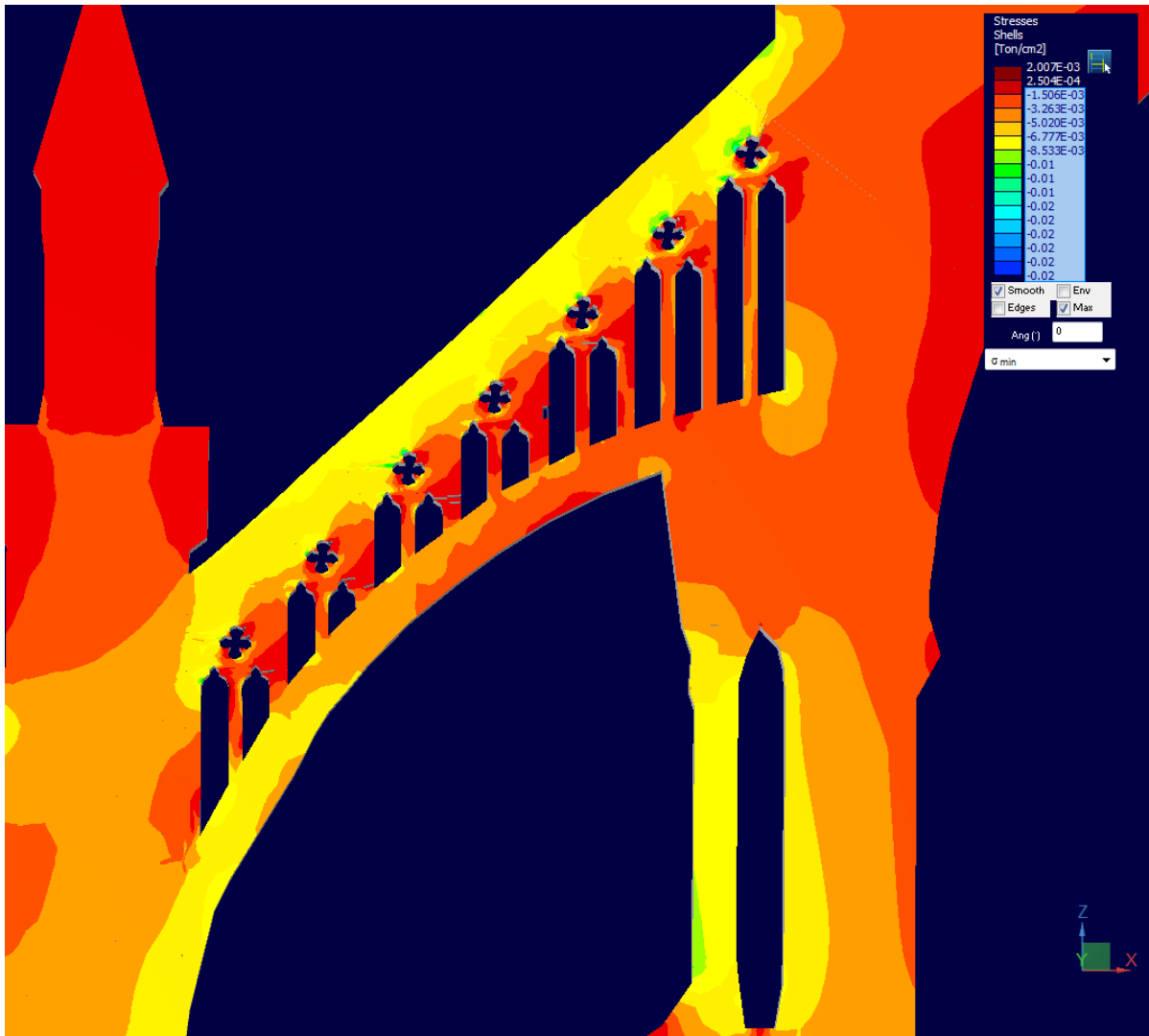
Maximum Principal Stresses ($-4.315 \times 10^{-3} \sim -7.286 \times 10^{-4}$ ton/cm²) of Cathédrale d'Amiens (état antérieur à 1497) of Flying Buttress 1



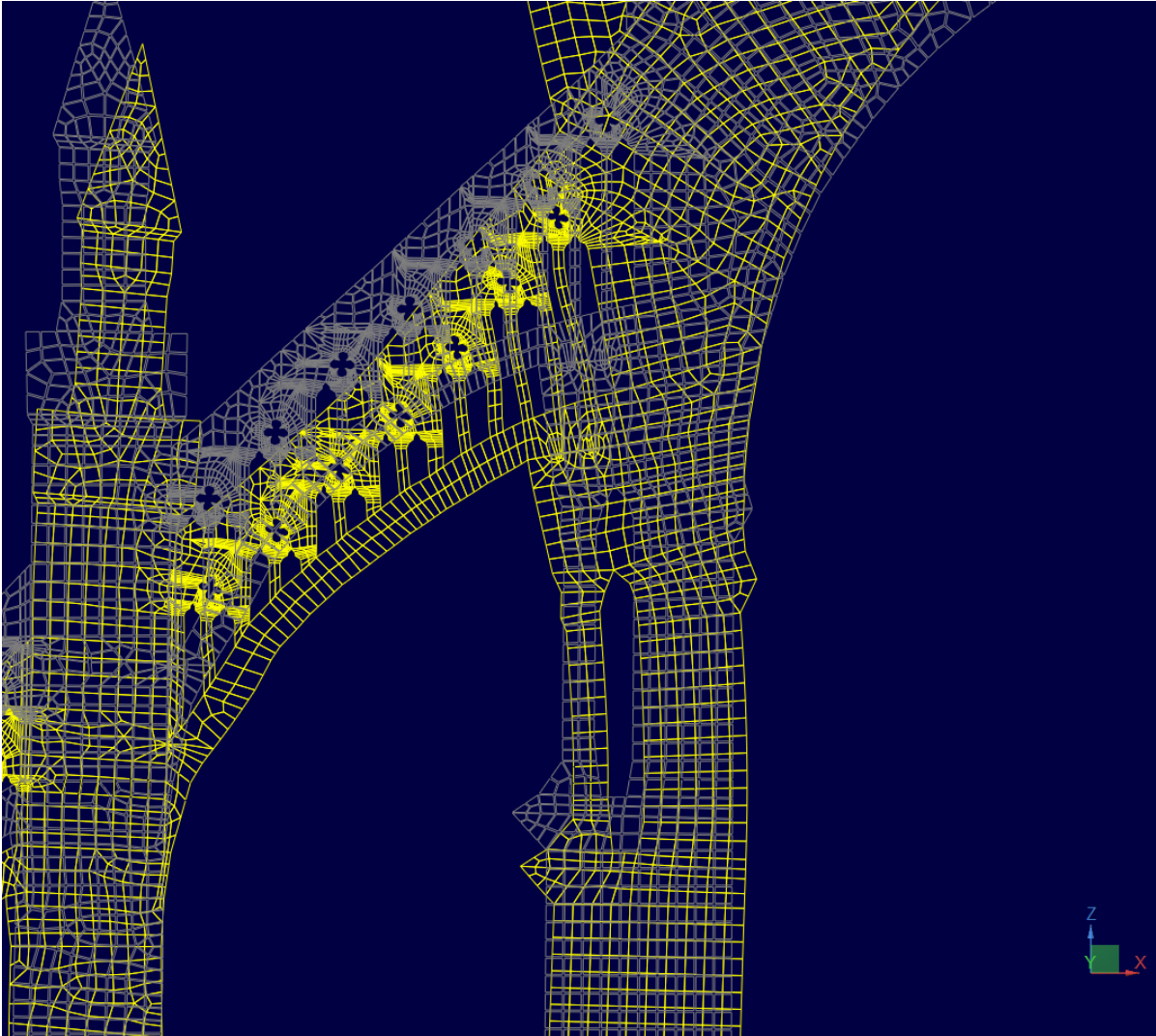
Minimum Principal Stresses ($9.383 \times 10^{-4} \sim 2.007 \times 10^{-3}$ ton/cm²) of Cathédrale d'Amiens (état antérieur à 1497) of Flying Buttress 1



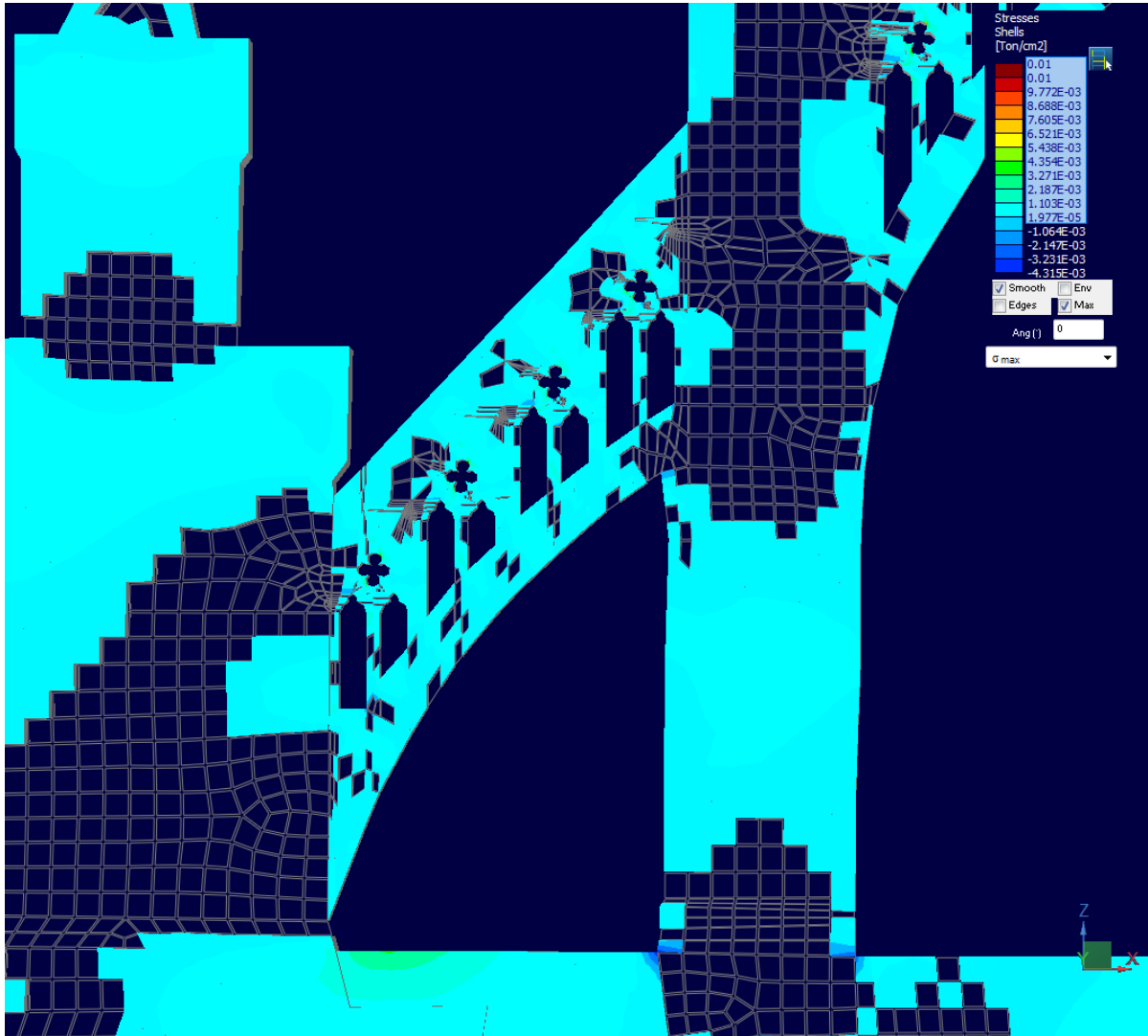
Minimum Principal Stresses ($-1.305 \times 10^{-4} \sim 9.383 \times 10^{-4}$ ton/cm²) of Cathédrale d'Amiens (état antérieur à 1497) of Flying Buttress 1



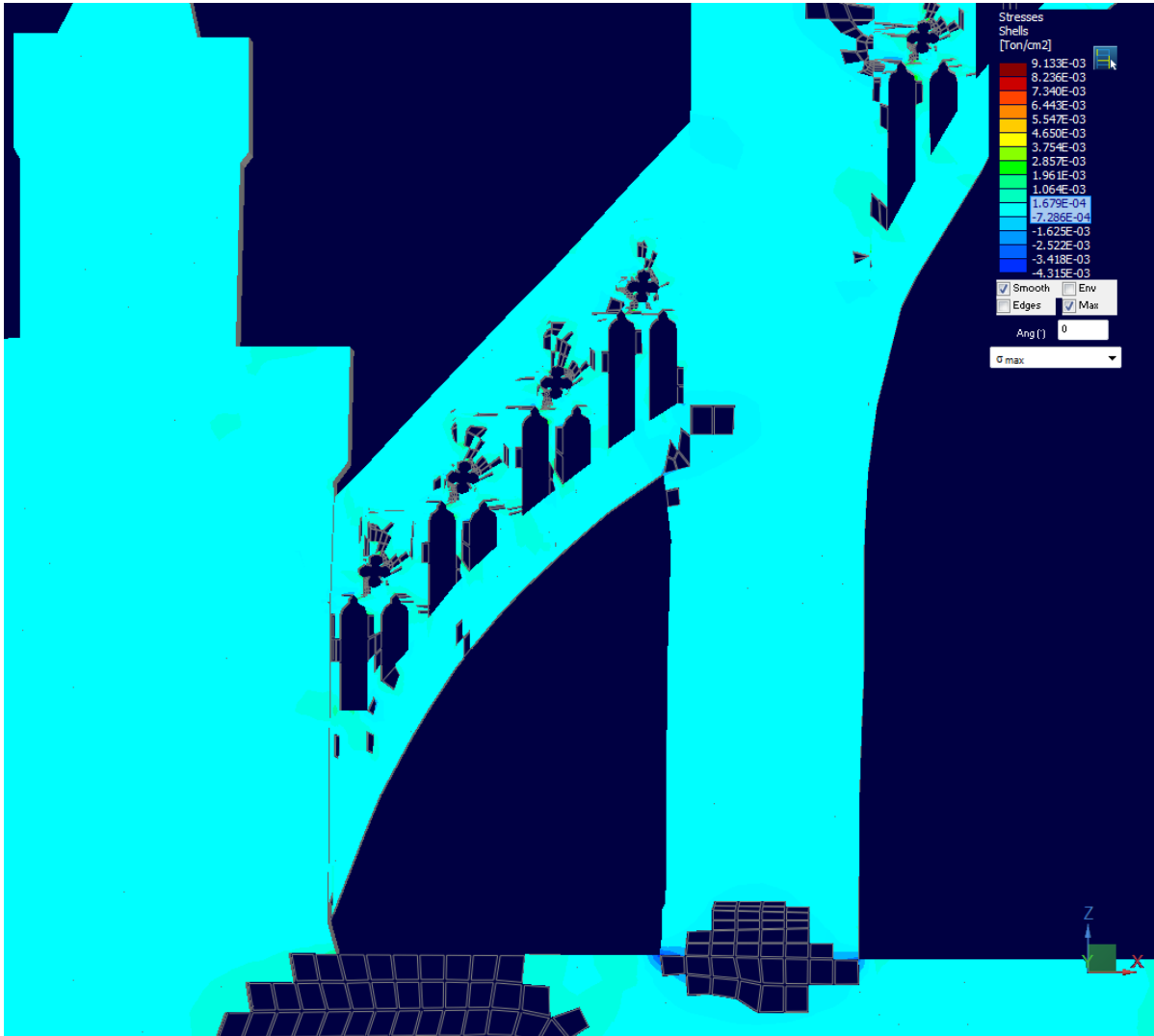
Minimum Principal Stresses ($-0.02 \sim -1.506 \times 10^{-3}$ ton/cm²) of Cathédrale d'Amiens (état antérieur à 1497) of Flying Buttress 1



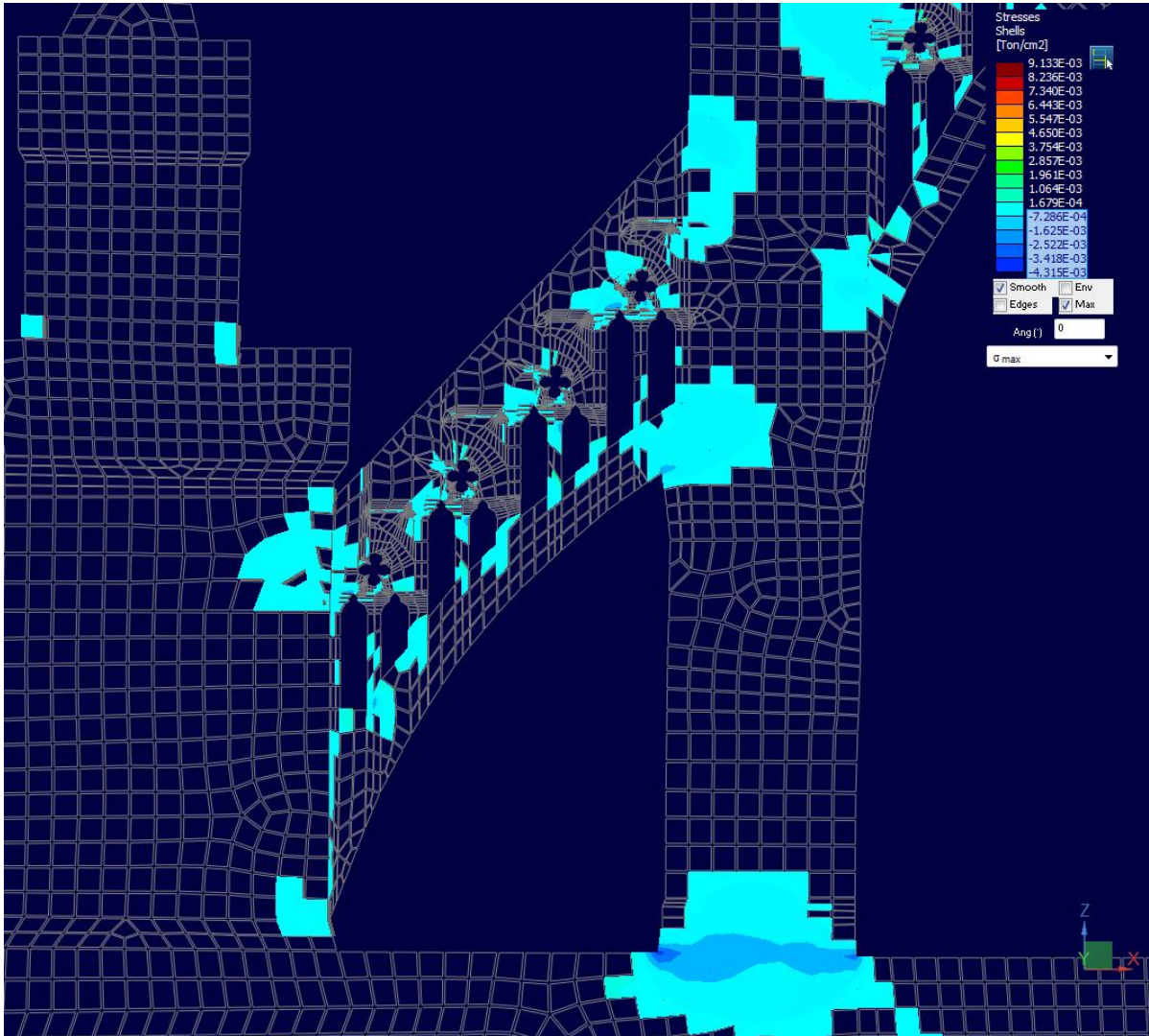
**Projected Cross Section Profile Deflection of Cathédrale d'Amiens (état antérieur à 1497)
of Flying Buttress 1**



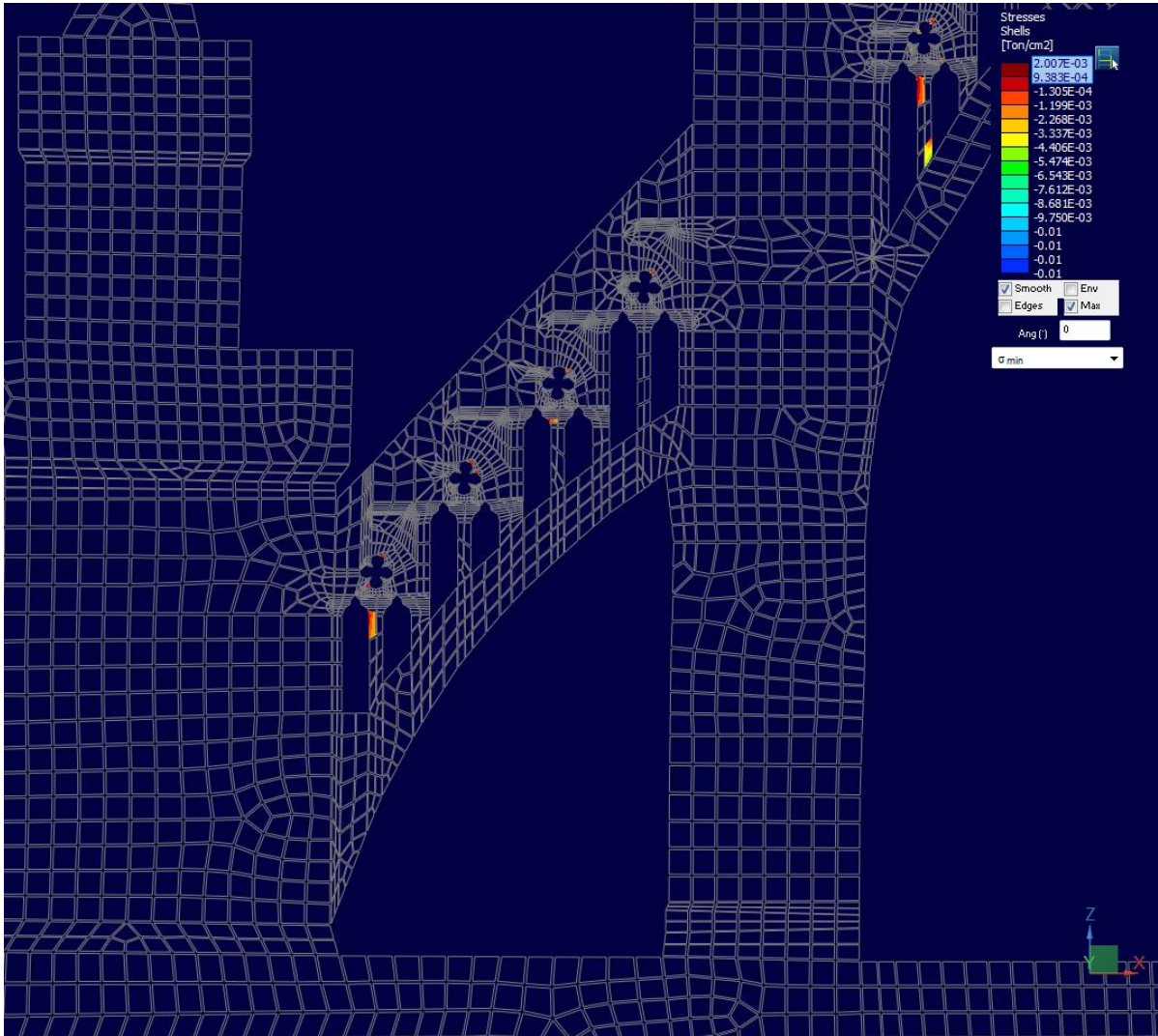
Maximum Principal Stresses ($1.977 \times 10^{-5} \sim 0.01$ ton/cm²) of Cathédrale d'Amiens (état antérieur à 1497) of Flying Buttress 2



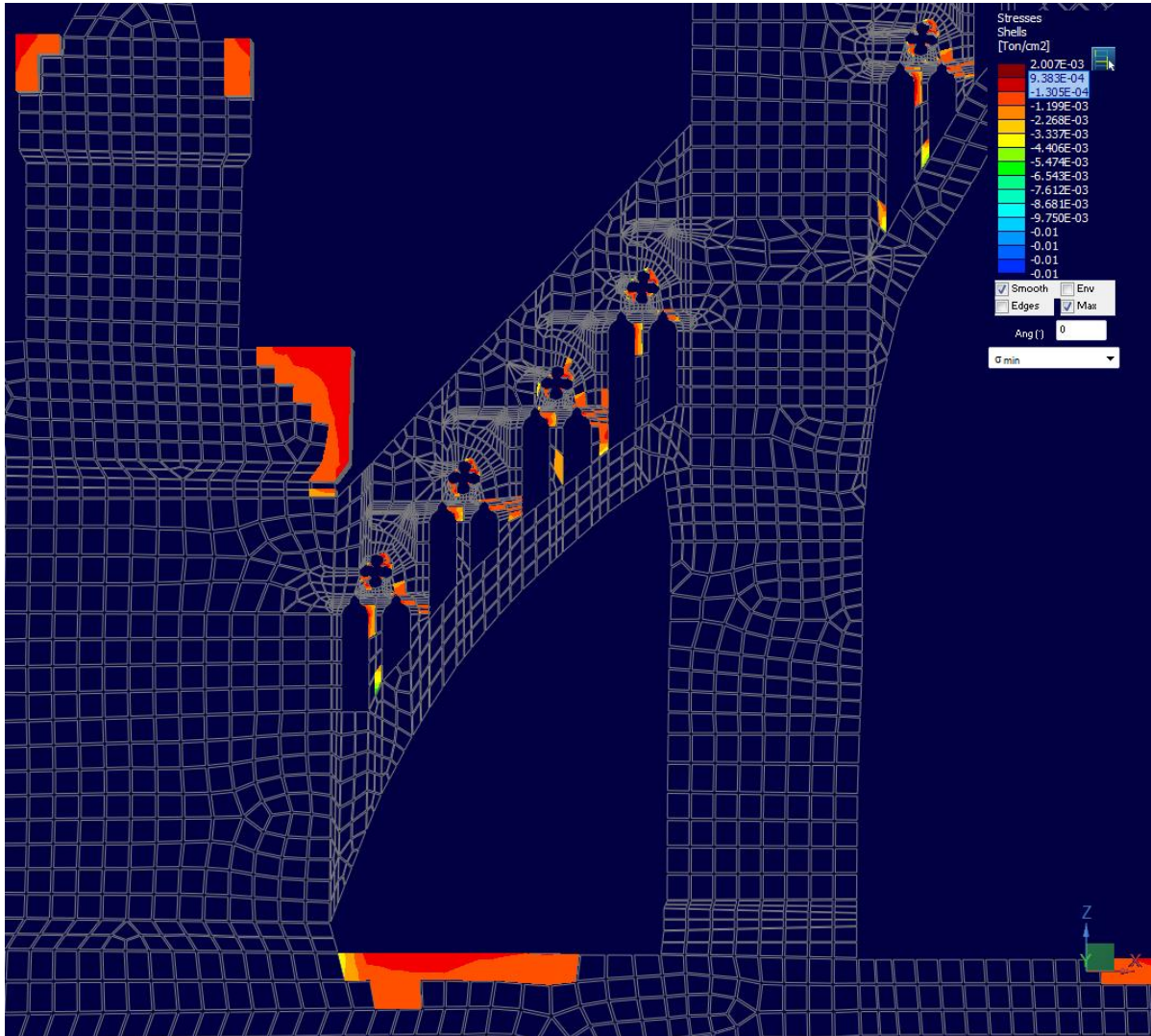
Maximum Principal Stresses ($-7.286 \times 10^{-4} \sim 1.679 \times 10^{-4}$ ton/cm²) of Cathédrale d'Amiens (état antérieur à 1497) of Flying Buttress 2



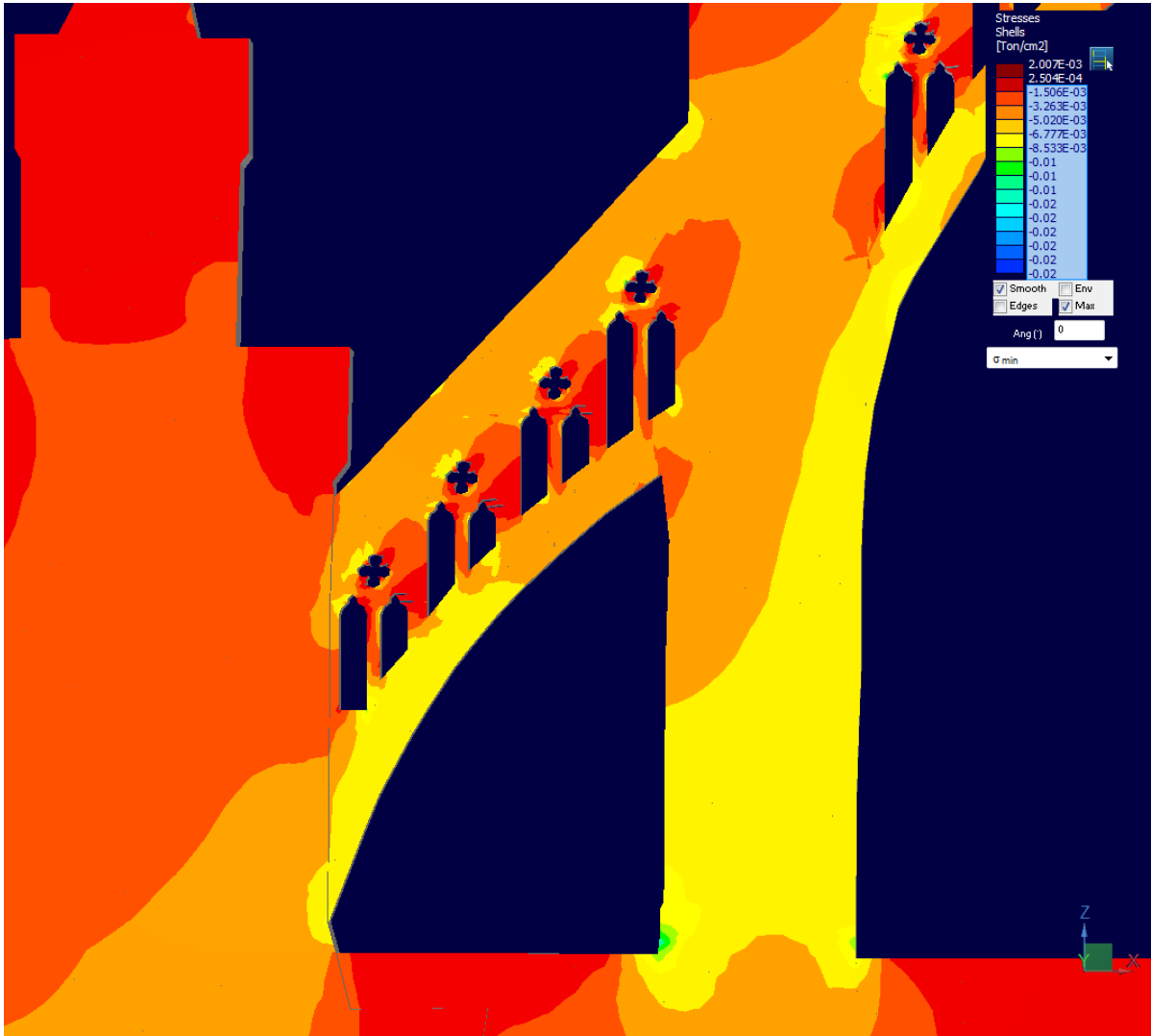
Maximum Principal Stresses ($-4.315 \times 10^{-3} \sim -7.286 \times 10^{-4}$ ton/cm²) of Cathédrale d'Amiens (état antérieur à 1497) of Flying Buttress 2



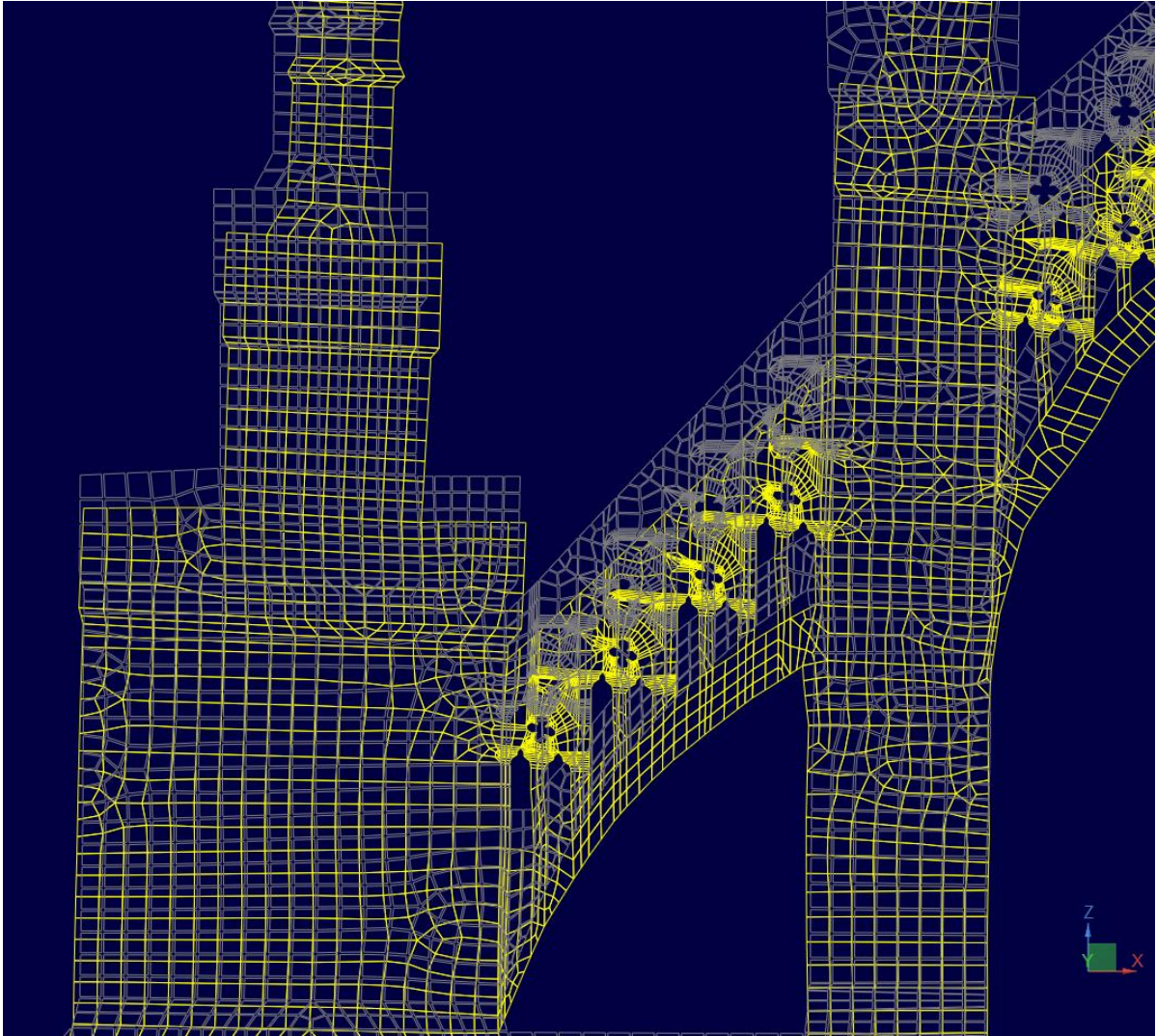
Minimum Principal Stresses ($9.383 \times 10^{-4} \sim 2.007 \times 10^{-3}$ ton/cm²) of Cathédrale d'Amiens (état antérieur à 1497) of Flying Buttress 2



Minimum Principal Stresses ($-1.305 \times 10^{-4} \sim 9.383 \times 10^{-4}$ ton/cm²) of Cathédrale d'Amiens (état antérieur à 1497) of Flying Buttress 2



Minimum Principal Stresses ($-0.02 \sim -1.506 \times 10^{-3}$ ton/cm²) of Cathédrale d'Amiens (état antérieur à 1497) of Flying Buttress 2



**Projected Cross Section Profile Deflection of Cathédrale d'Amiens (état antérieur à 1497)
of Flying Buttress 2**

Appendix D – Source Permission

2/14/2016

John Wiley and Sons pending request requires YOUR ATTENTION - Richard Kim

John Wiley and Sons pending request requires YOUR ATTENTION

Copyright Clearance Center <rightslink@marketing.copyright.com>

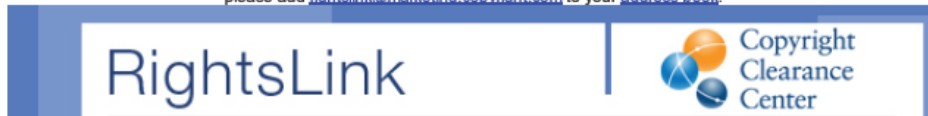
Wed 1/27/2016 3:31 PM

To: Richard Kim <rdykim@ksu.edu>;

To view this email as a web page, go [here](#).

Do Not Reply Directly to This Email

To ensure that you continue to receive our emails,
please add rightslink@marketing.copyright.com to your address book.



Permissions Request Requires Your Acceptance

Dear Mr. Richard Kim,

John Wiley and Sons has approved your recent permission request - see the details below. Prior to reusing this content, you must accept the license fee and terms.

To accept or decline this order, please click the link below to open RightsLink.

<https://s100.copyright.com/CustomerAdmin/FC.asp?ref=dd83d133-11c0-4128-b067-a4d5a102daa3&oName=wiley>

(If the link above is displaying on two lines, it may not open your browser window properly. Copy and paste the entire link into your browser address field and try again.)

Order Details

Licensee:	Richard Kim
Order Date:	Jan 27, 2016
Order Number:	501102470
Publication:	Wiley Books
Title:	Form and Forces: Designing Efficient, Expressive Structures
Type of Use:	Institutional Repository

Note: Payee for this order is Copyright Clearance Center.

B.3:v5.7

<https://outlook.office.com/owa/#viewmodel=ReadMessageItem&ItemID=AQMkADYxYzFmMzVjLWQ0ODQtNGM5NS1hMTkzLWQzYThiMWJhOTZkZgBG...> 1/2

2/14/2016

RE: Images from 'Form and Forces' by E. Allen and W. Zalewski - Richard Kim

RE: Images from 'Form and Forces' by E. Allen and W. Zalewski

Wiley Global Permissions <permissions@wiley.com>

Fri 2/12/2016 9:10 AM

To: Richard Kim <rдыkim@ksu.edu>;

Dear Richard,

Thank you for your request.

Permission is granted for you to use the material requested for your thesis/dissertation subject to the usual acknowledgements (author, title of material, title of book/journal, ourselves as publisher) and on the understanding that you will reapply for permission if you wish to distribute or publish your thesis/dissertation commercially. You must also duplicate the copyright notice that appears in the Wiley publication in your use of the Material; this can be found on the copyright page if the material is a book or within the article if it is a journal.

Permission is granted solely for use in conjunction with the thesis, and the material may not be posted online separately.

Any third party material is expressly excluded from this permission. If any of the material you wish to use appears within our work with credit to another source, authorisation from that source must be obtained.

Best wishes,

Aimee Masheter
Permissions Assistant
John Wiley & Sons Ltd
The Atrium
Southern Gate, Chichester
West Sussex, PO19 8SQ
UK

WILEY

From: Richard Kim [mailto:rдыkim@ksu.edu]**Sent:** 04 February 2016 15:37**To:** Wiley Global Permissions**Subject:** Re: Images from 'Form and Forces' by E. Allen and W. Zalewski

<https://outlook.office.com/owa/#viewmodel=ReadMessageItem&ItemID=AQMkADYxYzFmMzVjLWQ0ODQ0tNGM5NS1hMTkzLWQzYThiMWJhOTZkZgBG...> 1/2

2/14/2018

RE: Images from 'Form and Forces' by E. Allen and W. Zalewski - Richard Kim

Wiley Global Permissions,

Here are the following images that I would like to include for my thesis:

- figure 8.7 (a), (b) (page 219)
- figure 8.8 (a) (page 220)
- figure 8.9 (a), (b), (c) (page 221)
- figure 8.16 (a), (b), (c) (page 226)
- figure 8.22 (a) (page 231)

Please do not hesitate if you have any questions.

Thank you

Richard Kim

<https://outlook.office.com/owa/#viewmodel=ReadMessageItem&ItemID=AQMkADYxYzFmMzVjLWQ0ODQhNGM5NS1hMTkzLWQzYThiMWJhOTZkZgBG...> 2/2

2/14/2016

RE: Permission to use images - Richard Kim

RE: Permission to use images

alison stones <mastones@hotmail.com>

Fri 2/5/2016 10:32 AM

To: Richard Kim <rdykim@ksu.edu>;

No problem: the cross-sections were copied from Dehio, a book out of copyright and in public domain. So all you need to say is "after Dehio". Good luck finishing up! Alison Stones

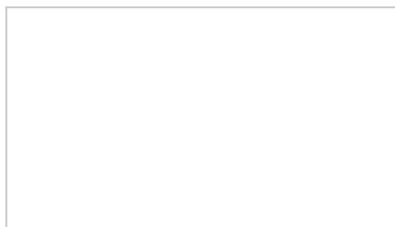
Professor Emerita M. Alison Stones, Ph.D., F.S.A., Chevalier de l'Ordre des Arts et des Lettres
(Department of History of Art and Architecture, University of Pittsburgh)
255 W 95th St # 5A, New York, NY 10025 tel 646 678 3671
French address: Chauzanaud, Savignac-les-Églises, 24420
tel (33) 553 07 81 03 mobile (33) 607 437385

From: rdykim@ksu.edu
To: mastones@hotmail.com
Subject: Permission to use images
Date: Fri, 5 Feb 2016 15:22:57 +0000

Dear Alison Stones,

I am currently in the process of finalizing my Masters thesis on flying buttresses to Kansas State University.

During my research, I happened to come across detailed cross sections of several cathedrals from www.medart.pitt.edu and I would like to request your permission to include these images when I submit my thesis electronically to the Kansas State University research archives.



IMAGES OF MEDIEVAL ART AND
ARCHITECTURE
www.medart.pitt.edu
MEDART - Images of Medieval Art and Architecture -
created by Alison Stones and designed by Jane Vadnal
and Philip Maye - is a series of webpages devoted to ...

By submitting my thesis to the Kansas State University archives, it will be easily accessible to anyone. I believe that including the cross sections and plan views of selected cathedrals would be an essential part to my thesis and I would be grateful if you can grant me permission to use them. The three cathedrals used for my research are Cathédrale Notre-Dame de Paris, Amiens Cathédrale Notre-Dame, and Bourges

<https://outlook.office.com/owa/#viewmodel=ReadMessageItem&ItemID=AQMkADYxYzFmMzVjLWQ0ODQtNGM5NS1hMTkzLWQzYThtMWJhOTZkZGZG...> 1/2

2/14/2016

RE: Permission to use images - Richard Kim

Cathédrale Saint-Etienne.

I will fully reference your work and include any acknowledgement that you deem appropriate.

Please let me know if you need any further information. Thank you in advance for your consideration.

Sincerely,

Richard Kim

<https://outlook.office.com/owa/#viewmodel=ReadMessageItem&ItemID=AQMkADYxYzFmMzVjLWQ0ODQhNGM5NS1hMTkzLWQzYThiMWJhOTZkZgBG...> 2/2

2/14/2016

Re: Permission to use images from mappinggothic - Richard Kim

Re: Permission to use images from mappinggothic

Gabriel Sussman Rodriguez <gsr2101@columbia.edu>

Fri 2/5/2016 11:42 AM

To: Richard Kim <rdykim@ksu.edu>;

Cc: Media Center for Art History <mediacenter@columbia.edu>;

Hi Richard,

Here are citations for those three images. Please still include "Image courtesy of mappinggothic.org, Media Center for Art History, Department of Art History and Archaeology, Trustees of Columbia University" below the image in your thesis.

--Notre Dame de Paris, transverse section of nave,
from Baudot, Anatole de, and A. Perrault-Dabot. Cathédrales De France. Paris, France: H. Laurens, 1905-1907.

--Notre Dame d'Amiens, section of choir (from Durand, Monographie, 1, plate XIX),
from Murray, Stephen. Beauvais Cathedral - Architecture of Transcendence. Princeton, N.J.: Princeton University Press, 1989. 143.

--Saint-Étienne de Bourges, transverse section,
from Dehio, Georg. Die Kirchlche Baukunst Des Abendlandes. Vol. 4. 5 vols. Stuttgart, Germany: J. G. Cotta, 1887-1901. 375.

Best,
Gabe

On Fri, Feb 5, 2016 at 11:25 AM, Richard Kim <rdykim@ksu.edu> wrote:

Thank you very much!

I would like to obtain the original source to theses images.
Both cross sections and plans of the cathedrals seemed to be linked to google.

Here are the links to the three cathedrals

Paris, Cathédrale Notre-Dame:

<http://mappinggothic.org/building/1164#/>



Paris, Cathédrale Notre-Dame - Mapping Gothic France

mappinggothic.org

Three levels of interpretation may be entertained. E. E. Viollet-le-Duc, considered the monument a radical breakthrough, a revolt against feudalism and monasticism ...

<https://outlook.office.com/owa/#viewmodel=ReadMessageItem&ItemID=AQMkADYxYzFmMzVjLWQ0ODQtNGM5NS1hMTkzLWQzYThiMWJhOTZkZgBG...> 1/2

<http://mappinggothic.org/image/40340?mode=naked&view=zoom>

Amiens, Cathédrale Notre-Dame:

<http://mappinggothic.org/building/1063>



Amiens, Cathédrale Notre-Dame - Mapping Gothic France

mappinggothic.org

Notre-Dame of Amiens is by far the tallest cathedral built at this time with a new level of rigor and an attention to form drawing upon masonic expertise from the ...

<http://mappinggothic.org/image/30580?mode=naked&view=zoom>

Bourges, Cathédrale Saint-Etienne:

<http://mappinggothic.org/building/1096>



Bourges, Cathédrale Saint-Étienne - Mapping Gothic France

mappinggothic.org

The western frontispiece of Bourges is articulated by a program of five sculpted portals. These portals are dedicated, from north to south, as follows: the ...

<http://mappinggothic.org/image/39057?mode=naked&view=zoom>

--
Gabriel Rodriguez
Digital Curator, Media Center for Art History
Department of Art History and Archaeology
Columbia University
824 Schermerhorn Hall
212-854-3044
gsr2101@columbia.edu

2/28/2016

RE: Permission to use images for Masters Thesis - Richard Kim

RE: Permission to use images for Masters Thesis

Masheter, Aimee - Chichester <amasheter@wiley.com> on behalf of
Wiley Global Permissions <permissions@wiley.com>

Tue 2/23/2016 7:56 AM

To: Richard Kim <rdykim@ksu.edu>;

Dear Richard,

Thank you for your email.

Permission is granted for you to use the material requested for your thesis/dissertation subject to the usual acknowledgements (author, title of material, title of book/journal, ourselves as publisher) and on the understanding that you will reapply for permission if you wish to distribute or publish your thesis/dissertation commercially.

You should also duplicate the copyright notice that appears in the Wiley publication in your use of the Material. Permission is granted solely for use in conjunction with the thesis, and the material may not be posted online separately.

Any third party material is expressly excluded from this permission. If any material appears within the article with credit to another source, authorisation from that source must be obtained.

Best wishes

Aimee Masheter
Permissions Assistant
John Wiley & Sons Ltd
The Atrium
Southern Gate, Chichester
West Sussex, PO19 8SQ
UK



From: Richard Kim [mailto:rdykim@ksu.edu]
Sent: 05 February 2016 16:08
To: Wiley Global Permissions
Subject: Permission to use images for Masters Thesis

To the Permissions Department at John Wiley & Sons Inc.,

I am currently in the process of finalizing my Masters thesis on flying buttresses to Kansas State University.

<https://outlook.office.com/owa/#viewmodel=ReadMessageItem&ItemID=AQMkADYxYzFmMzVjLWQ0ODQtNGM5NS1hMTkzLWQzYThiMWJhOTZkZgBG...> 1/2

Permission to use images for Masters Thesis



Richard Kim

To: Wiley Global Permissions <permissions@wiley.com>;



Reply all |

Wed 3/9/2016 9:43 AM

Sent Items

Hello,

Here is the final list of following images specified that corresponds to the page number for 'A Visual Dictionary of Architecture (2nd Ed.)' by Francis D. K. Ching. The descriptions shown in parenthesis indicate the words associated/labeled with the image.

- p. 4; masonry arch (showing voussoir, keystone, extrados, intrados, spring, rise and archivolt) (1 image)
- p. 5; the funicular arch (showing arch action, arch axis and line of thrust) (1 image)
- p. 6; Roman arch, equilateral arch (2 images)
- p. 28; campanile (1 image)
- p. 29; cathedral (flèche), (rose window, stained glass, triforium) (2 images)
- p. 280; vaulting shaft (shaft, flying buttress), (flying buttress, pinnacle, buttress pier, amortizement, nosing) (2 images)
- p. 293; quatrefoil, cinqfoil (2 images)

total images used: 11 images

Thank you

Richard